A record of paleoseismicity from the varved marine sediments of Effingham Inlet, Vancouver Island, British Columbia

Matthew Robert Skinner

B.Sc., Queen's University, 1999

Thesis Submitted in Partial Fulfillment of the
Requirements for the Degree of

MASTER OF SCIENCE

In the School of Earth and Ocean Sciences

We accept this thesis as conforming to the required standard

[redacted]

Dr. B.D. Bornhold, Supervisor (School of Earth and Ocean Sciences)

[redacted]

Dr. C.R. Barnes, Departmental Member (School of Earth and Ocean Sciences)

[redacted]

Dr. E. Van Der Flier-Keller, Departmental Member (School of Earth and Ocean Sciences)

[redacted]

Dr. I.J. Walker, External Examiner (Department of Geography, University of Victoria)

Supervisor: Dr., Brian D. Bornhold

ABSTRACT

Diatomaceous sediments in piston cores retrieved from the Effingham Inlet inner and outer basins represent a complex history of episodic bioturbated intervals, turbidites, debris flows, and deformation structures set against a background of varved sedimentation. The turbidites initiated as slope failures and were characterized by either an abrupt transition from slump/slide blocks to fluid flow, or by liquefaction and flow of slope sediments. A combination of varve counting and AMS ^{14}C dating has allowed accurate dating of 24 turbidites over approximately 3,300 years of the inner basin record. Known earthquakes recorded by turbidites include the AD 1946 Vancouver Island earthquake and AD 1700 plate-boundary earthquake. Eleven turbidites over the past 2,000 years of the inner and outer basin record are contemporaneous. Comparison of the event history obtained here and a similar record from Saanich Inlet has yielded 8 contemporaneous slope failures over the past 1,500 years, despite a physical separation of 130 km.

Examiners:

[redacted]

Dr. B.D. Bornhold, Supervisor (School of Earth and Ocean Science)

[redacted]

Dr. C.R. Barnes, Departmental Member (School of Earth and Ocean Science)

[redacted]

Dr. E. Van Der Flier-Keller, Departmental Member (School of Earth and Ocean Science)

[redacted]

Dr. I.J. Walker, External Examiner (Department of Geography, University of Victoria)

Table of Contents

List of Tables

List of Figures

List of Appendices

Acknowledgments

This work was made possible through logistical support from the Geologic Survey of Canada's Pacific Geologic Centre (PGC), in Sidney, B.C. and with funding from an NSERC grant to Dr. Tim Patterson, Carleton University.

My thanks to the crew and shipboard scientific party of the C.C.G. John P. Tully, for my first taste of life (and science) at sea. I would like to thank my supervisor Brian Bornhold, for offering me the opportunity to pursue this Master's degree, for his constant support, and for acting as steady guide while granting me the freedom to forge my own, somewhat winding path through the research process.

A special thanks must go to my friends at the UVic POLIS Project and Eco-Research Chair, for I feel that completion of this thesis would not have been possible without their warmth and support, or the place to hang my hat during the final stages of writing -it was a privilege.

I am grateful to my parents for all they have fostered in me, and for their unending love and support, and to a crew of remarkable friends and housemates who are responsible for much that has made my time here truly enriching and meaningful. To Lauren especially, I extend my deepest gratitude for being a friend above all.

Lastly, I am indebted to Cadboro Bay for letting me share but a small portion of the old and incalculable ocean, and to a dog, Ella, for reminding me that rain or shine, a walk along the beach is a rare treat.

Frontispiece

Historical science is "a search for repeated pattern, shown by evidence so abundant and so diverse that no other coordinated interpretation could stand, even though any item, taken separately, would not provide conclusive proof." (Steven J. Gould, 1989).

1.0. Introduction

Annually laminated marine sediments of Holocene age offer an unparalleled record of global change and disruptive events of past millennia (Bull and Kemp, 1995; Kemp, 1996). Clearly, by extending records into the past we help shape the view of present global and regional processes (Francis and Hare, 1994). In southwestern British Columbia and the Pacific Northwest, a region collectively known as Cascadia, the historical record of earthquake activity is short (less than 130 years). Earthquakes have left geologic evidence that is helping extend this record, albeit incompletely, further into the past.

The seismicity of Cascadia is influenced by interactions of the Pacific, North America, and Juan de Fuca plates (Riddihough, 1977), and from internal deformation of the North American plate (Wells et al., 1988) (Figure 1). The North American and Juan de Fuca plates are presently locked and accumulating elastic strain -i.e. strain that will be released in a future plate-boundary or great earthquake (Rogers, 1988; Dragert and Hyndman, 1995). Geologic evidence for plate-boundary events is essentially of four types: (1) buried marsh and coastal soils produced by sudden, seismically induced subsidence; (2) sheets of sand and gravel deposited by tsunamis; and (3) clastic dykes and sand blows generated by liquefaction during strong ground shaking; and (4) continental margin turbidites triggered by shaking (for reviews see Atwater et al., 1995, Clague, 1996; Clague, 1997). These combined phenomena provide the strongest evidence of past earthquakes along the Cascadia subduction zone (Atwater and Hemphill-Haley, 1997).

a.

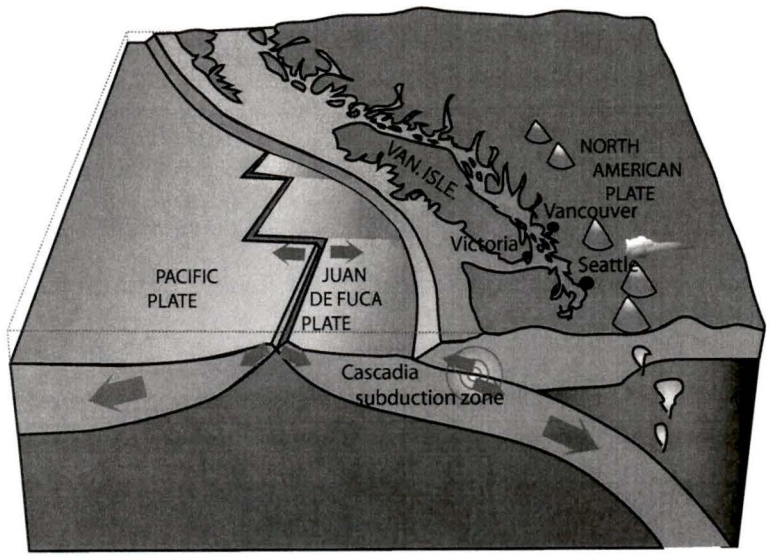

b.

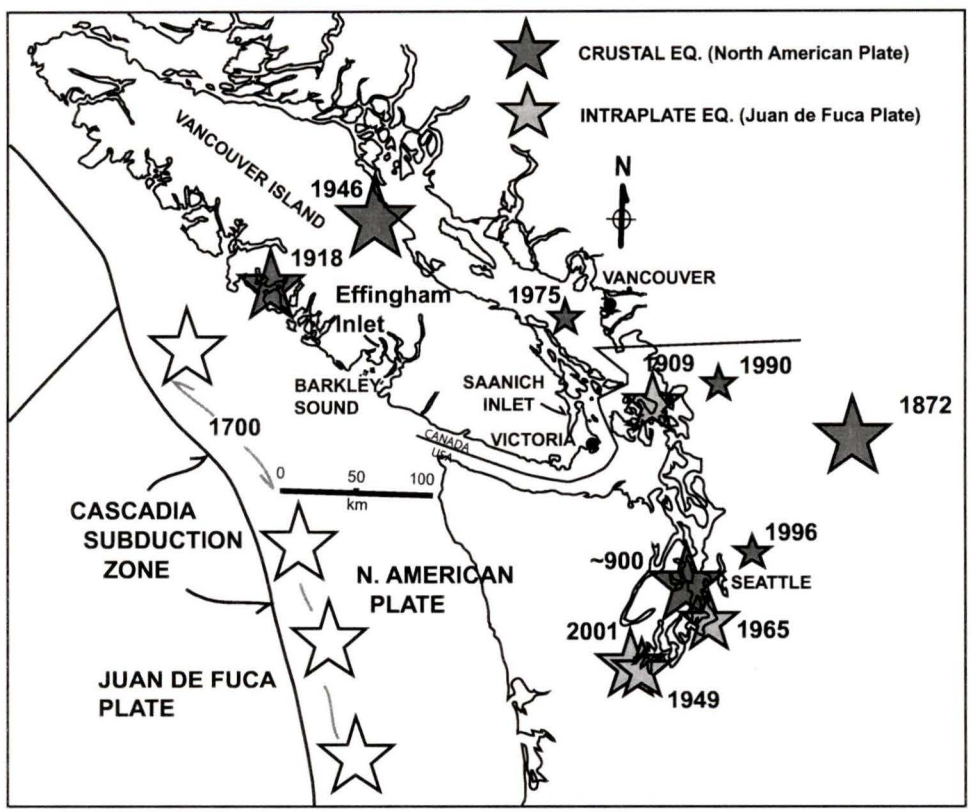

Figure 1. Tectonic setting and historical seismicity of southwestern British Columbia and northwestern Washington State. **a**. The oceanic Juan de Fuca plate is being subducted beneath the continental crust of North America along the Cascadia subduction zone - source of the "great earthquakes" (e.g. 1700 AD). Internal deformation and faulting of the North American plate and subducting Juan de Fuca plate also generates earthquakes. **b.** Significant historical earthquakes throughout the region. Deeper, intraplate earthquakes have tended to cluster around the Puget lowlands, while shallow, crustal earthquakes have occured throughout the region The largest stars indicate magnitude 7 or greater earthquakes, intermediate size stars indicate magnitude 6-7 earthquakes, the smallest stars indicate earthquakes of magnitude 4.5-6. (source: Geological Survey of Canada, 1999).

The amassed geologic and geophysical evidence has led to an improved understanding of the nature of the Cascadia subduction zone. Several key points are outlined below (Clague et al, 2000):

1. The Cascadia subduction zone produces great earthquakes, the most recent of which occurred in 1700 and was of moment magnitude (M_w) 9.
2. Most or all of the 1100 km long plate-boundary ruptured during a single event on January 26, 1700.
3. The sizes of earlier Cascadia earthquakes are unknown; the subduction zone may have failed piecemeal over periods ranging from a few hours to a few years, or the entire length may have ruptured at once.
4. Great Cascadia earthquakes generate tsunamis, the most recent of which was probably 10 m high along the Pacific coast.
5. Strong ground shaking from a M_w 9 subduction zone earthquake will last three minutes or more and will be dominated by long-period ground motions.

The mean recurrence interval for Cascadia great earthquakes is 500—600 years with intervals ranging from a few hundred to almost one thousand years (Adams, 1990; Atwater and Hemphil-Haley, 1997). However the recurrence intervals are poorly constrained and no pattern has yet emerged.

Although no plate-boundary earthquakes have struck Southwestern British Columbia during historical time, the region experiences over 200 crustal and intraplate earthquakes a year, making it Canada's most seismically active region (Rogers, 1998). Most earthquakes are too small to be felt, however, ten moderate to large earthquakes (moment magnitude, M_w 6-7) have occurred within 250 km of Victoria and Vancouver

over the last 130 years (Rogers, 1998). This record of seismicity is short and may misrepresent the actual seismic hazard for the region (Clague, 1999). Geologic evidence for moderate to large crustal or intraplate earthquakes (i.e. earthquakes occurring *within* the North American or Juan de Fuca plates, respectively) is less abundant in the record (e.g. Clague et al., 1992; Mathewes and Clague, 1994; Adams, 1992, and ref. therein; Bourgeois and Johnson, 2001), however their potential for damage is quite large, especially if centered near populated areas (Clague, 1999). Despite their destructive potential, these types of earthquakes typically do not leave abundant and "strong" geologic evidence, such as that left by the larger plate-boundary earthquakes (e.g. land subsidence, tsunami deposits etc.). In order to gain a more complete picture of the seismic hazard for the region, the problem remains: is there geologic evidence sensitive enough to record these moderate to large events?

Subaqueous slumping, turbidites and sediment disturbance structures have long been associated with earthquake activity (Heezen and Ewing, 1952) and have therefore been used as paleoseismic tools (Sims, 1975; Adams, 1990; Doig, 1990; Gorsline, 1996; Inouchi et al., 1996; Karlin and Abella, 1996; Gorsline et al., 2000; Nakajima and Kanai, 2000; Blais-Stevens and Clague, 2001). Lacustrine basins lend themselves to paleoseismic studies as they hold continuously deposited sedimentary records that may be punctuated by seismically triggered events. Recent work in Swiss lakes is linking small-scale deformation structures in varved lake sediments (Monecke et al., 2001) as well as large slump deposits (Schnellmann et al 2001) to paleoseismic activity in the Swiss Alps. Holocene sediments from Lake Washington contain many episodic turbidites deposited throughout the lake as a result of slumping of the steep walls (Karlin and Abella, 1996).

The unequivocal identification of a "coseismic" origin for geologic phenomena remains critical in paleoseismic studies (Vittori et al., 1991). While it remains difficult to determine whether slope failures in subaqueous environments are coseismic or nonseismic in nature, many can be linked convincingly to past known earthquakes (e.g. Inouchi et al., 1996; Karlin and Abella, 1996; Blais-Stevens and Clague, 2001). However, there remains a collective unease with linking mass wasting to earthquakes since a direct causal relationship can usually not be confidently established, as indeed it can be with evidence of land-level change, tsunamis or liquefaction. Seismic activity need not be the only plausible explanation for the generation of turbidites in a particular setting. In order to determine whether mass wasting "events" were coseismic, or not, all other possible nonseismic mechanisms must be ruled out. The generic term "event" is often used in order to connote uncertainty in judgement of a triggering mechanism.

Each type of paleoseismic evidence has its own set of advantages and disadvantages in terms of the length and resolution of record, ease and accuracy of dating, and strength of the coseismic link. Geographically widespread and contemporaneous failure events offer quite compelling evidence of a seismic trigger (Blais-Stevens, 1995 and Blais-Stevens and Clague, 2001), especially when the setting in question precludes other possible triggering mechanisms, such as storms, wave action, or slope oversteepening. The precise dating of geological events over widespread areas forms the crux of any paleoseismic study yet the uncertainties can be greatly reduced in settings where annually-laminated or varved sediments accumulate.

Paleoseismicity from varved sediments

Given the difficulty in obtaining precise dates for prehistoric earthquakes from the many coastal settings along Cascadia, paleoseismic evidence is being sought that offers high temporal resolution. A continuous, high-resolution record of past seismic events compiled from several locations would be a valuable contribution to seismic characterization and hazard assessment of the region. The varved marine sediments of Saanich Inlet, an anoxic fjord in southern Vancouver Island, have been perceived increasingly as a potential high-resolution record of past earthquakes (Bobrowsky and Clague, 1990; Blais 1995; Blais-Stevens et al., 1997; Bornhold, Firth et al., 1998).

Late Holocene sediments from the Saanich Inlet central basin consist of fine-grained, diatomaceous varved sediments, punctuated by event beds attributed to "debris flows" (Blais, 1995). Earthquakes likely triggered debris flows along the sides of the elongate basin; while the background varved sedimentation which blanketed the deposits served to date accurately each flow. The varve-based chronology in Saanich Inlet was extended to include most of the Holocene following the Ocean Drilling Program (ODP) Leg 169S (Bornhold, et al, 1998; Blais-Stevens and Clague, 2001; Nederbragt and Thurow, 2001). It was argued that the debris flows were likely coseismic since discrete failures had occurred at the same varve horizon at various sites along 15 km of the basin axis. In addition, varve counting and biomarkers placed the age of several flows close to that of known large earthquakes (Blais-Stevens and Clague, 2001). Most of the debris flows in the ODP Leg 169S cores could be matched between disparate sites and their ages determined through image analysis (Nederbragt and Thurow, 2001) and manual varve counting (Blais-Stevens and Clague, 2001).

The event chronology established from the Leg 169S cores from Saanich Inlet record must now be compared, if possible, to other such records in the area, in order to further test the proposed regional earthquake history generated from Saanich Inlet. Several fjords and former fjords (now meromictic lakes) along the west coast of Vancouver Island and the mainland are characterized by anoxic deep basins due to the presence of sills. Laminated sediments or varves are being deposited in these basins due to anoxia, the exclusion of benthic burrowing organisms and seasonally driven sedimentation. Effingham Inlet, an anoxic fjord on the west coast of Vancouver Island, was chosen for a paleoseismic study because of its varved sediments, its sedimentological and morphological affinities to Saanich Inlet (130 km to the southeast) and its proximity to the plate-boundary earthquake zone (90 km to the west).

Study Area - Effingham Inlet

General setting

Effingham Inlet is a 17-km long fjord, mostly less than 1 km wide, that opens into the Imperial Eagle Channel portion of Barkley Sound on the west coast of Vancouver Island (Figure 2). During the last glacial maximum, piedmont glaciers scoured Barkley Sound, Effingham Inlet and the adjacent inlets (Herzer and Bornhold, 1982). The fjord cuts into steep and forested slopes of the Coastal Mountains that rise more than 1000 m above the waters of the inlet. The region immediately to the southeast is underlain by basaltic extrusives and intrusives of the Upper Triassic Vancouver Group as well as by tuffs of the Lower Jurassic Bonanza Group (Yorath et al, 1999). Plutonic and intrusive rocks of

intermediate to mafic composition from the West Coast Crystalline complex are also distributed throughout the area.

Due to the presence of sills, the inlet can be subdivided into inner and outer basins that have maximum depths of approximately 150 m and 200 m respectively (Figure 2, Figure 3). Laminated sediments are preserved in the deeper portions of these basins due to anoxic bottom water and the virtual exclusion of benthic organisms. Terrigenous sediment input is derived from the fjord-head Effingham River as well as from several side-entry streams that are building fan deltas into the fjord. As a result of high annual rainfall in the area, many ephemeral streams present all along the fjord walls likely contribute small amounts of coarse sands and gravels, and organic litter to the nearshore environment, as has been observed in other B.C. fjords (Prior and Bornhold, 1988). Two streams discharge directly into the outer basin, three discharge near the head of the inlet, while none discharges directly into the inner basin proper.

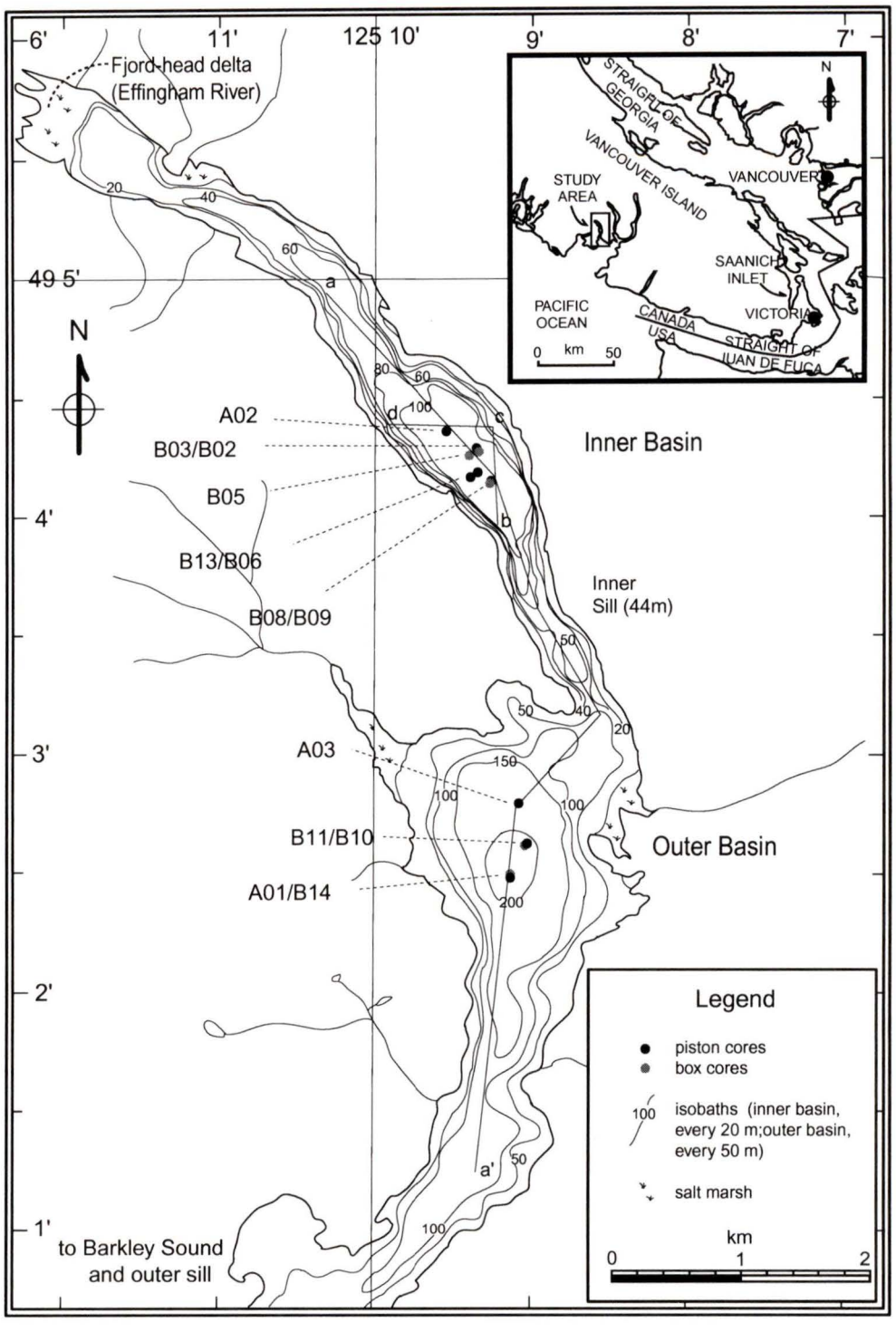

Figure 2. Effingham Inlet: bathymetry and core locations. Chart of Effingham Inlet showing position of basins, sills, piston cores (black dots), and box cores (grey dots).

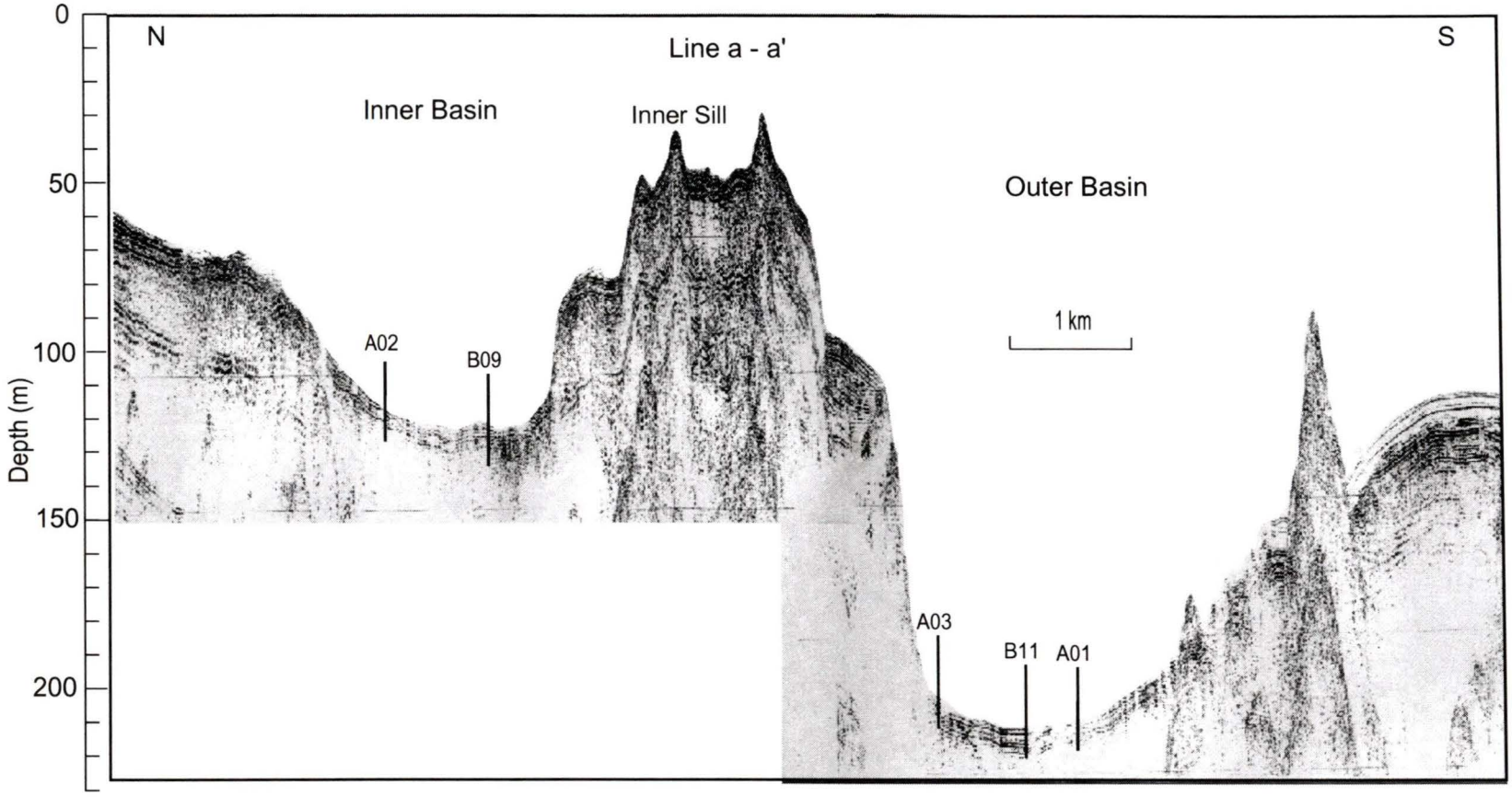

Figure 3. Seismic profile a-a' through the inner basin showing piston cores located along ship track. Note that sediment drape along the inner basin axis is dominantly from the direction of the head river; sediment drape along the outer basin axis is dominantly from the direction of the outer sill. (See Fig. 2 for location).

Oceanography

Distinct oceanographic conditions are responsible for much of the scientific interest in the varved sediments of Effingham Inlet. Restricted circulation due to the presence of sills, combined with high surface productivity and sedimentation rates lead to persistent anoxia in the deeper portions in the inlet. Seasonally driven sedimentation, i.e., a bimodal sediment source (Grimm et al., 1996) of diatoms and terrigenous material produces seasonal laminae or varve couplets. This picture is, of course, a simplification, due to the dynamic interplay of climate, ocean conditions, and sediment supply through time.

Marked variability in water property structure along the inlet arises due to seasonally changing wind-induced mixing, surface heating and cooling, local runoff, and coastal upwelling (via Barkley Sound). Tidal forces in the inlet are small and tidal currents are weak, except in the vicinity of the shallow sills where some degree of constriction exists. A series of sills present along the length of Effingham Inlet restricts ocean circulation and subdivides the deeper portions into *inner* and *outer* basins. The inlet is stratified with respect to temperature and salinity: surface waters are relatively cool and fresh; bottom waters are relatively cool and saline; middle waters are relatively warm with intermediate salinity. The inner basin is about 150 m deep and has anoxic bottom water conditions that inhibit bioturbation of sediment and that ideally, allow the preservation of annual layering or varves. The outer basin is about 200 m deep and has somewhat more oxygenated bottom waters with less ideal preservation of laminae. Two representative water property profiles, for the inner basin (Figure 4) and outer basin

(Figure 5), show the vertical oxygen concentrations, water transmissivity (a measure of clarity), and temperature.

The position of Effingham Inlet immediately adjacent to the Pacific coastal upwelling zone bears on the stability of anoxia in the basins through time. Dense, oxygenated water, periodically upwelled along the coast can enter the inlet and temporarily displace anoxic basin water. Anoxic water masses persisted through 1995-1998, although surveys made from the fall of 1998 to the fall of 1999 showed that dense, oxygenated water had entered both basins, displacing stagnant, deep water (R. Thomson, 1999, Department of Fisheries and Oceans, unpublished data). However, by early 2000, oxygen in this water had been largely depleted due to the ongoing decay of organic matter.

Basin flushing, like that observed in 1999, is essentially governed by the strength and timing of two main forces; (1) density stratification within the inlet and (2) northwesterly winds, leading to upwelling along the coast. Density stratification, and estuarine circulation, are most pronounced during times of high river runoff. Discharge along the west coast of Vancouver Island is tied to rain events, which are more frequent in the fall and winter, although snow melt can provide additional runoff during the spring. Persistent moderate to strong northwesterly winds along the coast of Vancouver Island lead to upwelling onto the shelf of high-density, low-oxygen (1-3 ml/l) water that may be dense enough to displace the basin water in Effingham Inlet. The moderate to low oxygen content of upwelled water is due to its origin in the oxygen minimum zone off the continental margin. Because moderately augmented re-oxygenation of the basins may lead to increased benthic activity and potentially, to bioturbation of the sediments, an

understanding of the oceanographic and climatic forces at play in Effingham Inlet is essential for an informed interpretation of the varved, and non-varved record.

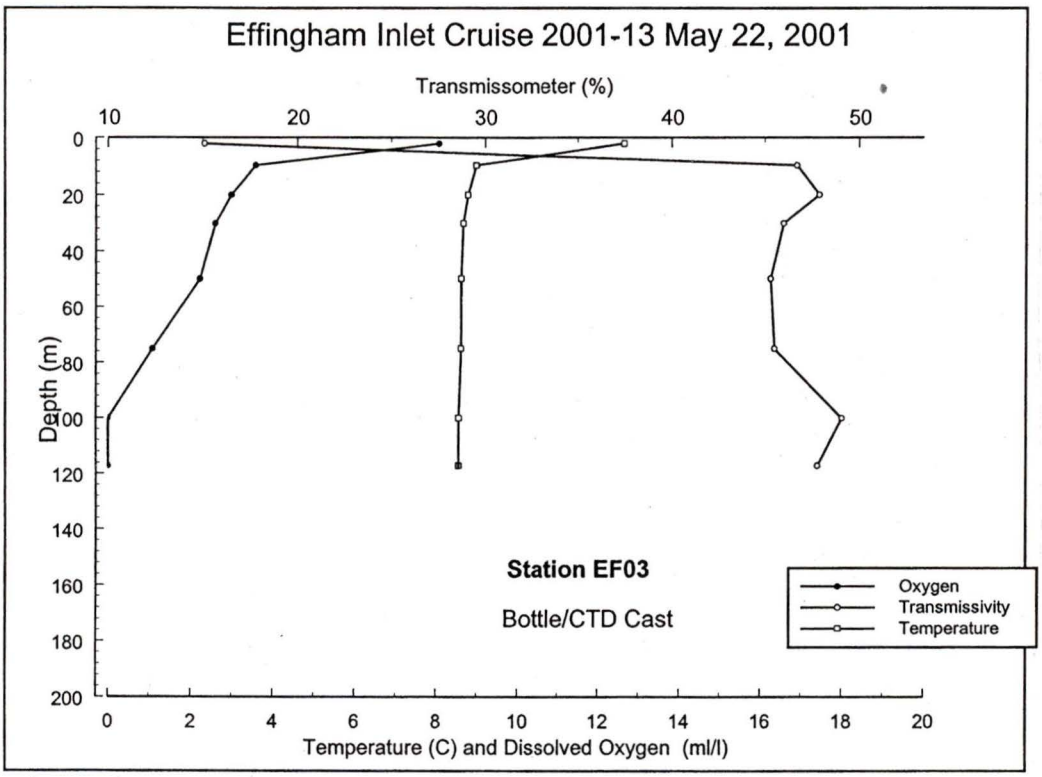

Figure 4. Water property structure of Inner Basin

Dissolved oxygen transmissivity, temperature profile from the Inner Basin of Effingham Inlet during the spring of 2001, at a station located in the centre of the inner basin. Dissolved oxygen level reached zero at about 100 m depth. (Data courtesy Dr. R. Thomson, DFO)

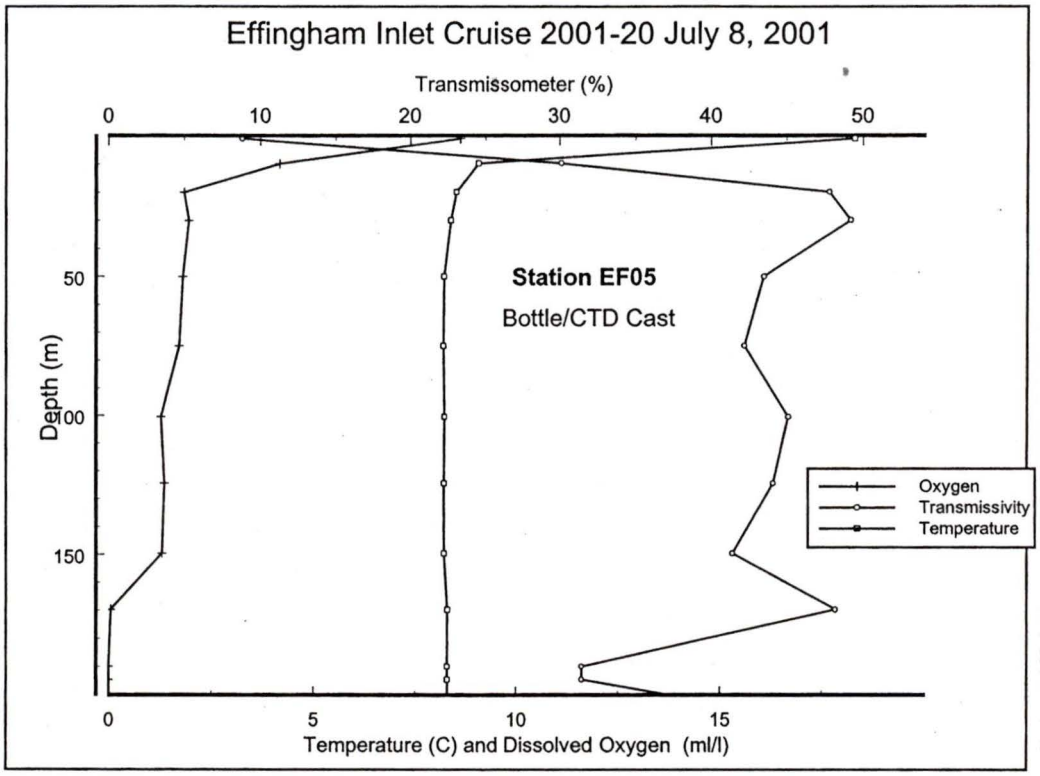

Figure 5. Water property structure of the Outer Basin.

Dissolved oxygen transmissivity, temperature profile from the Outer Basin of Effingham Inlet during the summer of 2001, at a station located in the centre of the outer basin. Dissolved oxygen level reached zero at about 170 m depth. (Data courtesy Dr. R. Thomson, DFO)

2.0. Materials and Method

The sediments of Effingham Inlet were cored in 1997 and 1999 aboard the C.C.G. John P. Tully. Three piston cores were taken in 1997 using a 6-cm diameter by 9 m long ship-mounted coring device. In 1999, an additional 5 piston cores were taken using a 10 cm diameter by 11 m long device. Box and freeze cores were also obtained in order to ensure that the uppermost water-saturated sediments were recovered. Figure 2 shows the distribution of cored sites throughout the inlet. Shipboard 3.5 kHz and air-gun seismic surveys were conducted during each cruise in order to highlight target locations that appeared undisturbed and relatively free of gas. Sediment from the piston cores was contained in plastic inner liners that were sectioned into 1.5 m lengths while on board. Upper, water-saturated core sections were stored upright for up to two months following the cruise so that some degree of dewatering and consolidation could occur. The cores were then eventually split longitudinally by electric saw and steel wire in the laboratory. This produced working and archival core halves that were kept in sealed plastic D-tubes and stored at the Pacific Geoscience Centre (PGC) in Sidney B.C..

Table 1. Core Locations

Core Identification	Core Type	Location	Water Depth
		Inner Basin	
	Piston Cores		
TUL97A02		49 04.360 125 09.540	100 m
TUL99B03		49 04.275 125 09.359	120 m
TUL99B06		49 04.188 125 09.337	121 m
TUL99B09		49 04.145 125 09.279	122 m
TUL99B13		49 04.173 125 09.401	122 m
	Freeze Cores		
TUL99B01		49 04.269 125 09.399	119 m
TUL99B04		49 04.218 125 09.429	120 m
TUL99B07		49 04.145 125 09.337	121 m
	Box Cores		
TUL99B02		49 04.277 125 09.334	118 m
TUL99B05		49 04.266 125 09.417	120 m
TUL99B08		49 04.145 125 09.279	122 m
		Outer Basin	
	Piston Cores		
TUL97A01		49 02.480 125 09.130	200 m
TUL97A03		49 02.790 125 09.090	
TUL99B11		49 02.632 125 09.023	205 m
	Freeze Cores		
TUL99B10		49 02.642 125 09.043	205 m
TUL99B12		49 02.632 125 09.023	205 m
	Box Cores		
TUL99B14		49 02.495 125 09.127	204 m

Detailed descriptions of the piston and box cores were carried out at the Pacific Geoscience Centre in Sidney, B.C.. Sedimentological textures, thickness and internal structure of the sedimentary units were described from visual analysis of core and x-

radiographs of core. X-radiographs of half cores and subsampled (slabbed) material were taken at a local veterinary hospital. Stratigraphic marker beds used for correlation were pinpointed and assessed visually by laying out core half-sections side by side in the lab or by comparison of x-radiographs. These included turbidite beds as well as distinctive thickness and colour patterns in the laminae. Manual varve counting from core and x-radiographs was performed several times on each core to check for repeatability of the counts. Sedimentary horizons that were represented in every core were employed to match cores and to elaborate the varve chronology.

The Institute of Ocean Sciences (IOS) in Sidney, B.C., has been monitoring the spatial and temporal variability of oceanographic conditions in Effingham Inlet and adjoining Barkley Sound through shipboard profiling, and using moored instruments under the direction of Dr. Richard Thomson (IOS). Profile data are derived from Conductivity-Temperature-Depth (CTD) probe, a transmissometer, a flourometer, and a 24-Niskin bottle rosette sampler for measuring concentrations of oxygen, nutrients, and other dissolved constituents taken at several stations along the axis of the inlet. Profile data span the period of 1995 to 2001 (13 surveys) while data from sediment trap and current meters have been collected from 1998 to 2000.

Accelerator Mass Spectrometry (AMS) ^{14}C dating of wood, shell and fish bone samples was conducted at the University of Toronto Isotrace Laboratory. Calendric ages were calibrated to the Holocene ^{14}C temporal scale using the program CALIB v.4.3, developed by Stuiver and Reimer (1993). and Stuiver and Reimer (2000). Radiocarbon dates from marine material were adjusted using the combined global and local reservoir correction of R = 801 +/- 23 (Robinson and Thompson, 1981; Stuiver and Braziunas,

1993). By convention, radiocarbon dates quoted in the literature as "BP", imply an age in "*calendar years before 1950 AD*". However, in this study, to avoid confusion between the varve chronology and radiocarbon dates, all ages given as "y BP", whether varve-derived or ^{14}C-derived, are *calendar years before 2000 AD*, unless otherwise stated. To ease comparison with other paleoseismic studies, radiocarbon and varve ages quoted hereafter have also been converted to this "2000 AD" format..

3.0. Results

3.1. Sedimentology

Inner Basin

The sediments retrieved in cores from the inner basin of the inlet comprise laminated to non-laminated, olive-coloured, diatomaceous silts. The sediments are >95 wt.% silt-sized (mostly diatoms and lithic particles) although some gravity flow deposits have sand content up to 14 wt.% (Dallimore, 2001). Clay content is low (<1%) while organic carbon content is high (5 wt.%) with a high percentage of the carbon derived from terrestrial sources (Dallimore, 2001).

Seismic profiles of the inner basin show preferential draping of sediments along the western side (Figure 6). Average sedimentation rates, calculated from varve thicknesses in core, also reflect the preferential sedimentation along the western margin; B06 and B13 on the western side, have the highest average sedimentation rates (2.8 mm/a), while B03 close to the eastern side has the lowest (2.2 mm/a) (see Figure 12 for a full description of sedimentation rates). Given that the diatom bloom forms the bulk of the annual sediment flux, this may be due to preferential circulation patterns in surface waters containing suspended sediment that force diatom blooms to the west in the inner basin. This may be either brought about by a dominant local wind stress pattern, or by tidal eddying in the inner basin.

Textural variations in sediments from the inner basin of Effingham Inlet were based on visual analysis of archived core halves as well as x-radiographs of core halves and sub-sampled slabs. Although frequently gradational in nature, the sedimentary structures of these sediments were divided into five general categories: *laminated*;

indistinctly laminated to *non-laminated*; *gravity flow units; deformed strata*; and *thin sandy beds*.

Laminated sediment

Although variable in character, the laminated intervals consist of alternating light-coloured laminae (composed of diatoms) and darker laminae (composed of lithic particles) (Figure 7). The light-dark couplets average about 2.7 mm in thickness in the inner basin, with the light (diatom) portion comprising most of the couplet material. The laminae reflect the seasonal changeover in sedimentation in the inlet - spring-summer diatom blooms lead to the light-coloured laminae while fall-winter pluvial runoff produces the dark-coloured terrigenous laminae, similar to varves in Saanich Inlet (Sancetta, 1989). The laminae couplets are annual in nature and can be called varves. Uninterrupted varved intervals range in thickness from a few cm's to 60 cm.

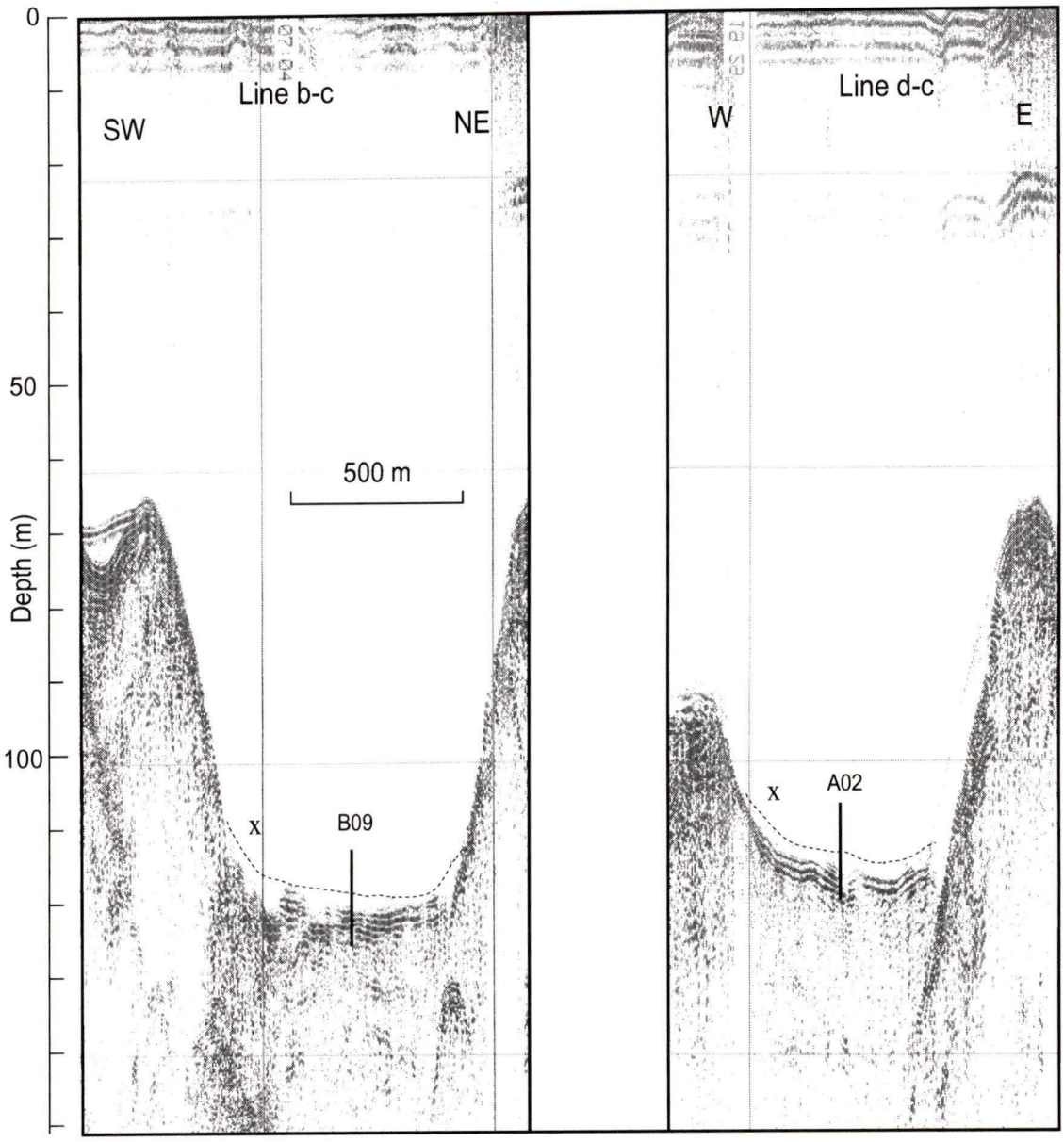

Figure 6. Seismic profiles b-c and d-c through the inner basin showing piston cores located adjacent to track (See Figure 2 for location). Note, line d-c is essentially perpendicular to the basin axis . Sediment draping the western sidewall, on the lefthand side of each basin sweep (x) is thought to be the source slope for many of the failures in the inner basin. Dashed line highlights a faint sediment-water interface.

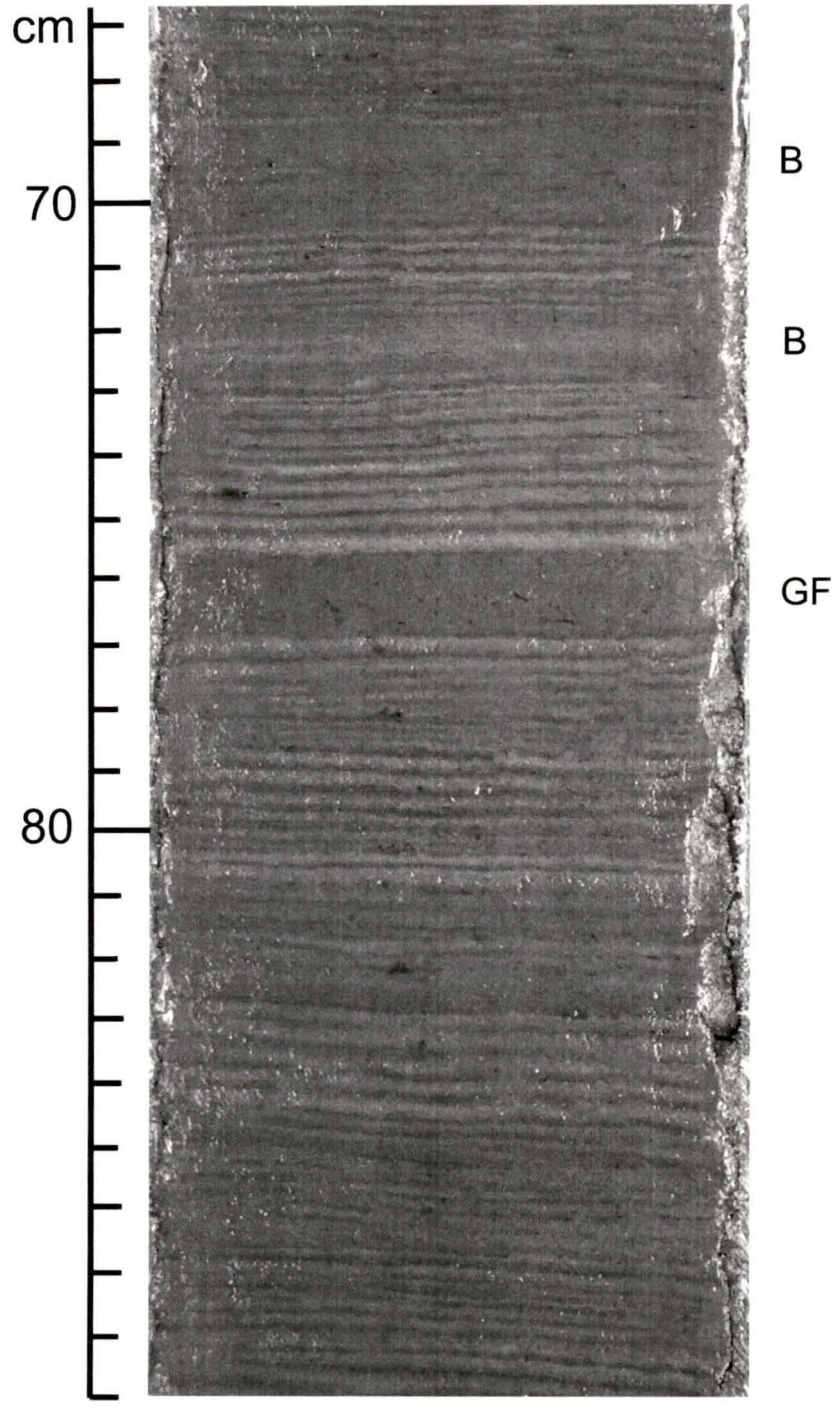

Figure 7. Photograph showing characteristic laminated diatomaceous mud from the inner basin of Effingham Inlet. Pale laminae are diatom ooze and diatomaceous mud; darker laminae are terrigenous silts. Laminae style is variable in character and interupted by one distal gravity flow (GF), and two short intervals of bioturbation (B). (TUL99B09 - Sec. 7: 67-89 cm)

Indistinctly laminated to non-laminated units

In addition to varves, many faintly laminated and entirely non-laminated intervals are distributed throughout the Effingham inner basin cores at all sites. Units comprising wavy, discontinuous or faint laminae, or homogeneous pelleted mud with faint internal laminae are interpreted as bioturbated sediment (Figure 8). Faint mottling seen in x-ray images is also evidence of burrowing. Bioturbated horizons comprise sharp tops and diffuse bases, often with faint internal laminae with thicknesses ranging from as little as one centimetre to as much as 25 cm at some sites. Rare burrows take the form of 2-3 mm, sub-horizontal traces that truncate or cross-cut laminae. Laminae may appear blurred or have indistinct boundaries.

Clearly defined, classical burrows are not seen within or below the homogeneous intervals. The internal texture of the individual bioturbated intervals is not consistent core to core, reflecting the spatial variability in the extent of destruction of laminae at each site. Faint laminae seen in x-ray are remnants of laminae within a bioturbated interval and attest to the 3-dimensional variability in microsite destruction by small (mm-scale) burrowing organisms (De Diego and Douglas, 1989). Pelletized material is likely an indication of small, deposit-feeding organisms disrupting the laminated sediments (Savrda and Ozalas, 1993; Brodie and Kemp, 1994).

Discussion

Fabrics in organic-rich muddy sediments are related to seafloor oxygenation, which controls the activity of macrobenthic organisms (Savrda and Bottjer 1991; Bottjer and Savrda, 1993, De Diego and Douglas, 1999). Bioturbated beds in laminated

sediments typically consist of two parts: so-called "primary strata", consisting of thoroughly homogenized sediment, and an underlying "piped zone", consisting of recognizable burrow tubes that cross-cut previous laminations (Ozalas et al., 1994, and ref. therein). Unequivocal vertical traces (i.e. piped zones) were not observed below the homogeneous beds in inner basin cores, however, benthic macrofauna in this setting are not expected to be great in size or particularly diverse, and likely could not penetrate anoxic sediments due to persistent hydrogen sulphide. Horizontal traces and wavy laminae are consistent with depleted oxygen (>0.1 ml/l) and a redox boundary just below the sediment-water interface (De Diego and Douglas, 1999). The sharp tops found in the bioturbated zones are consistent with abrupt termination of the macrobiological activity precipitated by a return to anoxia.

Thickness of the bioturbated interval and nature of the laminated/bioturbated transition are strongly influenced by diversity and size of the macrobenthos (Savrda et al. 1984; De Diego and Douglas, 1999). Basin centre benthic organisms are expected to be sparse and possibly limited to small polychaetes, whereas the edges might support larger and more diverse organisms (Savrda et al., 1984). Consequently, bioturbation (substrate colonization) potential and burrow size are anticipated to be greatest at the basin edges. Paradoxically, in Effingham Inlet, the shallowest inner basin core (97A02) shows the least disturbance by bioturbation. This site is however the furthest from the sill, suggesting that oxygenated water may not always reach it during a renewal event. A similar arrangement was seen in Saanich Inlet whereby cores closest to the sill had a higher incidence of indistinctly laminated sediment, i.e. bioturbaton (Blais-Steven et al, 1997; Bornhold et al, 1998).

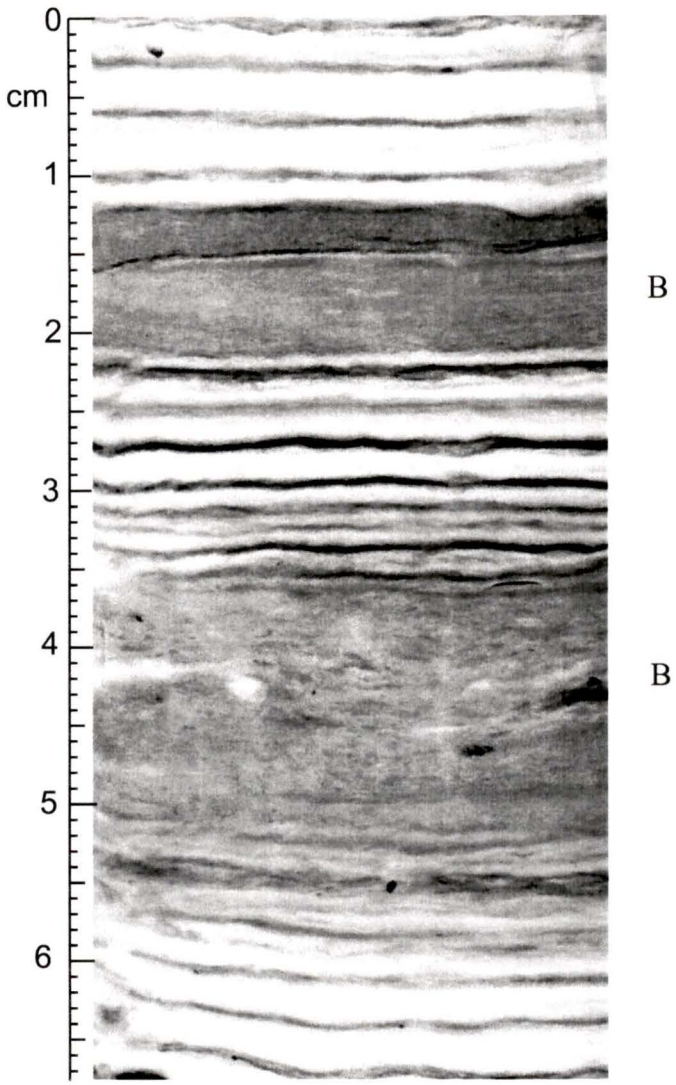

Figure 8. X-radiograph of core "slab" showing well defined laminae interrupted by bioturbated zones (B). Bioturbated sediment in Effingham Inlet comprises mottled, pelleted mud, disrupted or faint laminae, and rare, mm-scale sub-horizontal burrows that cross-cut varves. Lower zone represents 10-12 years of quasi-annual reoxygenation; upper zone represents about 5 years. From TUL99B03, sec. 4, 480 cm.

Large burrowers might explain some of the thick (>10cm), non-laminated intervals found in cores, however large traces and piped zones are absent from the sediment. In this respect the bioturbated zones from Effingham Inlet sediment resemble Monterey Formation "type IV" beds of Ozalas et al. (1994) (their figure 8). The absence of piped zones in these beds reflects the absence of deep burrowers that would leave such traces, possibly related to the magnitude and duration of the oxygenation period. Perhaps only small, rapidly reproducing organisms or juveniles have time to colonize substrates before anoxic conditions return. Given that the oxygenation in Effingham Inlet has been observed as intermittent, of short (several months maximum) duration, and of moderate to low O_2 levels (R. Thomson, pers. comm.), it is hardly surprising that larger organisms could not colonize basin substrates. Nor is it surprising that the 20th century record shows no sign of bioturbation, despite the occurrence of intermittent flushing. These findings eliminate the possibility that short-term (sub-annual) oxygenation led to thick bioturbated "events" seen in the pre-20th century record. The ichnology of Effingham Inlet sediments, therefore, only supports quasi-annual and short-lived oxygenation events, repeated over decadal time scales, followed by many decades of anoxia. This appears to corroborate the oceanographic data although events not represented in the modern (post-1946 AD) record are possibly responsible for older oxygenation-bioturbation "events".

In addition to flushing, the 1999 renewal event recorded in Effingham Inlet was accompanied by increased upper water-column turbidity (R. Thomson pers. comm.) and it has been hypothesized that, once settled out of suspension, the mud could lead to homogeneous, >10 cm ungraded beds (Dallimore, 2001). At present, it is not known whether the 1999 turbidity had any expression on the seafloor in terms of increased

deposition. However, the water column turbidity of a single event would likely not contain the equivalent of several decades worth of sediment at normal sedimentation rates. No evidence exists that the currents that accompany flushing events have the strength to erode sediments at depths greater than the sills, and there is no sedimentary evidence that turbidity currents are generated from the sill during flushing events. There is also no evidence from the varve counts and radiocarbon dates that would suggest that the bioturbated intervals represent times of higher sedimentation rates due to increased sediment supply. Given the high volume of precipitation experienced along Canada's Pacific coast in 1999 (5^{th} wettest year overall, Environment Canada, 1999), the most plausible explanation for the upper water-column turbidity observed in 1999 may in fact be that it was derived from the rivers and not the sill.

Further complicating the interpretation of the evidence for bioturbation in Effingham Inlet sediments is the possibility of variations in the relative amounts of terrigenous and biogenic sediment supplied to the basin. Bioturbation alone may be an unsatisfactory explanation for horizons that exhibit no internal fabric that intergrade with laminated sediments or that contain very faint, yet visibly undisturbed, laminae. Horizons lacking definitive evidence for redeposition or biological reworking in anoxic hemipelagic sediments from the Santa Barbara Basin may have arisen out of variations in the "bimodality" (seasonality) of sediment supply (Grimm et al., 1996). In a coastal fjord such as Effingham, normal seasonality of sedimentation may be absent or partially masked if spring-summer runoff is unusually high; the resultant terrigenous flux may dilute the spring-summer diatom bloom.

In a study of two fjords, (Saanich and Jervis inlets), Sancetta (1989) determined that mass flux to the sediments is primarily controlled by the seasonal cycle of diatom production, with terrigenous particles from runoff contributing only a background signal. However suppression of the bloom may occur if large volumes of runoff are introduced to the inlet during the spring and summer. This is the case in Jervis Inlet, an oxygenated, mainland fjord where meltwater, as opposed to rain precipitation, controls discharge. In contrast, terrigenous flux in Saanich and Effingham inlets is primarily controlled by pluvial events which are most abundant throughout the fall and winter (Sancetta, 1989, and references therein; Dallimore, 2001).

The mountains present in the Effingham River catchment basin may introduce an additional variable, snowmelt freshet, into the Effingham Inlet system. The end result for the nature of the annual laminae is uncertain. Meltwater runoff in spring may provide a negative feedback to varve preservation through distortion of the annual sedimentation regime, or through augmented flushing potential, due to its possible role in establishing stratified water structure within the inlet ahead of summer upwelling conditions. Results from ongoing monitoring of *in situ* sediment fluxes will greatly improve our understanding of the dynamics of the inlet. Given the surrounding physiography, position along a coastal upwelling zone, and small size, Effingham Inlet is probably a more complex system in terms of its climate-sediment dynamics than is Saanich Inlet.

Implications for past ocean conditions

The interpretation of thick (5-15 cm), extensively bioturbated or entirely homogeneous mud units in the older record from the piston cores (i.e. pre-1946 AD) is problematic, because 15 cm of sediment, at normal sedimentation rates, might represent 60 varve years. Does this represent one or two years of oxygenation that led to the destruction of 60 years worth of varved sediments, or does this represent the destruction of laminae during near-annual oxygenation events occurring over a 60 year period? Potentially analogous bioturbation of previously laminated sediments is presently occurring within the Alfonso Basin and the oxygen minimum zone of the Santa Rosalia slope, in the Gulf of California. Bioturbation has disturbed only the topmost 4-8 cm of sediments with the onset of the modern oxygenation-bioturbation cycle determined to be circa 1969 -1973 AD (De Diego and Douglas, 1999). Thirty years of intermittent yet persistent re-oxygenation has produced only minimal disturbance of the uppermost sediments. In the Santa Barbara basin, sub-annual oxygenation events are insufficient to permit complete bioturbation, and laminations (varves) are well preserved in the Holocene record (Soutar and Crill, 1977), yet marked variability still exists in the extent of bioturbation or "bioturbation index" of these sediments (Behl, 1995; Behl and Kennett, 1996).

It is clear from modern oceanographic monitoring that Effingham Inlet can readily be flushed with moderately oxygen-rich waters during times of coastal upwelling and strong estuarine circulation. However, the oxygenation in the deep basins is short-lived and of moderate oxygen concentration - high sedimentation rates and high organic content quickly return the basins to anoxia. It is arguably impossible for a fauna of

impoverished, millimetre-sized polychaetes, bivalves and crustaceans to reproduce, colonize and homogenize a bed 5-cm thick over the entire basin in the space of a few months. At most, the topmost varve couplet might be disrupted in any given oxygenation event. The 1999 cores were taken during full oxygenation of the inlet and after several renewal events had occurred over the course of the preceding year, and no evidence of bioturbation can be seen in the freeze cores. Nor is any dramatic disturbance seen from the varve years of 1946 to 1998 that could be attributed to biological activity.

This raises the interesting possibility that the thick bioturbated intervals in the pre-20-century record may represent many years or even decades of repeated, annual or quasi-annual oxygenation of the inlet. Oxygenation of the inlet is augmented by upwelling off the west coast as deep, dense water is brought to shallow coastal waters. Upwelling of deep, cold water is set in motion during times of persistent, moderate to strong northwesterly winds which are common in the summer along the west coast of Vancouver Island. Northwesterly winds during fall storms may also be sufficient to induce upwelling.

A key factor in basin flushing appears to be the timing and duration of sustained fresh water runoff. High runoff stratifies the upper layers of the inlet and diminishes vertical mixing, allowing for enhanced estuarine circulation that may bring compensatory, dense water masses over the sills and into the basins. On Vancouver Island, the fall and winter are peak times for runoff while northwesterly wind and upwelling are most prevalent during spring and summer. Requisite northwesterly winds can be produced by fall storms, however these do not occur frequently. Upwelling and high runoff can coincide in spring when strong northerly winds are present and when the

preceding winter had high snowpack. The most compelling link between high snowpack and basin flushing may be the 1999 La Ni a event when Vancouver Island had the thickest June snowpack in recorded history (Bryant, 1998; 1999) *and* when the basins underwent extensive flushing (R. Thomson, pers.comm.).

Given that the upwelled water that reaches the inlet is derived from the oxygen minimum zone (OMZ), at a depth of 300 -500 m off the continental shelf, it is difficult to explain how such relatively low oxygen content water could lead to significant re-oxygenation and benthic activity in the inlet. Low-oxygen water masses would rapidly decay in the inlet due to high sedimentation rates and the ongoing decay of sedimentary organic matter. There are three ways that dense, high-oxygen content water could arrive at the inlet:

- If upwelled water is mixed at the surface by wind stress, oxygen contents would be augmented however density would diminish. In order for the mixed water masses to remain dense enough to sink into the basins, marked cooling of surface waters must occur. This could occur at a quasi-annual frequency only if climatic conditions were much colder than today's, or if the region experienced a series of very severe winters.
- If very strong, sustained northwesterly winds are generated, moderately to well oxygenated dense water from *below* the level of the present-day OMZ (i.e. below 500 m) may be brought onto the shelf. It is not clear how this type of upwelling could occur consistently over several years on the west coast of Vancouver Island.

- Through changes in ocean *productivity*, the level, location and intensity of the OMZ off the west coast of North America may have fluctuated over the late Holocene; or through changes in *circulation* the age and level of oxygenation of Pacific Intermediate Water may have fluctuated. This would then be reflected in the oxygen contents of water upwelled onto the shelf off Vancouver Island on an annual basis, and on the potential for increased oxygenation of inlet waters.

While all three mechanisms remain speculative, the third option is the most intriguing since it is perhaps the only way to explain a consistent supply of well-oxygenated water available for upwelling and hence re-oxygenation of the inlet over decadal time scales. It is worth noting that very little work has been done on the Holocene paleooceanography of the *northern* northeast Pacific, and that our present-day conceptualization is based on an exceptionally short period of monitoring. It is thought that the paleo-oxygenation (i.e. bioturbation) record of the Santa Barbara Basin reflects the changing age and ventilation of East Pacific Intermediate Waters that are linked to Pacific and Atlantic ocean circulation, and ultimately to the general ocean-atmosphere system (Behl and Kennett, 1996). Possible widespread and synchronous changes in ventilation along the northeast Pacific margin during the late Holocene may have been recorded in the frequency and intensity of oxygenation-bioturbation episodes in Effingham Inlet varves.

In order to test the link between *local* oxygenation/bioturbation in the varved record of Effingham Inlet and more widespread changes in climate and ocean dynamics, bioturbation indices (e.g. Behl, 1995; Behl and Kennett, 1996; De Diego and Douglas,

1999) need to be applied to the varved sediments of the inlet. As an extension of this study, extensively bioturbated intervals in the varved record were correlated throughout the inner basin stratigraphy, and although their full significance is uncertain, their frequency and duration have changed notably through time. Prior to 3,000 y BP, bioturbation appears to have been a rare occurrence; from 3,000 to 1,800 y BP bioturbation episodes in the inner basin were infrequent but of long duration; while after 1,800 y BP bioturbation episodes were frequent and short-lived, almost to the point of being the norm rather than the exception.

In summary, the incidence of bioturbation in the pre-20th century record of the inner basin of Effingham Inlet, probably necessitated a type of oxygenation outside of the present oceanographic mode, and warrants further attention. Whether paleo-oxygenation is coupled, positively or negatively, or not, to paleoproductivity or climate awaits results from ongoing paleobiological studies of the inlet.

Gravity flow deposits

Gravity flow units punctuate the varved intervals, ranging from a few centimetres at some core sites to almost a metre in thickness at others, with most falling within the 10 to 25 cm range. Units consist of homogeneous silty, sandy or clast-rich, diatomaceous sediment that is typically normally graded with respect to clasts (Figure 9) while in some cases a colour gradation exists (dark to light). Clasts comprise small diatom laminae intraclasts, terrigenous organic debris, and lithic/shell sand and gravel. Some units are entirely homogeneous both in core and in x-radiographs and exhibit no grading or basal sand, yet spatial variation in unit thickness supports a transported origin. A few units contain floating, elongate varve intraclasts, no more than a few centimetres in length.

The bases of many units comprise concentrations of sand, gravel or coarse wood debris. Normal grading is evident in core and in x-ray images of these deposits and possible planar laminations within the sandy material are evident in some x-ray images. Perhaps the most distinguishing feature of these units is a < 1cm-thick, light olive brown, diatom/silt-rich top that is gradational with antecedent deposits (Figure 9). This fine-grained top is composed of small centric diatoms, macerated diatom frustules, and silt and minor clay. These tops are distinguished from varve laminae due to their mixed lithic/biogenic composition, light brown colour, and gradational lower contacts.

Units are variable in coarse-grained fraction; some are simply composed of homogeneous mud with a fine-grained top, while others contain coarse sand granule clasts and organic debris suspended within a mud matrix. Units are thickest in core B13 and B06, thinner in B03 and B09 and thinnest in A02, i.e. thickest in the west, thinner to

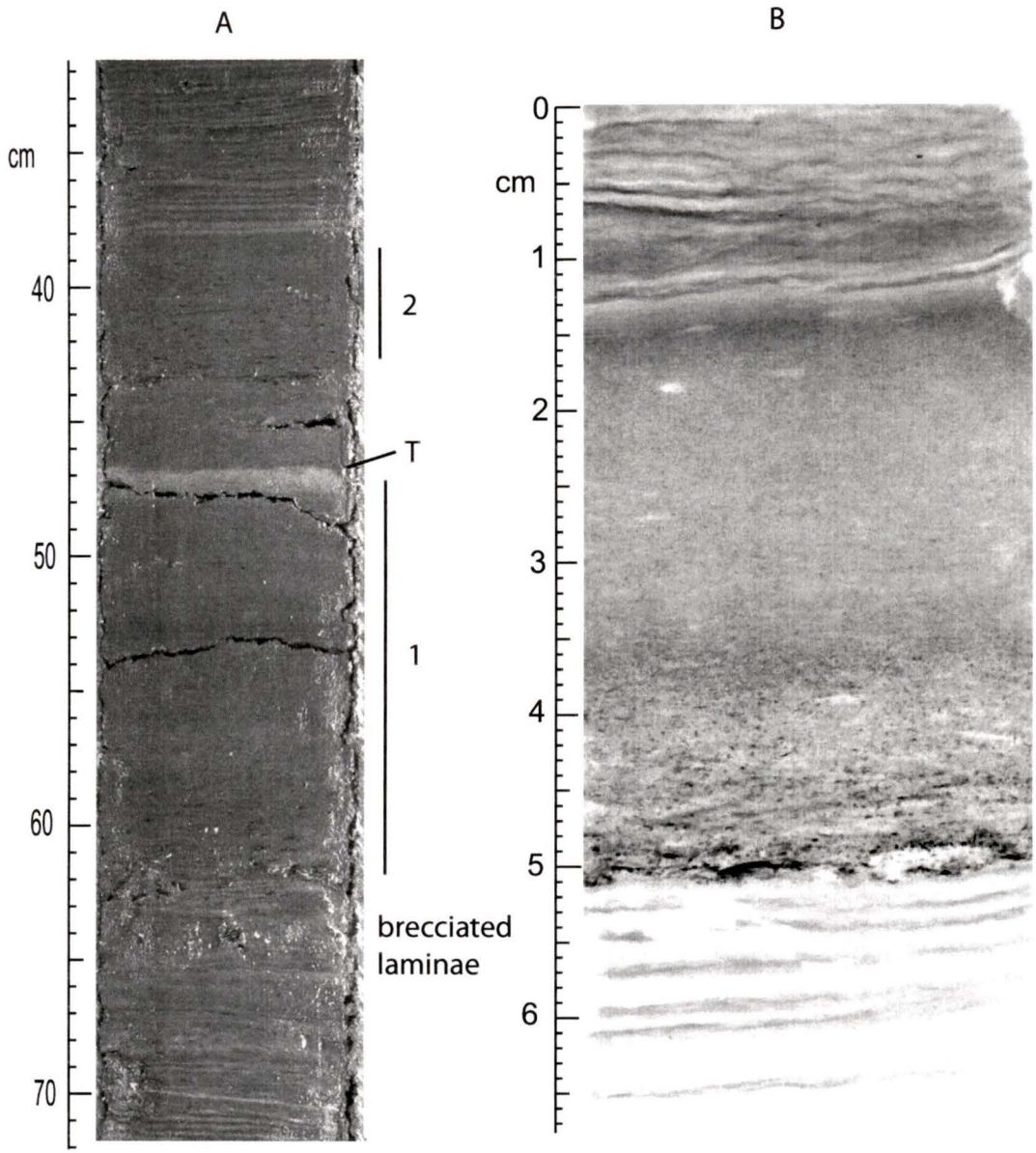

Figure 9. Turbidites from Effingham Inlet. A. Photomosaic showing two successive turbidites (1= lower; 2 = upper) within laminated sediment. Note disturbed laminae below unit and light-coloured, gradational top (T). (TUL99B06 sec 7: 42-72 cm). B. X-radiograph of core slab showing normal grading of varve clasts, sand and mud. Note brittle behaviour in underlying varve laminae that show minor offset, while overlying laminae are wavy and indistinct, probably due to moderate bioturbation at low oxygen levels. (TUL99B03, sec 3, 780cm)

the east and south and thinnest to the north (Appendix 1). An individual layer may vary in thickness yet the fine detail of the bed is generally consistent core to core. A zone of brecciated, sheared or folded laminae underlies the base of some graded units at some sites (see section below for a full description).

Most of the gravity flow deposits can be interpreted as turbidites due to the preponderance of normal grading, fine-grained tops, and paucity of large, intact varve clasts. These attributes are consistent with transport by a fluidized medium (turbidity current) and not by a cohesive, viscous flow (debris flow) (Middleton and Hampton, 1973; Shanmugam, 1996).

It is possible that some turbidity currents were gradational, in a spatial sense, with "mud flows" (i.e. muddy debris flows), as some units show floating varve clasts, little to no grading, and no obvious fine-grained top (Middleton and Hampton, 1976; Shanmugam, 1996; Chang and Grimm 1999). Viscous type flows can progress to turbidity currents through dilution by ambient water (Fisher 1983).

The fine-grained, silt/diatom tops resulted from suspension fallout of fines after the sediment-water mass came to rest (Middleton and Hampton, 1973). The same effect was replicated in the lab with disaggregated mud from the inlet, if stirred into suspension in a water-filled container and allowed to settle. The same light-coloured silt/diatom cap is formed as the material settles out of suspension at the bottom of the container, reflecting the lower settling velocities of these fine-grained materials relative to the coarser mud particle fraction.

The mud fraction is not a complete disaggregate of constituent silt-sized biogenic and lithic particles; rather it contains silt and sand-sized mud aggregates that were not

completely broken up during transport. The tops represent the "winnowed" fine-grained constituents of a hydraulically macerated and sorted, formerly laminated, sediment mass, and are a further indication of transport by a fluidized medium. These distinct tops were also noted from many of the Saanich Inlet "debris flows" of Blais (1995).

Erosion at the base of the turbidites was likely not extensive, especially at sites where units are only 2-4 cm thick. The varve counts generally agree between sites where thick (potentially erosive) turbidity currents and flows occurred and sites where correlative thin units are found in the basin centre and edges. This corroborates Blais (1995), Blais-Stevens and Clague, (2001), and Nederbragt and Thurow (2001), who interpreted minimal amounts of erosion beneath similar sediment gravity flows in Saanich Inlet. However, some of the thicker units at some sites show evidence of erosion. For example, differences in varve counts below the youngest event (AD 1946, Event 1) indicate erosion of perhaps sixty varve years in B06, when compared to a more distal site of B09 (Table 3, varve years between "ML" 1 and 2).

Due to their composition and colour, similar to background laminated and indistinctly laminated sediments, the turbidites likely emanated from lower side-wall and basin-fill slope failures which traveled downslope to come to rest in the basin plain. The slightly elevated sand contents suggest a depth of origin shallower than the basin plain (Blais 1995), although they are not likely to have been derived from fan-delta or shoreline deposits. The proximal to distal thickness trends indicate that a majority were derived from the western side of the basin where the thickest beds are found. Individual beds pinch out towards the north, south and east. This is evident in the core stratigraphy depicted in Appendix 1 where individual turbidites are thickest in cores B06 and B13 and

pinch out laterally towards the other cores. Multiple, simultaneous failures of differing size may also have occurred, although there is less evidence for this. In a few cases, the B03 site, which is closest to the eastern side-wall, probably received slope failures from the western and eastern sides.

The most likely parent slope for the majority of the failures is the thick, inclined sediment wedge that drapes the western side of the basin (Figure 6.). Failures from river-derived flood deposits can be ruled out since the core closest to the fjord head river (97A02) has by far the thinnest, most distal turbidites (Appendix 1). The highest average sedimentation rates of the inner basin were also measured in cores close to the western margin (B06, B13), suggesting that a slightly high sedimentation rate in conjunction with higher slope angle is correlates to higher slope failure rates (Hein and Gorsline, 1981; Blais-Stevens and Clague, 2001).

Very similar gravity flow deposits in Saanich Inlet were interpreted as debris flows (Bobrowsky and Clague, 1990; Blais, 1995; Blais-Stevens et al, 1997). Debris flows exhibit plastic rheology, laminar flow and transport clasts through support by matrix strength and buoyant lift (Middleton and Hampton, 1976; Shanmugam, 1996). Several new lines of evidence point to a different transport mechanism acting in Effingham Inlet. Unlike in Saanich Inlet, the layers described here comprise a significant sand component, very little clay (Dallimore, 2001), and exhibit grading and other sedimentary textures that are uncharacteristic of debris flows. They did not freeze in place, as debris flows would, but rather spread throughout the basin, even travelling upslope. Cores 97A02 and 99B03 are updip of the other cores yet they contain the thin lobes of turbidites that likely emanated from the western slope of the inner basin.

The interpretation of Saanich Inlet "massive layers" as debris flows was largely based on a lack of classic Bouma sequence structures and a lack of grading or other structures (Blais, 1995; Blais-Stevens et al, 1997). However, the Bouma sequence was conceived for sandy deposits and therefore is not necessarily applicable in a silty clay-dominated setting such as Saanich Inlet. Many of the graded beds in Effingham Inlet were only recognized as such after x-ray images of the cores revealed sandy bases. The massive layers of Saanich Inlet contain less than 5% fine sand yet apart from one bed that had gravel at its base, no mention is made of how this sand is distributed throughout the individual units (no x-radiographs were presented). Since a clear lack of grading has not been shown, how can its absence be used as proof of gravity flow mechanism? The only positive proof of transport mechanism is the gravel at the base of one unit, which is consistent with traction transport at the base of a turbulent fluid (Lowe, 1982) and not transport by a debris flow (Middleton and Hampton, 1976; Shanmugam, 1996).

The sharply based "brecciated zones" noted below over half of the Saanich Inlet gravity flow deposits were thought to be the result of bed shearing by the overlying flow (Blais, 1995; Blais-Stevens et al, 1997). Subaqueous debris flows can travel over antecedent deposits without exerting significant shear (Mohrig et al, 1999), especially if the flows are composed of low-density, water-saturated material. In fact, the brecciated zones themselves have more affinities with debris or mud flows as they show obvious evidence of laminar, non-turbulent flow (Shanmugam, 1996), and the presence of floating, brecciated varve clasts within these units indicates that they froze in place as a visco-plastic flow.

Table 2. Evidence for turbidity currents

Summary of observed evidence for turbidites

Observed characteristic supporting deposition by turbidity currents	Interpretation
• Normal grading	→ sedimentation out of suspension
• sand gravel "traction carpets", planar laminations	→ traction transport of sand below turbulent sediment-fluid mixture
• sharp, lower contact; gradational, fine-grained tops	→ erosive body; hydraulic maceration and sorting; suspension settling of fine fraction
• pinch-out geometries; slope run-up	→ fluid, non-cohesive, non-freezing

Discussion

The laminated sediments and gravity flow deposits of Effingham Inlet are texturally and compositionally analogous to those of Holocene age from Saanich Inlet (Blais, 1995) and the California Borderland basins (Behl, 1995; Bull and Kemp, 1995; Grimm et al, 1996), the late Quaternary deposits of the Peru-Chile continental margin (Kemp, 1990; Brodie and Kemp, 1994) as well as the Miocene Monterey Formation diatomites from California (Grimm and Orange, 1997; Chang and Grimm, 1999). What baseline physical properties of these sedimentary analogues might influence the rheological behaviour of Effingham Inlet sediments?

Organic-rich (>4-5% TOC) sediments rapidly lose their strength following disturbance and are therefore highly susceptible to failure (Keller 1983). The combination of having sediments of high water content, low bulk density and high sensitivity in an environment where earthquakes can generate excess pore pressure is conducive to fluidized failures rather than failures of coherent slump blocks (Keller,

1983). Transition of debris flows to turbulent fluidized transport is readily achieved in laboratory models if initial water contents of the sediments are high (Hampton, 1972). Low clay and sand content also tends to prevent development of cohesive strength in flows. In the case of sediments with high organic carbon and water content, such as anoxic, diatomaceous sediments, abrupt transition from slump/slide blocks to fluid flow is therefore thought to readily occur following disturbance and failure (Keller, 1983; Einsele, 1990; Chang and Grimm, 1999).

Conclusions

Despite the absence of a complete set of physical properties for Effingham and Saanich Inlet sediments, a literature review of published data on organic-rich, laminated, diatomaceous sediments supports fluidized flows leading to turbidity currents rather than slump failures leading to debris flows.

Consistency of internal structures at sites and overall distal-proximal thickness trends suggest sources along one sidewall, specifically along a portion of the basin-fill muds that drape the western side of the inner basin (Figure 6.). Grading of clasts indicates fluidization of sediments during transport that must have occurred over an extremely short distance (a few tens of metres). The gravity flow deposits have affinities with turbidites although some may have been gradational with mudflows. Sediment gravity flows exist through a continuum of types (Middleton and Hampton,1976) and they are readily subject to dilution by ambient water during movement (Hampton 1972; Fisher, 1983). Behaviour of the individual failure events during initial slope destabilization and flow was likely governed by the baseline physical properties of these

organic-rich, diatomaceous sediments and by the extent of liquefaction induced by loading. Low clay and high water content of these sediments as well as slope aspect all undoubtedly influenced their behaviour during subsequent stages of transport.

Deformation zones

Conspicuous and thick (20-180 cm) zones of micro-faulted, folded, deformed, and brecciated laminae are found at several stratigraphic horizons in the cores of the inner basin (Appendix 1). Deformed strata are overlain by a graded layer or turbidite. The best developed and most extensive zone (circa ~3,300 y BP, recovered at the base of cores 97A01, 99B03 and 99B09) shows an upwards progression from: (1) undisturbed laminae to centimetre-scale, micro-faulting, folding, and pull-apart structures ("boudinage"); to (2) decimetre-scale recumbent and isoclinally folded laminae, and chaotically inclined laminae; to (3) finely brecciated laminae; and, finally, to (4) a graded layer (turbidite) with a preserved paleo-sediment-water interface (Figure 10). The micro-faults and folded laminae are all compressive stress (thrust) features. Chaotic, deformed laminae probably represent further deformation, folding and initiation of liquefaction of the sediment. Due to the presence of a way-up indicator in the varve couplet colouration, only minor overturning of varves could be detected in the most extensive of the deformed zones (i.e. 97A02, Appendix 1). Capping the deformed strata is a turbidite, identical to the other event deposits found throughout the cores.

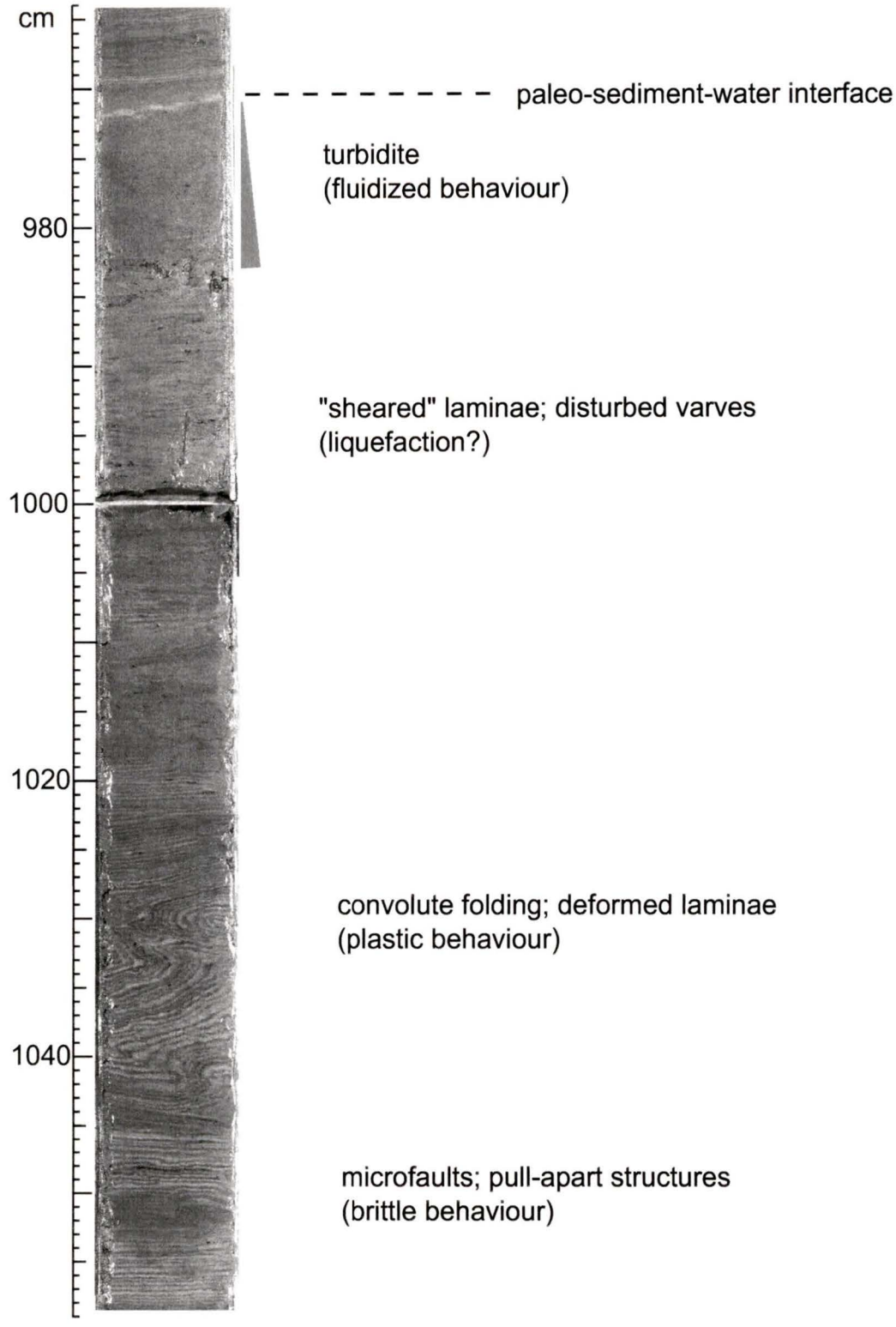

Figure 10. Photomosaic of piston core from Effingham Inlet with interpreted progressive, depth-related deformation and liquefaction of diatomaceous muds, illustrating the proposed relationship between water content and mode of failure following cyclic shear stress. See text and Figure 11 for a more complete explanation. (TUL99B09, sec 7/8, 965-1059 cm).

Discussion

All three deformed zones are overlain by a 10- 20 cm thick turbidite with the same characteristics as other the turbidites -including proximal-distal trends that point to an origin along the western sidewall. Since the underlying deformed zones are thick by comparison, they could not have resulted from loading either during, or following, passage of the turbidity current. Rather, the deformation resulted from displacement of uppermost strata that preceded, or was concurrent with initiation of the turbidity current. The displacement of these strata may have been related to slumping of sediment higher up on the basin slopes or to direct deformation of the basin centre sediments by earthquake shaking. Although the direction of slumping cannot be determined at this time, sites with no appreciable slopes, such as B09, contain deformed strata. The shallowest core (97A02), located near the northern slope of the inner basin, contains the thickest deformed interval. Therefore, basin-wide slumping of sediments appears to have occurred while a turbidity current was triggered on the western slope.

Deformation structures in laminated diatomaceous sediments from other settings offer useful analogues for comparison with these structures. Zones of progressively deformed strata in diatomaceous sediments have been noted from other settings including the Peru-Chile continental margin (Hill and Marsters, 1990), and the Miocene Monterey Formation of California (Seilacher, 1969 and 1984; Grimm and Orange, 1997). Interlocking diatom frustules can support a high proportion of the sediment load thereby making high diatom content a significant factor in the plasticity of laminated sediments (Hill and Marsters, 1990). The widely reported "fault-vein" structures (Hill and Marsters 1990; Lindsley-Griffin et al., 1990) or "intrastratal microfractured zones" (Grimm and

Orange, 1997) represent brittle fracture and ductile shear in diatomaceous sediments following slope destabilisation. However, apart from minor microfaulting, very little brittle fracture is observed in Effingham sediment, while plastic deformation to fluidized flow appear dominant. Plastic-fluid behaviour would theoretically be more prevalent in Effingham Inlet sediments given its lower organic carbon and clay content. Lower Atterberg (liquid and plastic) limits would therefore be expected for Effingham Inlet sediments (Keller, 1983).

In a recent study of Monterey Formation sediments, Chang and Grimm (1999) describe an array of sedimentary structures, including brittle fracture, plastic deformation and resedimented units, all produced by slope destabilisation, that are strikingly similar to those described here. In addition, Seilacher (1969) described deformed Monterey Formation sediments, termed "seismites", showing an upwards progression from undisturbed strata, a zone of *en echelon* fault-vein structures, a brecciated zone and an upper liquefied zone. The upper liquefied portions of these zones have been shown to represent a sediment-water interface (Seilacher, 1969, 1984; Grimm and Orange, 1997). Seilacher's "seismites" are thought to be more fluidized versions of the brittle failure (fault-vein) structures described by Grimm and Orange (1997) and others. A lower liquid failure limit, possibly related to slightly lower organic and/or higher clay content (Busch and Keller, 1981; Keller, 1983), would increase the likelihood of plastic deformation and liquefaction over brittle fracture and fault-vein deformation. Again, the structures observed in Effingham Inlet would appear then to represent the more fluidized behaviour expected from sediments having slightly lower liquid failure limits and organic carbon contents.

Paleoseismic implications of deformed strata

The liquid (w_L) and plastic (w_P) limits are the lowest boundaries of water content (w) at which a sediment experiencing deformation behaves as a liquid and plastic respectively (Keller, 1983). When in-situ water content exceeds the liquid limit, the inter-particle fabric is of sufficient strength to allow the natural sediment to exist as a coherent mass at a water content that would cause the sediment to flow if it were disturbed (Keller, 1983). In marine sediments, a gradient exists from high water content at the sediment-water interface ($w > w_L$) to lower water contents ($w < w_L$) over the first few metres of sediment (Einsele, 1990) (Figure 11). Following disturbance by cyclic shear stress, the uppermost sediments with $w > w_L$ may experience fluidized flow while those deeper in the column may undergo plastic (ductile) deformation or remain little changed. The Effingham Inlet cores appear to have recovered the transition from fluidized behaviour in uppermost sediments, through plastic deformation, to undeformed strata at depth.

This upwards liquefaction gradient is best explained by mobilization of uppermost, unconsolidated sediments by dynamic (cyclic) loading and not by soft sediment creep or slumping due to static (depositional) loading. In this protected setting, earthquakes are the only plausible mechanism for the development of cyclic shear stress. A similar concept postulated by Einsele (1990) emphasizes the role liquefaction plays in the generation of turbidity currents (Figure 11). The "paleo-disturbance" gradient at the 3,300 y BP level is therefore probably representative of the possible range in rheological effects of earthquake loading on these sediments. Sediment deformation was simultaneous and basin-wide, providing additional support for a coseismic hypothesis.

Taken together, these attributes make a strong case for the structures having formed under loading by a large earthquake. This earthquake would date to 3,280 y BP based on varve counting, placing it in the time window of coastal land subsidence related to a Cascadia plate-boundary earthquake (Atwater and Hemphil-Haley, 1997).

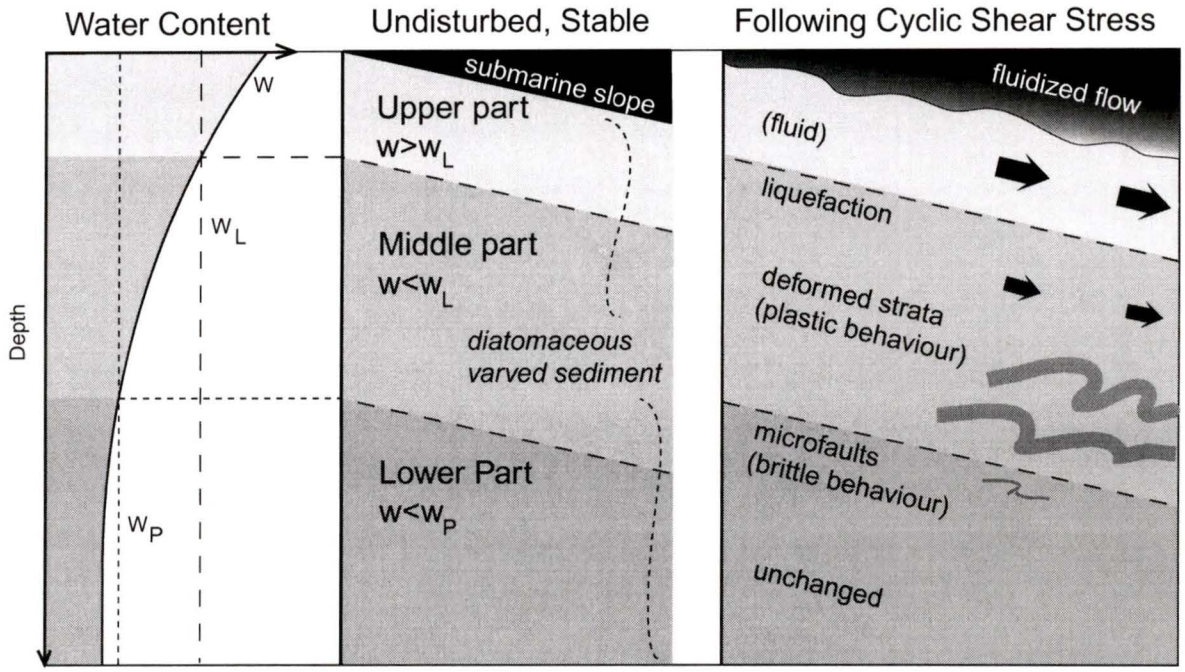

Figure 11. Conceptual model for the generation of sediment deformation gradients and turbidites in the diatomaceous oozes and muds of Effingham Inlet. In situ water contents w, equal to or in excess of liquid limit (w_L) permit liquefaction, while water contents less than the liquid limit and in excess of the plastic limit (w_P) allow plastic deformation of previously laminated sediment, following disturbance by cyclic shear stress, i.e. seismic shaking. Uppermost sediments form a fluidized flow (turbidity current). Concept adapted from Einsele, (1990, fig. 1).

Thin sandy beds

Thin (1-5cm) coarse layers, composed of sand, plant debris, varve clasts and mud are distributed throughout the cores. These units have sharp bases and tops and do not comprise the light-coloured diatom-clay tops seen in the turbidite units. Clasts are typically non-graded and float in matrix, although grading is evident in a few cases. These units can, in many cases, be correlated from site to site, however they do not show the thickness trends of the turbidites described above, suggesting multiple sources along the basin sides.

These thin units are likely allochthonous, having cascaded down from steep, shallow areas of the sidewalls either during periods of exceptionally high runoff or during tidal drawdown and undrained loading of shoreline sediments (Prior et al, 1984, and ref. therein). Ephemeral streams along the shores of fjords emanate from rugged high-relief catchments and can contribute coarse material (sand and organic debris) to the fjord basin during times of heavy rainfall, snow melt or snow avalanching. Ephemeral streams produce episodic, high-energy sediment influx when the flooding streams introduce large quantities of sand and gravel to the fjord margin. While some of this sediment accumulates along the shores as small fans, quantities are sufficiently mobile to continue downslope through chutes as debris flows that likely entrain some mud along the way (Prior and Bornhold, 1988). These small units probably represent deposits from exceptional floods.

Outer Basin

The outer basin sediments in general have been discussed by Dallimore (2001) and will only be given cursory treatment herein. Many of the sedimentary textures found in the inner basin can be identified in outer basin cores, including, laminated, indistinctly laminated to homogeneous; gravity flow units (turbidites); and deformed intervals. The gravity flow units can further be subdivided into mud-rich and sand/organic-rich.

Laminated sediment

Laminated sediment in the outer basin consists of alternating light-coloured laminae (diatom-rich) and darker laminae (lithic particles). Although analogous to varves in the inner basin, laminae in outer basin sediments are significantly thicker, averaging 4.3 mm. Considerable variability in the character, relative proportion of diatom and terrigenous constituents, and preservation, makes treatment of the laminae in the outer basin as varves somewhat problematic. There is little doubt that varves are present in the outer basin (Dallimore, 2001), however, they are often less visually distinct and often contain sub-laminae. Terrigenous sub-laminae present within varves likely represent exceptional pluvial events that are superimposed on the annual sedimentation cycle. The two streams discharging directly into the outer basin, its deeper sill, and its proximity to the open ocean likely all contribute additional variables to the oceanographic and sedimentary dynamics of the basin.

Indistinctly laminated sediment

In addition to erratic varve characteristics, varve preservation in the outer basin is patchy and adversely affected by bioturbation. Units comprising faint, discontinuous laminae or homogeneous, pelleted mud are interpreted as bioturbated sediment.

Mud-rich turbidites

Gravity flow units comprising graded or non-graded basinal mud are similar to graded units from the inner basin. Units consist of homogeneous olive-coloured, sandy diatomaceous sediment that is typically normally graded with respect to sand and colour (light to dark). A 1-2 cm thick, light olive brown, silt-diatom top, gradational with antecedent olive mud is also present.

Due to their mud composition and colour similar to background laminated and indistinctly laminated sediments, these event beds likely were derived from failures in basin and slope sediments. Normal grading and gradational, fine-grained tops indicate that sediment settled out of suspension in a fluid medium, i.e., that the failures initiated turbidity currents.

Sand/organic-rich turbidites

Up to 40% of the gravity flow deposits in the outer basin cores were distinctive sandy and organic-rich beds, comprising greater than 20 wt% graded, or massive sand and organic (woody and herbaceous) material (Dallimore, 2001). Some units show reverse grading, i.e., mud to sand. No other units in the Effingham Inlet cores contain

such high concentrations of coarse sand and organic debris. Due to their unusual composition and textures, these units are distinct from mud-rich beds in probable origin and may have originated from the fan deltas of the two streams that discharge directly into the outer basin on either side of the basin. Although the subaqueous aspect and sedimentary dynamics of the fan deltas in question have not been studied, these streams may periodically contribute larger than normal quantities of coarse material to the basin during times of exceptionally high runoff, as has been observed in other fjords (Prior and Bornhold, 1988). However, since these deposits are thickest in core A01, which is the furthest from the delta fronts, and thinnest in cores closest to the streams, it is perhaps more probable that these deposits resulted from mass wasting from sidewall sediments.

3.2. Inner Basin Stratigraphy

Essential for an age model based on varve counting is that the correlation of sites be as accurate as possible. Marker horizons including turbidites, bioturbated zones and varves arranged in characteristic patterns of thickness and spacing allow for unambiguous correlation between sites in the inner basin (Appendix 1 in back pocket). Gravity flow units were correlated between sites using distinct features in the varve character (i.e. colour and thickness pattern) both above and below the units. Varve counts between turbidites offered a further check on these correlations. These sedimentary units provide a framework of absolute time horizons within which the radiocarbon dates and varve counts can be placed. Despite gas expansion and consequent loss of core material between core sections, over 100% of the record can be accounted for in overlapping, correlative sections. Two independent age models thus emerged: a varve-based chronology and a radiocarbon chronology. The average sedimentation rates derived from both of these were further checked against the measured average sedimentation rates obtained from the varves themselves.

Couplet Measurements and Sedimentation Rates

In order to assess sedimentation rate over time, independently of the ^{14}C-derived average sedimentation rates, measurements of varve couplet thickness, a measure of the annual sedimentation rate, were taken throughout the cores. Since the topmost piston core sections were allowed to settle in cold storage following the cruise, and since no dramatic increase in couplet thickness in uppermost sections occurs, compaction of

sediments with depth does not appear to have affected the measured average sedimentation rates. Varve couplet thickness data from the cores is displayed in the form of "modified box plots", shown side by side for comparison (Figure 12). Although the degree of skewness of the data is seen to vary, the interquartile range, or IQR (i.e. 50% of the data, delineated by the box) does not. The position of the median line within the IQR box indicates the degree of skewness of the data and the "arms" of the box represent the spread in outlier data. Cores at the western margin of the inner basin (B06 and B13) had the thickest measured varve couplets and the highest average sedimentation rates (2.8 mm/a), the eastern margin site (B03) had the lowest sedimentation rates (2.2 mm/a), while sites and at the northern (A02) and southern (B09) ends of the basin had intermediate rates (2.6 mm/a). From the total population of varve couplet measurements, the mean thickness of varve couplets is 2.6 mm, with a standard deviation of 1 mm.

It should be noted that the mean of the measured couplets probably results in slightly inflated sedimentation rates since the data have more upper-end outliers. This may reflect a general bias towards measuring thick, highly visible varves, and hence a tendency to obtain more upper-end values. The median is less affected by outlier data and is in fact closer to the average sedimentation rate obtained from the radiocarbon chronology. Therefore, the mean values probably represent upper limits on the true sedimentation rates.

Figure 12. Measured Sedimentation Rates - Varve Couplet Thickness

Modified box plots of measured varve couplet thickness from selected cores from the Inner Basin. The box delineates the interquartile range (IQR), or half of all data points, while the arms delineate values within 1.5 x the IQR. Additional points are extreme outliers within the data set. A standard statistical output for each plot and dataset is also given below. Means are reported in millimetres per annum (mm/a).

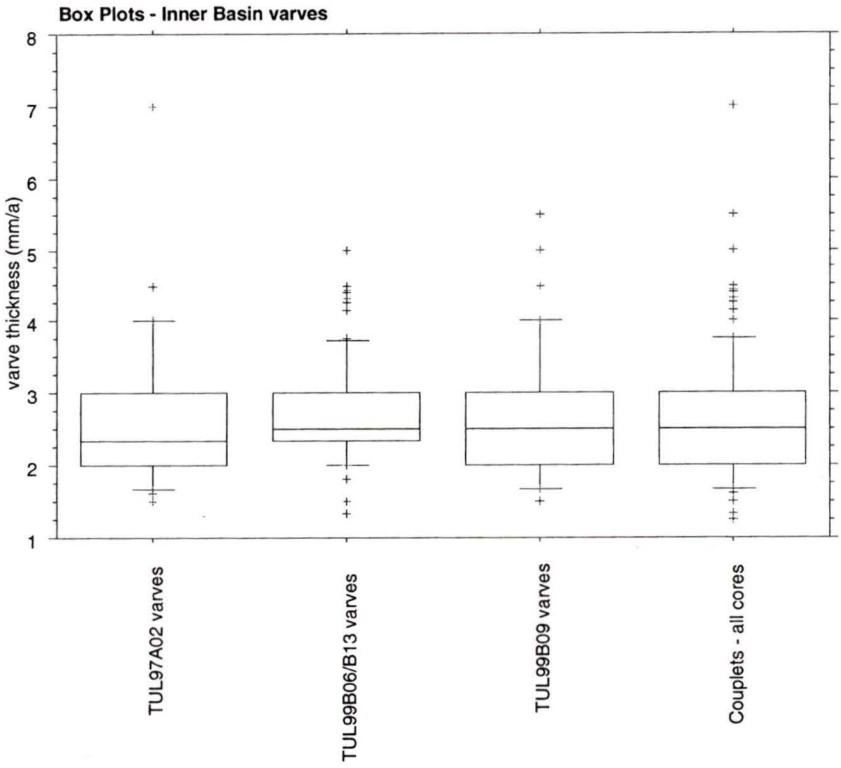

Descriptive Statistics for Couplet Thicknesses (measured in mm)

	TUL97A02 varves
Mean	2.597
Std. Dev.	.918
Std. Error	.115
Count	64
Minimum	1.5
Maximum	7

	TUL99B09 varves
Mean	2.607
Std. Dev.	.868
Std. Error	.099
Count	77
Minimum	1.5
Maximum	5.5

	TUL99B06/B13 varves
Mean	2.772
Std. Dev.	.725
Std. Error	.083
Count	76
Minimum	1.333
Maximum	5

	Couplets - all cores	
Mean	2.63	(mm/a)
Std. Dev.	.824	
Std. Error	.054	
Count	236	
Minimum	1.25	
Maximum	7	
Skewness	1.347	
Median	2.5	
IQR	1	

Varve chronology

Varve counts are a direct indication of the span of time between marker horizons and therefore provide a check on the radiocarbon-derived age model and sedimentation rates. The preservation of laminae in Effingham sediments is somewhat patchy, especially in the upper half of the cored record, since about 1,600 y BP. Although most of the record is well laminated, and varves could be counted throughout most of the sequence, incorporation of the indistinctly laminated and non-laminated horizons into the chronology was necessary because the bioturbated zones represent "time" in the final chronology. Assuming that this bioturbation disrupts only the surface sediment and that there is no net loss or gain in sediment volume at this horizon, it follows that the vertical thicknesses of the bioturbated zones translate into approximate time based on the mean varve couplet thickness (Brodie and Kemp, 1994). Average sedimentation rates obtained from the varve couplet thicknesses were applied to the short intervals where bioturbation had obliterated all trace of laminae. A hybrid varve-sedimentation rate age model was therefore employed to determine the ages of events.

The varve chronology extends to approximately 3,300 y BP in the inner basin (Table 3). Although laminated intervals were recovered below the 3,300 y BP horizon, they are not included in the chronology due to extensive in-situ folding and destruction of the varves below this horizon.

Table 3. Varve counts and thickness of bioturbated intervals between massive layers (ML), numbered consecutively from youngest to oldest, in all Inner Basin cores.

Effingham Inlet - Inner Basin varve counts

ML	TUL99B09 Varve years	TUL99B09 Varve Counts	TUL99B09 Bioturbated intervals (cm)	ML	TUL99B06 Varve years	TUL99B06 Varve Counts	TUL99B06 Bioturbated intervals (cm)	ML	TUL99B13 Varve years	TUL99B13 Varve Counts	TUL99B13 Bioturbated intervals (cm)	ML	TUL99B03 Varve years	TUL99B03 Varve Counts	TUL99B03 Bioturbated intervals (cm)	ML	TUL97A02 Varve years	TUL97A02 Varve Counts	TUL97A02 Bioturbated intervals (cm)	Inner Basin Varve-time Intervals	Final Event Ages
*	53	53		*	53	53														53	
1				1				1				1				1					53
	253	141	29	~	185	97	25										~			253	
2				2				2				2				2					306
	257	208	13						~				~				~			257	
3				3				3				3				3					562
													44	44			~			44	
4				4				4				4				4					606
~	70	56	3.6		128	92	10		135	117	5		130	103	6		~			135	
5				5				5				5				5					741
	108	93	3.8		132	114	5		110	97	3.5		106	83	5		~			132	
6				6				6				6				6					873
	48	35	3.5		36	36			48	41	2		43	43			47	41	1.5	47	
7				7				7				7				7					920
	31	31			43	34	2.5		36	27	2.5		36	36			34	30	1	36	
8				8				8				8				8					956
	219	211	2		201	147	15		234	221	4		242	203	9		230	220	2.5	234	
9				9				9				9				9					1189
	26	26			13	13			22	22			26	26			22	22		26	
10				10				10				10				10					1215
	290	248	11		~				294	247	13		~				>460			294	
11				11				11				11				11	+				1510
	~				~				224	199	7		239	225	3		+			239	
12				12				12				12				12					1748
	174	174			175	175			188	170	5		131	108	5					175	
13				13				13				13				13					1923
	289	260	8		287	216	20		262	166	27		254	224	7					289	
14				14				14				14				14					2212
	17	17			36	36			35	35			33	33						36	
15				15				15				15				15					2248
	46	46			21	21			35	35			40	22	4		?			35	
16				16				16				16				16					2283
	68	30	10		69	33	10		66	66			62	62			?			66	
17				17				17				17				17					2349
	193	139	14		175	50	35		151	137	4		185	140	10		189	154	9	189	
18				18				18				18				18					2538
	85	85			82	82			83	83			87	87			87	87		87	
19				19				19				19				19					2625
	15	3	3		15	4	3		14	3	3						11	3	2	15	
20				20				20				20				20					2639
	85	85			84	63	6		89	75	4		103	85	4		96	96		96	
21				21				21				21				21					2735
	287	156	34		281	177	29		268	161	30						330	299	8	287	
22				22				22				22				22	+				3022
	27	27			26	26			26	26							+			26	
23				23				23				23				23					3048
	232	232			230	230			227	227			235	235						235	
24				24				24				24				24					3283
Mean Sedimentation Rate:			0.26				0.28				0.28				0.22				0.26		

shading indicates intervals chosen for the final chronology

* interval taken from adjacent box cores and freeze cores

~ varved interval not present or incomplete due to non-recovery of core or disturbance

\+ count represents more than one interval due to missing massive layers

Radiocarbon ages and chronology

Twenty-five samples of marine and terrestrial material were removed from the piston cores for carbon dating with raw ^{14}C ages ranging from 160 to 4,190 ^{14}C years BP (Table 4). Tight stratigraphic control and the varves allowed for close scrutiny of these dates. Radiocarbon dates were treated as having been taken from specific varved horizons at "composite depths". Composite depths determined for each date are depths relative to basin-wide time horizons and a reference core TUL99B09 which had the thinnest gravity flow deposits and the most complete stratigraphic sequence. Thicknesses of turbidites were removed from the composite depths so that ages reflected sedimentation of varved and bioturbated intervals only.

Evaluated within this stratigraphic framework, many of the dates were too old given their context -e.g. old dates stratigraphically higher than young dates (Appendix 1), or dates separated by too few varves, or dates that showed considerable age deviation on depth-time plots (Figure 13). The nine dates that were retained gave an average sedimentation rate of 2.1 mm/a for the inner basin (Figure 14). Four dates (TO8671, TO872, TO8687, TO8675) form an age minimum trend giving an average sedimentation rate of 2.3 mm/a. This rate is closest to the average basin sedimentation rate obtained from the varve counts vs. depth plot for marker horizons of 2.4 mm/a, however it is lower than that obtained from varve couplet measurements (2.6 mm/a). The higher value from the measured rate may reflect a bias in measuring thick, highly visible varves. However, all the values lie well within one standard deviation of the mean, measured rate. While the actual sedimentation rate fluctuated with time, this comparison of means forms a good independent test of the varve-based age model for the inner basin.

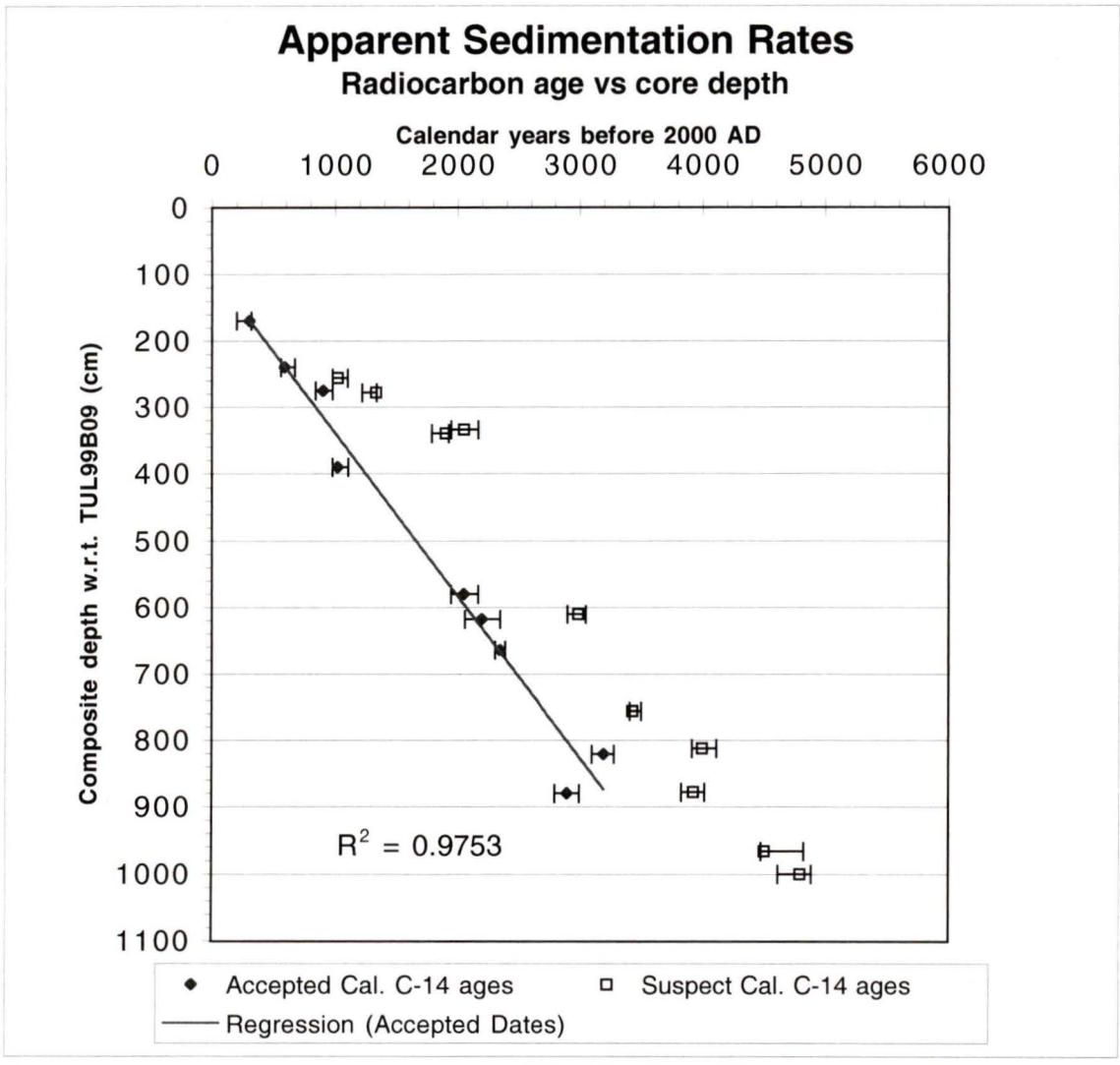

Figure 13. Aggregate Radiocarbon Ages vs. Core Depth (Inner Basin)

Plot of all available inner basin radiocarbon ages (calibrated) as a function of depth with respect to TUL99B09. Ages that deviate towards the right of the regression line for accepted dates are primarily from woody material that likely was deposited and remobilised prior to final deposition. Lag times for wood in the inlet system can be in excess of a thousand years.

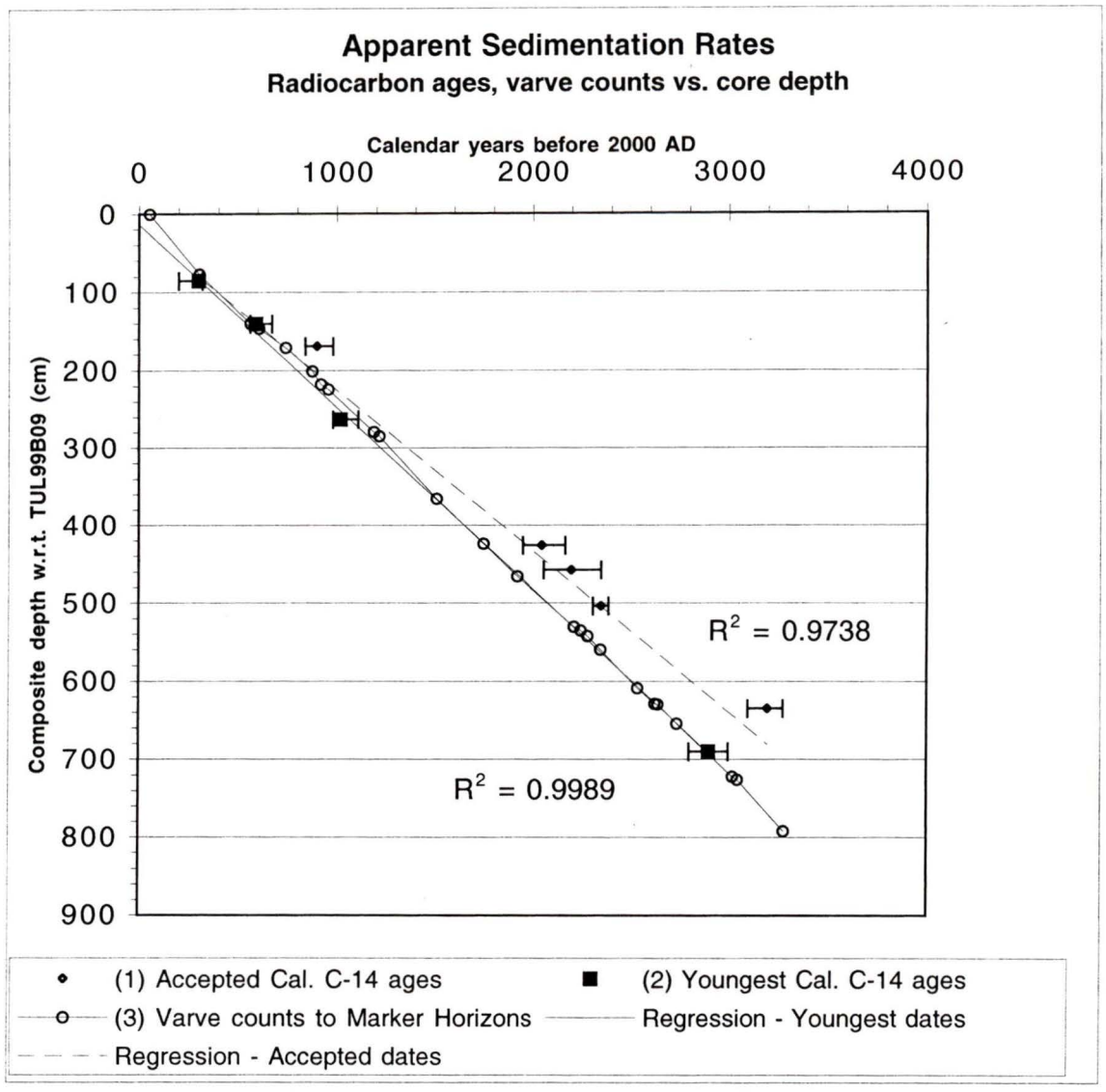

Figure 14. Accepted Radiocarbon Ages and Varve Ages (Inner Basin)

Plot of all "accepted" radiocarbon ages vs. core depth from the Inner Basin cores. Varve counts to marker horizons are also plotted against core depth to show for comparison, the age trend generated from varve counts. Core depths are relative to basin-wide marker horizons in the reference core TUL99B09. The four "stratigraphically youngest" radiocarbon ages are those furthest to the left.

Table 4. Radiocarbon ages

Summary of radiocarbon dated material

Sample ID	Depth (cm)	Material	^{14}C Age -/+ (yrs. before 1950)	Cal Age (yrs. before 2000) Age range (1σ) 95% c.i.	Comments
97A01-192M	192	Shell fragment	990 +/-40	310 (180-360)	Acceptable*
97A01-325	325	Wood fragment	730 +/-50	720 (700-740)	From a gravity flow deposit, although plausible age range*
97A02-14	14	Wood fragment	940 +/-50	900 (840-980)	Acceptable and in agreement with RC13S401
97A02-285M	285	Fish bones	3410 +/-50	2350 (2310-2390)	Acceptable
97A02-551	551	Wood fragment	4050 +/-50	4510 (4480-4830)	Too old
TO8671 RC03S101	97	Wood fragment	160 +/-40	? (50-320)	Acceptable (note several Cal. Ages possible)
TO8672 RC03S201M	169	Shell valves	1770 +/-60	590 (560-670)	Acceptable
TO8673 RC03S301	286	Wood fragment	2050 +/-70	2050 (1950-2170)	Too old, given varve counts to dates above
TO8674 RC03S501	553	Wood fragment	2830 +/-60	2990 (2900-3050)	From gravity flow deposit? Too old (by ~1000 yrs) and in disagreement with two dates near the same horizon
TO8675 RC03S601M	822	Shell valves	3890 +/-80	2800 (2900-3000)	Acceptable —youngest and deepest date
TO8676 RC03S701	937	Wood fragment	4190 +/-80	4800 (4620-4890)	From gravity flow deposit
TO8677 RC06S301	252	Wood twig	1080 +/-50	1020 (980 (1100)	Too old
TO8678 RC06S302	276	Wood fragment	1340 +/-50	1334 (1220-1340)	Too old
TO8679 RC06S502	629	Wood twigs	2050 +/-80	2050 (1950 2170)	Acceptable and in agreement with RC13S502
TO8680 RC06S801	1006	Wood twig	3590 +/-50	3930 (3830 4020)	Too old**
TO8681 RC09S302	340	Wood fragment	1890 +/-50	1900 (1790 1930)	Too old
TO8682 RC09S601M	821	Shell valves	4100 +/-60	3200 (3100 3280)	Acceptable, although in conflict with RC03S501 which is younger and deeper
TO8683 RC11S501M	531	Shell valve	2460 +/-90	1280 (1180-340)	Acceptable*
TO8684 RC11S801M	898	Shell fragment	2830 +/-60	1590 (1510-1670)	Acceptable (excludes RC11S801)*
TO8685 RC11S801	939	Wood fragment	2570 +/-100	2790 (2540-2820)	Acceptable (excludes RC11S801M)*
TO8686 RC11S802M	969	Shell fragment	1820 +/-60	660 (590-700)	Too young*
TO8687 RC13S401	377	Wood twig	1080 +/-60	1020 (980-1110)	Acceptable and in agreement with 97A02-14
TO8688 RC13S502	620	Wood twig	2140 +/-60	2200 (2060-2350)	Acceptable and in agreement with RC06S502
TO8689 RC13S603	779	Wood fragment	3170 +/-50	3430 (3410-3500)	Too old
TO8690 RC13S701	842	Wood fragment	3640 +/-50	4000 (3920-4120)	Too old and from gravity flow deposit

* Outer Basin samples

** taken from below the 3,300 BP deformed horizon

Discussion

Nine dates fit within the inner basin stratigraphic framework (post-3,300 varve years BP) and could be included in the chronology. Dates from below the 3,300 y BP horizon were not included due to extensive in situ sediment. Of the many dates regarded as too old given their stratigraphic context all were obtained from wood. Wood is a good dating candidate as it is unaffected by the marine reservoir correction and it is commonly believed that it could not have remained in the surface environment for a long time. However in this setting, where the gradient from source to basin is steep, and characterised by many subenvironments, anomalous old carbon can be readily explained by reworked and redeposited woody material. Wood deposited in streambed, fan-delta, shoreline sediments can remain there for extended periods of time before a flood or other erosive agent remobilizes it and sweeps it into the inlet. Material can also remain in fjord sidewall sediments until it is swept downslope during mass wasting. Further strengthening this interpretation is the fact that the accepted dates are a "mixed bag" of terrestrial woody material and marine material including three bivalve shells and one fish skeleton. Most of the marine material gave dates that fell close to the "accepted" radiocarbon age trend. Removing the marine material from the data set has little effect on the age trends established by accepted wood dates alone.

The reservoir correction applied to the Effingham Inlet dates was 801 +/-23, similar to that applied to inland coastal waters to the south and in Saanich Inlet (Bornhold et al, 1998). In some estuaries and large bays, where circulation may be restricted, nearshore waters may be ^{14}C-deficient, and may require an additional local ^{14}C reservoir correction greater than that commonly employed for the particular coastal region in

question. It is unlikely that this is required in Effingham Inlet since an older reservoir age would make the calibrated ages from marine material even younger than that calculated here. Regardless of their final deposition in a stagnant basin, the fish and bivalves necessarily lived and derived their carbon from the upper oxygenated (i.e. well mixed) layer of the inlet. Besides, even the stagnant deep water of the inlet is flushed periodically with upwelled water.

Despite the inherent complexities of the marine carbon pool, the reservoir correction of -801 +/- 23 (Robinson and Thompson, 1981) is applicable in Effingham Inlet. Similar consensus was reached following the ODP Leg 169S in Saanich Inlet where shell-wood pairs and varves allowed for a precise determination of the local marine reservoir effect that varied little from that quoted for the region (Bornhold et al, 1998; Bornhold pers. comm.).

In interpreting the radiocarbon ages, the reverse situation, whereby anomalous young carbon has been systematically sampled is difficult to explain. One way to achieve this is by creating out-of-sequence material during coring - i.e. through material being picked up from higher in the sediment column and dragged down the side of the core barrel. However, given that material was sampled from bedding planes, it is unlikely that this could have occurred in so many instances. Post-depositional sample contamination through surface uptake or exchange of non-coeval carbon may have affected the samples, due to the anoxic, organic carbon-rich diagenetic environment in Effingham Inlet. Whether diagenetic contamination by mobile, sedimentary organic compounds occurred or not cannot be determined at this time; physical and chemical lab pretreatment of samples, however, should have removed any such error. If diagenetic contamination

were occurring in Effingham Inlet sediments, then radiocarbon ages would deviate from varve ages to greater extents, with depth and age, and this is not the case.

Based on the radiocarbon age-depth model, the thickness (i.e. time) missing from the tops of the piston cores can therefore be determined. The youngest date in the chronology, taken from TUL99B03 (TO-8671; 160 +/-40 ^{14}C yBP), falls within an age range where the calibration curve has several inflection points and therefore several possible calibrated age results (Stuiver and Reimer, 1993). However, due to the presence of varves above this dated horizon in B03 and correlative horizons (i.e. B09), it can be concluded that the dated material must be *at least* as old as the number of overlying varves. As a result, several of the calibrated ages can be removed giving a tighter age range of 200 - 360 y BP (1800-1640 AD). The small turbidite (Event 2) ~15 cm above this radiocarbon dated horizon is approximately 240 varve years from the base of the topmost gravity flow deposit recovered in piston cores (i.e. Event 1). Therefore, Event 2 (at a depth of 54 cm in TUL99B03 or 156 cm in TUL99B09 etc.) likely has an age between 240 to 360 years before 2000 AD. Based on this there is a minimum of zero and a maximum of 120 years missing from the topmost sections of piston cores B03, B06, B13 and B09.

Core stratigraphy and age model

Mud at the sediment-water interface has a high water content and low density and is commonly not recovered (i.e. is 'overshot') during long-barrel piston coring. An extreme example of this is core 97A02 that sits stratigraphically well below the other piston cores of the inner basin and is missing the top 2.5 m of sediments, or about 500 years of the record (Appendix 1). An effort was made during the 1999 coring operations

to minimize piston core penetration and to recover the surficial sediments in short, gravity cores, i.e. freeze cores and box cores. The short cores were highly effective at sampling the uppermost layers, including the twentieth century record. The pilot or trigger cores that accompany the long cores also recovered the uppermost sediments. The 1999 piston cores retrieved sediment very close to the sediment-water interface based on several lines of reasoning.

- Section 1 from most of the piston cores is a partial section, containing only a few tens of centimetres of mud, suggesting that the core barrel had stopped moving through the sediment before its topmost section could move past the sediment-water interface. If the core barrel had overshot the sediment-water interface, it would have pushed mud up through the topmost section thereby recovering a ~1.5 m section of mud in section 1. This occurred in core 97A02, where the topmost section is ~1.5m in length and where there was significant overshooting based on stratigraphic evidence.
- A thick gravity flow deposit (Event 1, dated to AD 1946 from box and freeze cores) is a feature of every box, freeze and pilot core in both basins, in addition to the tops of the piston cores TUL99-B06, -B09, and -B13. This layer is unsurpassed in thickness and scope in the cored record of the inlet and forms a unique 20^{th} century marker horizon.
- The varve age trend from the piston cores matches the radiocarbon chronology when the topmost gravity flow deposit in the piston cores is assumed to have an age of ~50 y BP. The varve chronology obtained from the piston cores was initially treated as a floating chronology, since the topmost sections could not be assumed to correlate to any dateable horizon. The varve chronology was plotted next to the radiocarbon

chronology with three possible top horizon dates: 50, 120 and 300 y BP. The best fit was obtained when the topmost event was assumed to be 50 years old. Since the twentieth century record recovered in box cores shows only one sediment gravity flow that occurred in 1946, it was concluded that the topmost event in the piston cores likely also corresponds to 1946.

- The varve counts, sedimentation rates, radiocarbon dates and stratigraphy throughout the inner basin piston cores do not readily support an age model older than that which was determined through the reasoning above. Varve counts do support an age model whereby about 3,200 years separate the youngest and oldest sediment gravity flows (Events 1 and 24, respectively) with the youngest event most likely corresponding to AD 1946 and the oldest dated to slightly older than 3,200 y BP.

Comparison of the regression analysis of the varve age and radiocarbon age trends emphasizes that the stratigraphy, varve counts and radiocarbon ages must reinforce each other in order to derive a fully coherent age model for the basin. By incorporating all of the radiocarbon data in depth-time plots (Dallimore, 2001), unsatisfactory regression values are obtained, due to considerable spread in the radiocarbon dates. There is little support therefore for the claim the topmost sections of Effingham Inlet piston cores date to approximately 500 y BP (Dallimore, 2001). This analysis corroborates a similar stratigraphy-based treatment of radiocarbon dates from Saanich Inlet ODP Leg 169S cores (Nederbragt and Thurow, 2001).

Inner Basin Event Chronology

Once the measured (couplet thickness) and radiocarbon-derived average sedimentation rates and varve counts were rationalized, the age model for the turbidites and failure events within the basin was strengthened. With greater than 100% coverage among all the cores, the varve record could be extended to 3,280 y BP during which time 24 slope failure events occurred within the inner basin; the youngest being the AD 1946 event and the oldest being the 3,280 y BP event.

There is excellent agreement between the varve age trend and the trend for the minimum stratigraphic ages in the depth-time plots, i.e. the "youngest" radiocarbon dates (Figure 14). It is therefore highly likely that much of the radiocarbon material represents material that was reworked with varying lag times and that consequently these dates do not reflect the true age of the horizon they are derived from. Separation between the varve age trend and the total accepted radiocarbon age trend is apparent, although it was felt that the youngest radiocarbon dates represented a better age model for reasons explained above. The four shallowest dates (TO8671, TO8672, 97A02-14, TO8687) establish an age trend early on in the sequence that matches the varve chronology. A close match between the age trends means that there was no age-cumulative "loss" of varves in the varve chronology that could have arisen through cumulative varve undercounting or erosion of varves beneath turbidite beds. Further supporting this, varve counts show overall agreement between sites with thick, potentially erosive turbidites, and those with thin, distal turbidites.

The final varve-time intervals between events were obtained from varve counts and sedimentation rates applied to bioturbated intervals (i.e. thickness of the bioturbated interval divided by the average, measured sedimentation rate in centimetres per annum). Table 3 outlines the interval counts for each core and highlights the intervals chosen for the final chronology. Each interval was chosen based on criteria such as its completeness, lack of coring disturbance, and the relative proportion of laminated versus bioturbated sediment. Intervals with the highest varve counts and/or thinnest bioturbated intervals were also given preference. The final chronology is therefore a composite chronology from all cores.

Turbidites linked to known earthquakes

1. Event 1 and the 1946 Vancouver Island (M 7.3) earthquake

Approximately fifty varves below the sediment water interface, there is a thick unit composed of mud and terrigenous organic material. This layer is a ubiquitous feature in freeze and box cores, as well as in the pilot cores that accompany the piston cores. This mass wasting event occurred in both the inner *and* the outer basins during the same varve year. Accurate varve counts over the interval from the sediment-water interface to the top of this deposit obtained from freeze cores give a count of about 52 varve couplets before 1999. Since the cores were obtained in the fall of 1999, the topmost dark layer likely would not yet have been deposited. Adding the 1999 couplet would then give 53 years before 1999, or 1946. The first lamina deposited immediately after the event was composed of diatoms, suggesting that the failure occurred sometime in the spring or summer of 1946. Sedimentologically, this layer is much the same as the

other gravity flow deposits found throughout the cores; i.e. somewhat coarser than surrounding varves, with sand at the base and a fine-grained, diatomaceous top.

This unit corresponds in time to a large (M_w 7.3), crustal earthquake that struck central Vancouver Island the 26th of June 1946. This earthquake triggered extensive subaerial slumping, sediment failure, and liquefaction, as well as subaqueous slumping and flow of Holocene deposits in lakes located within several tens of kilometres of the epicentre (Rogers, 1980). A coseismic slump and sediment gravity flow of delta deposits in Comox Lake has been recognized from subbottom profiles (Shilts and Clague, 1992) and piston cores (Linden and Clague, 1993). Effingham Inlet is located approximately 70 km from the epicentre and lies within the projected VII isoseismal (Modified Mercalli Intensity), a zone that experienced extensive liquefaction and sediment failure (Rogers and Hasewega, 1978; Rogers 1980). The 1946 earthquake also triggered subaqueous debris flows in Saanich Inlet (Blais-Stevens et al., 1997), located much farther from the epicentre than Effingham, albeit within the VI (MMI) isoseismal of Rogers (1980).

2. Event 2 - AD 1700 plate-boundary earthquake

Event 2 is a candidate turbidite for the 300 y BP plate-boundary earthquake due to its presence approximately 301 cumulative varve years before 1999. The coincidence of the varve age with the known age of the approximate M_w 9 subduction earthquake is striking. The derived varve ages of an event should, if anything, underestimate the age of a known earthquake since varves may be lost during gravity flow emplacement. Varve counts in Saanich Inlet cores underestimate the age of the 1700 AD earthquake by about

26 years (Blais-Stevens and Clague, 2001). For Effingham Inlet, the derived varve age is slightly higher than anticipated, suggesting that perhaps few varves were lost. Alternatively, the sedimentation rate over the Event 1 - 2 interval may have been slightly higher than that used to determine the time represented by intervening bioturbated zones. This would relate to reduced compaction of sediment in the uppermost core sections.

Independent radiocarbon dates suggest that Event 2 is close to the age determined through varve counting. A radiocarbon age of 200-360 y BP (1800-1640 AD) was obtained from a wood sample (TO 8671; TUL99B03.1) 15 cm (i.e. ~ 50 varve years) below the Event 2 horizon, placing the event itself in the right time window for the last plate-boundary earthquake.

3.3. Outer Basin Stratigraphy

Radiocarbon dates and age model

As with the inner basin, radiocarbon ages from the outer basin piston cores were assessed within a proposed stratigraphic framework (Appendix 2). Four out of six radiocarbon dates were retained for the chronology and plotted against core depth (Figure 15). Thicknesses of gravity flow deposits were removed from the composite core depths so that ages reflected pelagic sedimentation only. The four dates (97A01-192; 97A01-325; TO8683; TO8684) show a satisfactory regression line and yield an average sedimentation rate of 4.3 mm/a, almost twice that of the inner basin.

The regression line shows that the uppermost sections of the outer basin cores likely recovered sediment from the 20th century. Preliminary work also suggests that the top few centimeters of section 1 of core B11 contains a 1940's *Rhizosolenia* sp. diatom biomarker (M. Hay, pers. comm.). As with the inner basin, the AD 1946 event deposit is a ubiquitous feature in box cores and freeze cores from the outer basin. Based on this, it is highly probable that the youngest massive layer in the piston cores (i.e. massive layer # 1 in cores A03 and A01) corresponds to the 1946 event.

Without the benefit of a varve-based "micro-stratigraphy" due to poor preservation of laminae over significant portions of the outer basin record, average sedimentation rates were applied to the core depths of each gravity flow deposit in order to derive age estimates of the flows. The composite core depths of each massive layer were adjusted by subtracting the cumulative thickness of overlying gravity flow deposits. Derived intervals between events were checked against varve counts wherever varve

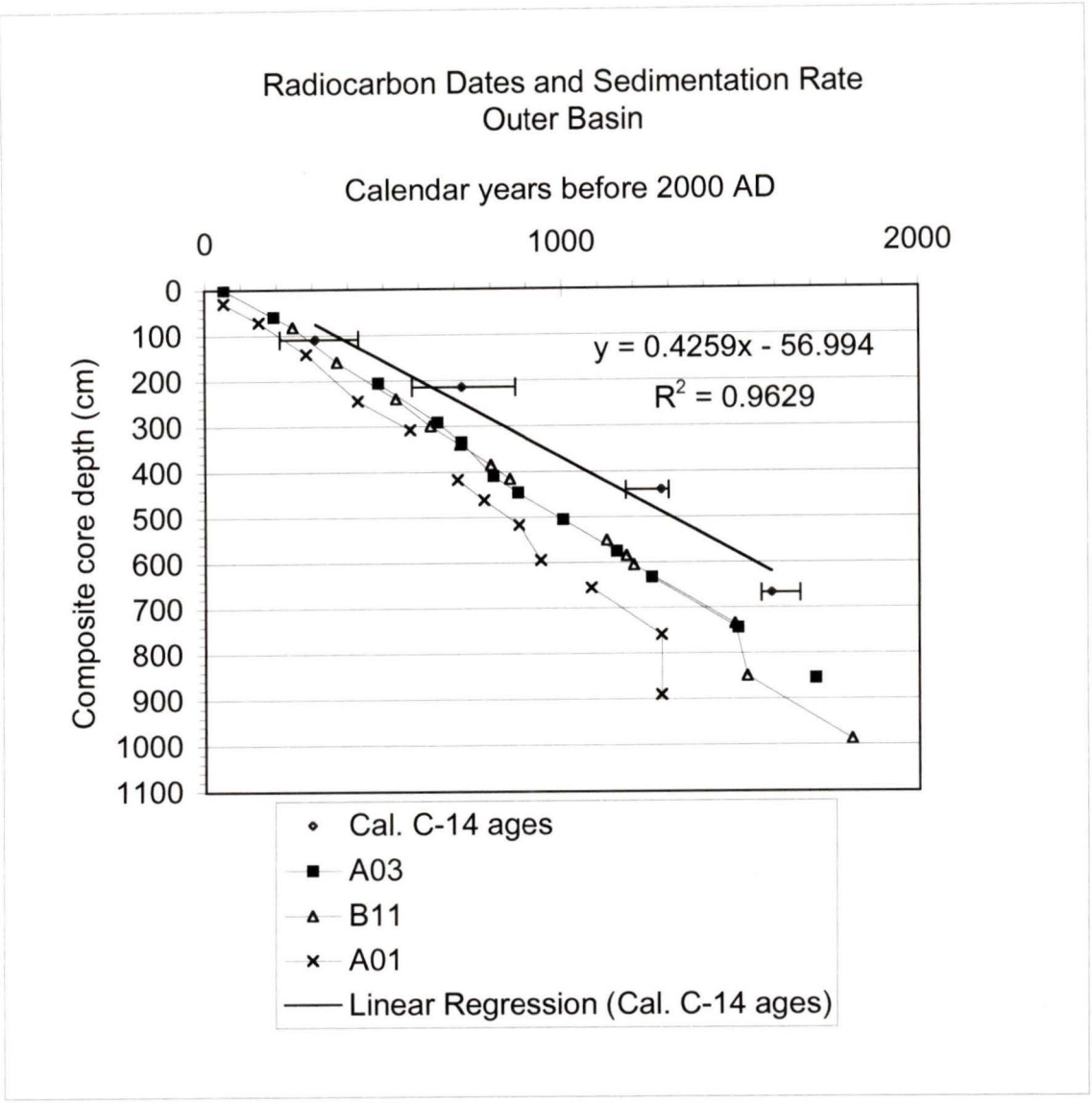

Figure 15. Plot of radiocarbon ages vs. core depth for the Outer Basin of Effingham Inlet. The average sedimentation rate of 4.3 mm/a was then applied to the depths to gravity flows in the three outer basin cores to derive event ages for the outer basin. The age trends for each core are plotted next to the radiocarbon age trend for comparison. Jumps in the event age trend occur below particularly thick turbidites. Core TUL97A01 has the thickest deposits and consecuently the most pronounced "age drift".

quality permitted, and they were generally found to be in agreement. Plotting the derived ages for events in each core (97A01; 97A03; 99B11) next to the radiocarbon trend proved to be revealing (Figure 15). Since the slope of each line in Figure 15 should ideally be a function of the average sedimentation rate, any age-cumulative deviation of the event age trend away from the radiocarbon age trend is likely the result of erosion of pelagic sediments by gravity flows. The increase in event age deviation, or "age drift", with core depth is readily apparent for all cores, however it is particularly marked in core 97A01 where, coincidentally, the thickest flow deposits are found. In addition to the overall drift in event ages with depth, several distinct jumps occur along each core's age trend. The fact that these jumps tend to occur below the thicker gravity flow deposits further implies that larger flows likely eroded and incorporated more antecedent deposits than thinner ones. Based on the separation between the radiocarbon age trend and the massive layer age trends, the age drift could be quantified as about 15% of the calculated event age.

Outer Basin Chronology

This method of deriving event ages yielded age estimates that were fairly well matched between all three cores. A narrow range in ages exists between the three cores up to about 1,000 y BP whereas thereafter, they show increasing inaccuracies (> +/-100 years). Age drift was least dramatic in A03 and B11, consequently it was felt that these cores probably gave the most reliable age estimates for outer basin gravity flows. The resultant chronology represents the calculated ages and varve counts from A01 and B11 verified against varve counts (Table 5).

The outer basin "history" was then compared against the inner basin event history (Table 6). The record of the last 2,000 years shows 13 events in the inner basin, 15 events in the outer basin, leading to a tentative match for 11 out of 15 events in the last 2,000 years. The histories from the two basins of Effingham Inlet show a matching "barcode" pattern that is likely attributable to contemporaneous slope failures in both basins. Since the two basins are separated by a sill at 44 m water depth, no failures could have traveled from one to the other. Flood deposits were ruled out for the inner basin turbidites, and although some of the sand-rich deposits from the outer basin could be derived from floods, they could equally be the result of slope failures for reasons given above.

Table 5. Outer basin massive layer ages based on average sedimentation rates

	TUL97A03			TUL99B11			TUL97A01		
ML#	Depth to ML	ML thickness, cm	Calculated age	Depth to ML	ML thickness, cm	Calculated age	Depth to ML	ML thickness,cm	Calculated age
1	0		*54*	0		*54*	30	30	*54*
2	60	20	194	83	24	247	72	13	152
3	~			160	10	370	142	40	284
4	206	15	487	241	17	535	244	1	428
5	292	14	652	300	5	633	308	52	575
6	335	37	719	340	8	714	~		
7	410	6	807	385	8	801	417	13	707
8	446	5	877	416	18	854	462	14	782
9	506	5	1005	~			518	50	880
10	575	15	1154	551	10	1126	595		942
11	~			585	12	1182	~		
12	632	8	1252	606	7	1203	656	20	1084
13	745	17	1496	735	100	1487	760	130	1280
14	~			850	12	1521	890	60	1280
15	855		1712	988		1814			

~ massive layer not present

Ages in italics refer to an age inferred from freeze cores

Table 5.
Outer Basin massive layer (ML) ages calculated from average sedimentation rates and depth in core (minus the thickness of all overlying massive layers). Note core TUL97A01, with its thicker deposits. Calculated ages show considerable aggreement between TUL97A03 and TUL99B11 except near the very top and very bottom.

Inner basin			Cumulative	Cumulative			Outer Basin
ML#	ML Ages	Intervals	Intervals	Intervals	Intervals	ML Ages	ML #
Sed-water interface							
			54	*54*			
1	54					54	**1**
		252	*252*	*193*	193		
2	306					247	**2**
					123		
		257			+	370	**3**
3	562	+					
		44	*301*	*288*	165		
4	606					535	**4**
		135	*135*	*116*	116		
5	741					652	**5**
					67		
					+	719	**6**
		132	*132*	*156*	88		
6	873					807	**7**
		47					
7	920	+					
		36	*83*	*70*	70		
8	956					877	**8**
					128		
					+	1005	**9**
					149		
					+	1154	**10**
		296	*296*	*305*	28		
9	1189					1182	**11**
		26	*26*	*21*	21		
10	1215					1203	**12**
		294	*294*	*293*	293		
11	1510					1496	**13**
					26		
					+	1521	**14**
		239	*239*	*242*	216		
12	1748					1712	**15**
		175					
13	1923						

+ Shading and plus sign indicates intervals that were summed

Table 6.

Comparison of massive layer (ML) ages from the inner and outer basin cores. Inner basin varve counts are from Table 3, outer basin ages are from Table 5. Column with cumulative intervals give values summed over several consecutive massive layers to generate proposed event correlations between basins.

3.4. Paleoseismicity

Event return periods

Over the entire cored record in Effingham Inlet, the crude, average "*event* return period" (i.e. the span of the record divided by the number of events) in the outer basin is 133 years, compared to 140 years for the inner basin. The generic term "event" is used here to connote uncertainty in judging a triggering mechanism. These numbers may have little bearing on actual *earthquake* return periods yet they nevertheless are useful for making bulk comparisons between basins, and eventually, between different inlets . The average return periods in both basins therefore compare quite favorably despite the fact that the sedimentation rate in the outer basin is nearly double that found in the inner basin. With sediment properties largely the same in both basins, sedimentation rates would exert primary control over the development of overburden pressure on sediment masses, while slope angles would control the factor of safety, or failure potential. Since these event deposits emanated from the inlet sidewalls and were not triggered by floods or delta front failures, the only remaining nonseismic triggering mechanism left is sidewall slope oversteepening. Assuming that sediment fails in each basin in a similar manner, from similar slopes, a mechanism that generates failures at the same rate, in spite of the dramatically different sediment loading rates, would appear to point to an earthquake trigger. Geotechnical analysis of inlet sediments is required to further probe this relationship.

The recurrence of paleoearthquakes is a critical characteristic in assessing the hazard from large earthquakes (McCalpin and Nelson, 1996). Assuming that all slope failures from Effingham Inlet were coseismic, the hypothetical average recurrence

interval, or return period for large (morphogenic) earthquakes is 133-140 years, compared to 150 years from Saanich Inlet (Blais-Stevens and Clague, 2001). The return period for regional crustal and intraplate earthquakes may be postulated by subtracting the number of known plate-boundary earthquakes (6 in the last 3,600 years) from the Saanich and Effingham inlet histories. From the Saanich Inlet ODP sites, 18 local events in the last 3,600 years at site 1033 gives an average return period of 200 years. Assuming that the last six plate-boundary events were recorded in the Effingham Inlet chronology, a similar calculation for Effingham Inlet gives a minimum of 17 non plate-boundary events in 3,280 years or an average return period of 193 years. This may be a maximum value as the possibility exists that fewer than 6 plate-boundary events were recorded in Effingham Inlet, or that not all local earthquakes triggered slope failures. The hypothetical return periods for moderate to large earthquakes from submarine slope failures in the two inlets on Vancouver Island are very similar; 193 to 200 years.

Earthquake statistics suggest that southern Vancouver Island should experience earthquake accelerations of 0.1 g or greater (i.e. sufficient to cause slope failures) approximately every 100 years (G. Rogers pers. comm.). Given that the event rates from Saanich Inlet and Effingham Inlet cores are roughly twice that of the statistically generated rate, earthquakes may be frequent enough in the region to be the main triggers, perhaps the only triggers, for slumps in these inlets.

Seismic constraints on slope failure

Historic earthquakes may help place some constraints on the seismic shaking required for slope failure in these inlets. The 1918 Vancouver Island earthquake (M 7 approx.) *likely* did not produce slope failures in Effingham Inlet. The possibility exists

that the *1946* failure, due to its size, cannibalized underlying sediments, thereby obliterating evidence of any early 20th century slope failures, whether coseismic or nonseismic. In shallow cores from the outer basin, an additional turbidite of unknown age immediately underlies the 1946 deposit in B10 and the pilot core from A03. Since there are no varves between the two deposits, no age could be assigned to the older of the two, although it is likely a 20th century event. Effingham Inlet lies 95 km south of the 1918 earthquake epicentre, close to the upper limit of the Modified Mercalli intensity V isoseismal, while Saanich Inlet, 220 km south of the epicentre, lies within the mid-IV isoseismal (Cassidy et al. 1988). No massive layers corresponding to 1918 have been reported from Saanich Inlet (Blais-Stevens et al., 1997).

The 1946 (M_W 7.3) Vancouver Island earthquake produced failures in both inlets, however they were much more widespread in Effingham Inlet than in Saanich Inlet (Blais-Stevens et al. 1997; Blais-Stevens and Clague, 2001). During the 1946 earthquake, Effingham Inlet would have been within the Modified Mercalli intensity VII isoseismal, while Saanich Inlet was within the mid-VI isoseismal (Rogers and Hasewega, 1978). Although only three piston cores (89-3, 91-4, 91-3) recovered the late 1800's interval in Saanich Inlet, no core shows a failure event that would correspond to the 1872 (M 7.4) northern Washington State earthquake, despite the likelihood that Modified Mercalli Intensities at Saanich Inlet were on the order of V to VI (Shedlock and Weaver, 1992). Evidence from these historic earthquakes might suggest that a Modified Mercalli intensity of >VI is required to trigger slope failures in these inlets. Some preliminary yet limited conclusions can be drawn from this. The inlets may be well situated to *both* record large earthquakes (e.g. M >7.3) occurring on Vancouver Island, however it is

likely that only Saanich Inlet could record large earthquakes (M >7.4) from northern Washington State, including the seismically active Puget lowlands region.

Standard seismic wave attenuation curves used in hazard mapping suggests the following ground motion levels in Saanich and Effingham inlets resulting from three major known earthquakes, shown below (Table 7).

Table 7. Site shaking level.

Site ground acceleration relative to gravity (g), based on hypothetical moment magnitudes (M_w) for three regional earthquakes.

Shaking Level — (g) acceleration due to gravity	Saanich Inlet	Effingham Inlet
Subduction events (M_w9)	0.14 g	0.15 — 0.17 g
1946 Vancouver Island (M_w7.3)	0.05 — 0.06 g	0.07 — 0.08 g
1100 AD Seattle Fault event (M_w >7.5?)	0.07 — 0.08 g	< 0.05 g ?

A sustained horizontal ground acceleration of 0.1 g is required to trigger liquefaction at many on-land (National Research Council, 1985, p.34) and submarine sites (G. Rogers, pers. comm.). In addition, a significant number of cycles of strong ground motion must be experienced rather than one peak acceleration of 0.1 g. However ground acceleration as low as 0.05 g clearly triggered failures in Saanich Inlet from the 1946 earthquake and the same earthquake produced the largest failure in Effingham Inlet in 3,000 years (and the second largest event in 3,200 years), with accelerations of 0.07 - 0.08 g.

The AD 1700 great earthquake produced only very small event deposits in Effingham Inlet yet the hypothetical ground motion that would be experienced during a plate-boundary earthquake is quite large (0.15 -0.17%g). In Saanich Inlet, this same earthquake triggered gravity flows much more limited in areal extent than other, older deposits. The level of shaking at Saanich Inlet during the 1700 earthquake is thought to have been around 0.14 g (G. Rogers, pers. comm.).

It is therefore not apparent from this analysis whether the extent of a failure deposit can be related to the ground acceleration of an earthquake. Many factors contribute to this relationship including the number of cycles of strong ground motion, the amplitude of this ground motion, the amount of sediment accumulated since the last failure, as well as local ground motion amplification factors. Local ground motion amplification effects in these inlets are not known, however, in a general sense, they are governed by the thickness of underlying, water-saturated Holocene deposits. Thick, water-saturated Holocene deposits are prone to ground motion amplification of low-amplitude, long-period seismic waves while thin Holocene deposits are more susceptible to amplification of high-amplitude, short-period waves. Holocene deposits that pinch out along steep fjord walls may not experience the kind of ground motion amplification that thick delta fans or basin centres do. In Effingham Inlet, and probably in Saanich Inlet, these sediment wedges are the likely source areas of the slope failures and turbidites. It may be that earthquakes producing an abundance of low-amplitude, long-period ground motions are less conducive to submarine failures in these instances.

Event Histories and Regional Paleoseismicity:

Saanich Inlet has been repeatedly cored (Appendix 3) and studied as a potential source of paleoseismic information. The stratigraphy and varve counts from Saanich Inlet piston cores investigated by Bobrowsky and Clague (1990), Blais (1995) and Blais-Stevens et al. (1997) were revisited by this author and found to contain very few gravity flow deposits that were not contemporaneous along approximately 15 km of the axis of the basin over the last 1700 years (Table 8, Part B; and Appendix 4). This revised stratigraphy placed emphasis on the matching of varved intervals between events and it resulted in event beds that could be traced over 15 km of the axis of the inlet (Appendix 4). The stratigraphy and varve counts from the piston cores were then checked against those from the ODP Leg 169S cores (Sites 1033 and 1034) (Blais-Stevens and Clague, 2001; Nederbragt and Thurow, 2001), and all were found to be well matched (Table 8, Part A; and Appendix 5). The two ODP sites have very little offset in their chronologies as a result (< 0.5% at 3000 years BP). These flows did not travel along the axis of the basin since no proximal to distal thinning trends are evident (Appendix 4). Rather, the flows originated along the adjacent sidewalls of the inlet as discrete slope failures. Therefore, in order for an individual event to be represented in piston cores distributed over 15 km of the basin axis, numerous, contemporaneous slope failures must have occurred. Since agents such as storm waves and flood deposit can be ruled out for this setting, only earthquakes remain as possible triggers for such extensive, and *simultaneous* mass wasting events in the inlet (Appendix 6).

The varve-based event chronology from Effingham Inlet (EI) was compared with the revised chronology from Saanich Inlet (SI). There have been a comparable number of

slope failure events in each basin over the last 3,500 years (EI = 24; SI = 22); despite the fact that Saanich Inlet has a sedimentation rate more than double that of Effingham Inlet's inner basin (Bornhold et al, 1998). This suggests that, given the similar slope aspects and sediment properties in each basin, there does not appear to be a strong correlation between sedimentation rates and failure rates, which would lend support to the coseismic nature of these deposits.

The event histories from the inner and outer basin of Effingham Inlet were merged to give a local event history, and this was in turn compared to the Saanich Inlet history. Without adjustments, a first-order comparison of the two inlet histories shows a near-symmetrical recurrence pattern over many consecutive events to about 1,500 y BP (Figure 16). Correlation of varve intervals obtained from core stratigraphy also corroborates this pattern (Appendix 7). This matching "barcode" pattern could plausibly be a product of contemporaneous slope failures in both inlets. Only large earthquakes could produce such a repeated pattern in two inlets that are 130 km distant from each other. Eight events show a close match with very little offset in age; 6 events correlate to with 3% of their age. These events are dated from the Effingham Inlet chronology, in years before 2000 AD, as: 54, 300, 606, 873, 920, 1189, 1215, and 1510.

Any match between the event histories prior to about 1,500 y BP, however, is limited, even with the degree of leeway provided by varve dating uncertainties and inaccuracy. Slight offsets in the absolute varve ages of events in Saanich Inlet and Effingham Inlet might arise out of varve counting errors or uncertainties generated when sedimentation rates were applied to the bioturbated intervals in the Effingham Inlet cores, however these are likely small. The largest potential source of error arising out of the

chronostratigraphy in Effingham Inlet lies in the choice of the topmost datum, however manual varve counting and incorporation of the bioturbated intervals in the chronology also give rise to dating inaccuracy. Regardless of possible inaccuracies, the two varve chronologies should not be treated as "elastic" in an effort to correlate events that may not be contemporaneous. Age discrepancies of no more than a few decades may therefore be accommodated.

If the varve ages in Effingham Inlet approach the actual age of the failure events then there does appear to be a credible temporal correlation between failures in the two basins (Appendix 7). Given the 130 km separation between the two inlets what might the coeval events say about regional paleoseismicity? Paleo-earthquakes occurring south of Saanich Inlet - such as the intraplate earthquakes that tend to cluster around the Puget lowlands (Rogers, 1998), may not have produced sufficient strong shaking in Effingham Inlet. By the same reasoning, paleo-earthquakes occurring north of Effingham Inlet may not have produced strong shaking in Saanich Inlet. Therefore, failures that occurred simultaneously in both inlets must have resulted from earthquakes that were very large - either shallow and located within less than 200 km radius of both basins, or from plate-boundary ruptures. The histories from these inlets combined with other coastal earthquake histories may contribute to the long-standing question of whether most great earthquakes rupture in a piecemeal fashion over several decades or centuries, or whether the entire length has ruptured many times.

Table 8 **Saanich Inlet Event Chronology**

Part A

Part B

Intervals		Events								Previously unrecognized correlations					
***89-3* & 1033**	***91-4* & 1034**	**Massive Layer Varve Ages**				**Saanich**	"Key core"	Comments	Massive Layers - Piston Cores					
		1033		1034		**Inlet**	89-3		(ML# from top of each core)					
Intervals	Intervals	Yrs before 2000	yrs AD	Yrs before 2000	yrs AD	**Event**	ML #		91-1	89-1	91-2	89-3	91-4	89-2
54	60	54	1946	60	1940									
						1	1	1946 earthquake				1		
220	*214*													
		274	1726	**274**	1726	2	2	1700 earthquake?			1	2	1	
182 **	*171*													
		456	1544	**445**	1555	3	3			1	2	3	2	2
113	112						4							
		569	1431	**557**	1443	4	5	Marker layer	2	2		5	3	
258	260													
		827	1173	**817**	1183	5	6	Marker layer	4	3	4	6	4	3
72	71													
		899	1101	**888**	1112	6	7		5	4	5	7		4
132	133													
		1032	969	**1021**	979	7	8		6	5	6	8		5
142	141						9							
		1174	827	**1162**	838	8	10		7	6	7	10		
59	57													
		1233	768	**1219**	781	9	11		8	7	8	11		6?
324	325													
		1558	444	**1544**	456	10	12		9?	8	9	12		
76	638													
)+		**1634**	368			11			10?		10			
151														
)+		**1785**	217			12			11?					
379														
		2164	-162			13								
30	27													
		2194	-192	**2182**	-182	14								
227	228													
		2421	-419	**2410**	-410	15								
403	402													
		2824	-822	**2812**	-812	16								
129	130													
		2953	-951	**2942**	-942	17								
202														
		3155	-1153			18								
139														
		3294	-1292			19								
31														
		3325	-1323			20								
247														
		3572	-1570			21								

Part A Varve counts from Blais-Stevens et al. (1997); Blais-Stevens and Clague, (2001); Nederbragt and Thurow, (2001)
Italics indicate varve counts from piston cores (Blais-Stevens et al., 1997)
Normal font indicates intervals form ODP counts (Nederbragt and Thurow, 2001)

** Varve count of 182 from correlative section in 91-2
Note: This interval in 89-3 was reassessed as an undercount due to core loss and because in several other correlative core sections, including the ODP Leg 169s cores, this interval had higher counts ranging from 171 to 192 varve years. As a result of this adjustment, 1033 and 1034 have event ages that are closely matched.
The AD 1726 event (Blais-Stevens & Clague's (2001) proposed 1700 AD earthquake) has the same age throughout the basin and is much more widespread throughout the basin (Part B), making its link to an earthquake stronger.
Surface datum used to derive ages was AD 1940 *Rhizosolenia* sp. diatom horizon and AD 1946 debris flow.

Part B Proposed correlation scheme for Saanich Inlet piston cores originally studied by Blais (1995); Blais-Stevens et al. (1997)
Massive layers are much more widespread than previously thought, lending support to the coseismic nature of these deposits.
Massive layers are numbered from the top of each core; missing numbers are layers that did not correlate.

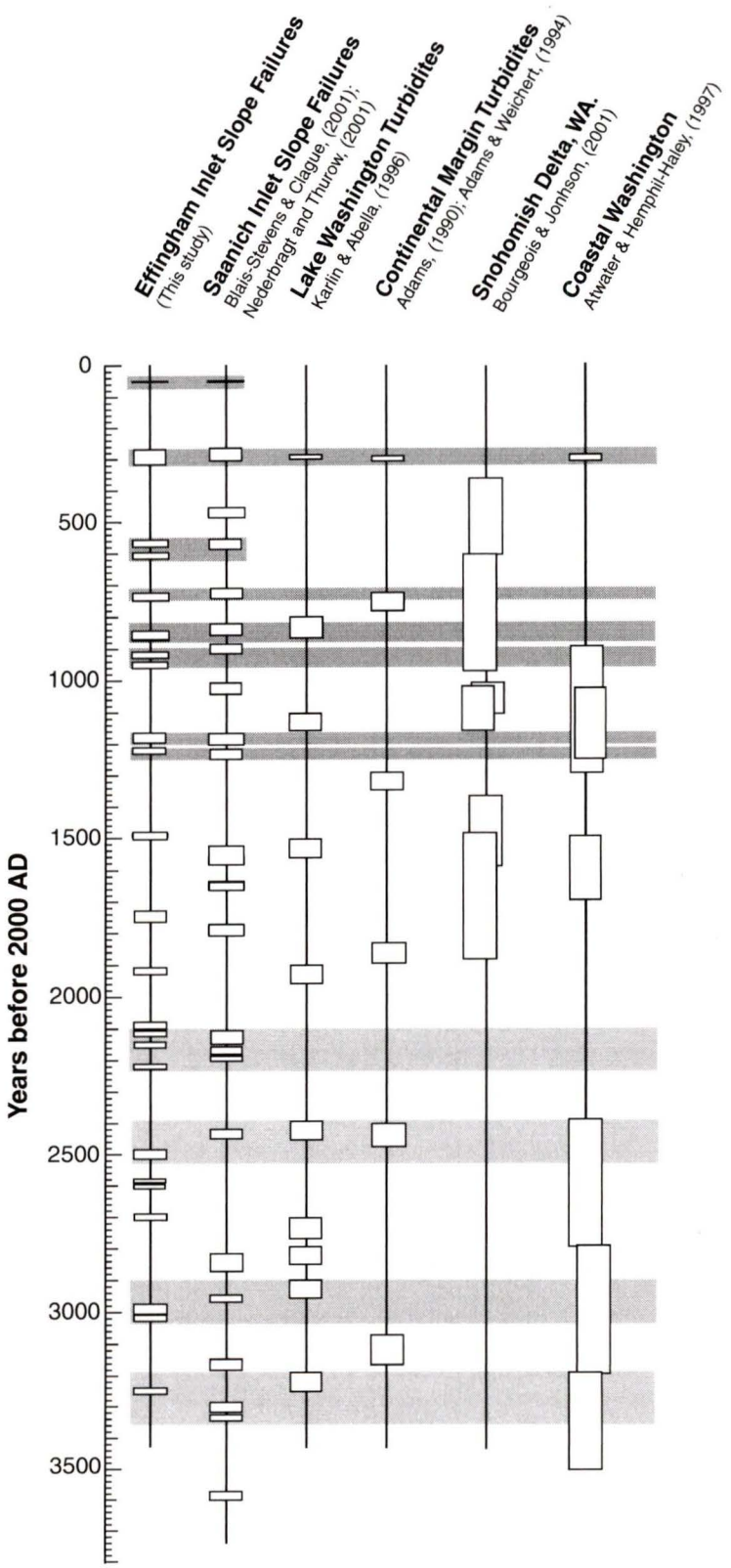

Figure 16. Paleoseismic histories from Vancouver Island to coastal Washington and Oregon, showing potential correlation in timing of events. Effingham Inlet history shows close match with Saanich Inlet until 1,500 y BP (dark shading), after which few correlations seem apparent (light shading). Thickness of event time "windows" for the varve chronologies are estimated uncertainties based on thickness of the preceding interval and thickness of bioturbated zones. Overlapping event windows on right-hand columns arise out of radiocarbon dating uncertainties.

4.0. Discussion

Since the coseismic nature of these deposits can readily be called into question, their potential as a record of paleoseismicity will only be accepted when a high degree of varve dating accuracy can be demonstrated *and* when contemporaneous events are found at distant sites. In theory, varved sediments offer an unparalleled chance at dating accuracy, however in practice, establishing a reliable varve age model requires an understanding of basin stratigraphy and "microstratigraphy" arrived at through repeated coring and concerted effort to recover undisturbed, uppermost sediments in order to establish bio- and chemo-markers.

Hampering many efforts to further refine the paleoseismic record of the Pacific Northwest has been the reliance on radiocarbon as a dating tool. Although the uncertainty associated with radiocarbon dating of paleoearthquakes does not diminish the strength of the paleoseismic evidence itself, large ranges in event ages have made it difficult to infer anything but broad, often conjectural correlations of supposed regional earthquakes (Atwater and Hemphil-Haley 1997; Bourgeois and Johnson, 2001; Blais-Stevens and Clague, 2001). However, despite the relative accuracy of varve-based dating, no regional paleoseismic conclusions can be confidently asserted until the age models of the basins are demonstrably very close to their *true* ages. This is partly because the record of paleoseismicity in varved sediments lies more in the precise chronology than in the deposits themselves.

Accuracy of the chronology remains crucial in comparative studies of proxy records from varved sediments, so that local variations can be extracted from broader

regional events and trends. While this study demonstrates this well for paleoseismic records, the same might be said of other records. Holocene proxy records of marine environmental change may be subtle in comparison to those of the late Quaternary (Behl and Kennett, 1996), nevertheless, they may yet be deciphered and compared regionally in order to test ocean-atmosphere-climate linkages under present-day interglacial conditions. The benefits of multiple, and multi-tier coring, and site-to-site correlation of microstratigraphy, combined with an understanding of basin sedimentary and hydraulic dynamics are underscored.

Conclusions

1. Indistinctly laminated to homogeneous sediments recovered in piston cores are the result of bioturbation, arising from past oxygenation of the basins. Based on present-day oceanographic conditions and laminae-scale observations, bioturbated intervals in Effingham Inlet sediments likely resulted from quasi-annual and short-lived oxygenation, repeated over decadal time-scales, that destroyed at most a few varves during each episode. Periods of enhanced oxygenation of the inlet were followed by many decades of anoxia. The Effingham Inlet record of oxygenation-bioturbation pulses likely has paleoclimatic and paleoceanographic implications and may correlate to other similar late Holocene records from the northeast Pacific margin (e.g. Santa Barbara Basin).

2. Graded units from the inlet were for the most part the result of turbidity currents that were initiated by slope failures. In the inner basin, these originated along the western basin slope. Progressively deformed laminae in the inner basin displaying, from bottom to top, brittle, plastic and fluid behaviour were likely produced by paleoearthquakes and provide a window on the rheological transformation of these sediments under cyclic shear stress.
3. Sedimentation rates obtained from varve thicknesses averaged 2.6 mm/a in the inner basin, with average rates slightly higher at sites along the western margin (2.6 mm/a) and lower along the eastern sites (2.2 mm/a). Although the mean rates differ depending on the site, the range of values was the same over the whole basin. The outer basin had much higher rates that averaged 4.3 mm/a. Rates of slope failure in each basin are similar (inner, 140; outer, 133) and do not appear to reflect the large difference in sedimentation -i.e. loading rate.
4. Many radiocarbon dates from wood samples were too old given their stratigraphic context, probably due to erosion and redeposition of old material. The dates (wood, shell and fish bone) that were retained for the chronology gave an average inner basin sedimentation rate of 2.3 mm/a. Based on stratigraphic, radiocarbon and sedimentological evidence, very little of the varved record was lost during coring or eroded during emplacement of the turbidites.
5. Varve ages were obtained for 24 slope failure events over approximately 3,300 years of the inner basin record. Events that coincide closely in varve

age with known large earthquakes include the AD 1946 Vancouver Island earthquake, and the AD 1700 plate-boundary earthquake. Eleven slope failure events were coeval in both basins of the inlet over the past 2,000 years. Comparison of the Effingham Inlet history with a similar varved record from Saanich Inlet (130 km distant) has yielded 8 closely matched events over the last 1,500 years of the record with 6 of these events correlating to within less than 3% of their age. Large earthquakes, such as the AD 1946 and 1700 earthquakes, are required to trigger simultaneous turbidites and debris flows in these two inlets.

References

Adams, J. 1990. Paleoseismicity of the Cascadia subduction zone: evidence from turbidites off the Oregon-Washington margin. Tectonics. 9, 569-583.

Adams, J., 1992. Paleoseismology: A search for ancient earthquakes in Puget Sound. Science, 258: 1592-1593.

Adams, J., Weichert, D., 1994. Near-term probability of the future Cascadia megaquake. ILP Paleoseismology Workshop, Sept. 1994, unpublished material. 3pp.

Atwater, B.F., Hemphil-Haley, E., 1997. Recurrence intervals for great earthquakes of the past 3,500 years at northeastern Willipa Bay, Washington, U.S. Geological Survey professional paper 1576. 108pp.

Atwater, B.F. 1992. Geologic evidence for earthquakes during the past 2000 years along the Copalis River, southern coastal Washington. Journal of Geophysical Research. 97, 1907-1919.

Atwater, B.F. 1994. Geology of liquefaction features about 300 years old along the lower Columbia River at Marsh, Brush, Price, Hunting, and Wallace Islands, Oregon and Washington. United States Geological Survey, Open File Report, 94, p.64

Atwater, B.F., Nelson, A.R., Clague. J.J., Carver, G.A., Yamaguchi, D.K., Bobrowsky, P.T., Bourgeois, J., Darienzo, M.E., Grant, W.C., Hemphill-Haley, E., Kelsey, H.M., Jacoby, G.C., Nishenko, S.P., Palmer,. S.P., Peterson, C.D., Reinhart, M.A., 1995. Summary of coastal geologic evidence for past earthquakes at the Cascadia subduction zone. Earthquake Spectra, 11(1): 1-18.

Behl, R.J., 1995. Sedimentary facies and sedimentology of the late Quaternary Santa Barbara Basin, Site 893. In Kennet, J.P. Baldauf, J.G., and Lyle, M. (Eds.) Proceedings of the Ocean Drilling Project, Scientific Results. 146 (pt. 2): 295-308.

Behl, R.J. and Kennett, J.P., 1996. Brief interstadial events in the Santa Barbara basin, NE Pacific, during the past 60 kyr. Nature, 379: 243-246.

Blais, A. 1995. Foraminiferal biofacies and Holocene sediments from Saanich Inlet, British Columbia. Implications for environmental and neotectonic research. Unpublished Ph.D. Thesis, Carleton University, Ottawa, Ontario, Canada. 280 pp.

Blais-Stevens, A., and Clague, J.J., 2001, Paleoseismic signature in late Holocene sediment cores from Saanich Inlet, British Columbia. Marine Geology, 175(1-4): 131-148.

Blais-Stevens, A., Clague, J.J., Bobrowsky, P.T., and Patterson, R.T. 1997. Late Holocene sedimentation in Saanich Inlet, British Columbia, and its paleoseismic implications. Canadian Journal of Earth Sciences. 34, 1345-1357.

Bobrowsky, P.T. and Clague, J.J. 1990. Holocene sediments from Saanich Inlet, British Columbia, and their neotectonic implications. Geological Survey of Canada, Current Research Part E, Paper 90-1E, 251-256.

Bornhold, B.D. 1983. Sedimentation in Douglas Channel and Kitimat Arm. Can. Tech. Rep. Hydrogr. and Ocean Sci. 18: 88-114.

Bornhold, B.D., Firth, J.V. et al. 1998. Proceedings of the Ocean Drilling Program. Initial Reports. 169S, 5-61

Bornhold B.D. and Harper, J.R. 1998. Engineering geology of the coastal and nearshore Canadian Cordillera. Proceedings of the 8th international congress association. for engineering geology and the environment. 63-75

Bornhold, B.D. Ren, P., Prior, D.B. 1994. High-frequency turbidites in British Columbia fjords. Geo-Marine Letters. 14: 238-243.

Bottjer, D.J. and Savrda,C.E. 1993. Oxygen-related mudrock biofacies. In Sedimentology Review 1. V.P. Wright (ed), Blackwell London, 92-102.

Bourgeois, J., Johnson, S.Y., 2001. Geologic evidence of earthquakes at the Snohomish delta, Washington in the past 1200 years. GSA Bulletin, 113: 482-494.

Brodie I. and Kemp. A.E.S., 1994. Variation in biogenic and detrital fluxes and formation of laminae in late Quaternary sediments from the Peruvian coastal upwelling zone.Marine Geology, 116: 385-398.

Bryant, A.A. 1998. Metapopulation ecology of Vancouver Island marmots (Marmota vancouverensis). Ph.D. dissertation, University of Victoria, (Victoria, BC). 125 pp.

Bryant A.A. 1999. Vancouver Island Marmot Recovery Foundation. 1999 Annual report. *Web:* http://www.islandnet.com/~marmot/subdir/99diary.html

Bull, D. and Kemp, A.E.S., 1995 Composition and origins of laminae in late Quaternary and Holocene sediments from the Santa Barbara Basin. In Kennet, J.P. Baldauf, J.G., and Lyle, M. (Eds.) Proceedings of the Ocean Drilling Project, Scientific Results. 146 (pt. 2): 77-87.

Busch, W. H. and Keller. G. H., 1981. The physical properties of Peru-Chile continental margin sediments - The influence of coastal upwelling on sedimentary properties. Journal of sedimentary Petrology. 51:705-719.

Busch, W. H. and Keller. G. H., 1982. Consolidation characteristics of sediments from the Peru-Chile continental margin and implications for past sedimentary instability. Mar. Geol. 45: 17-39.

Chang, A. S. and Grimm, K. A., 1999. Speckled beds: distinctive gravity-flow deposits in finely laminated diatomaceous sediments, Miocene Monterey Formation, California. Journal of Sedimentary Research. 69(1): 122-134.

Clague, J.J., 1996. Paleoseismology and seismic hazards, southwestern British Columbia. Geological Society of Canada Bulletin. 494, 88pp.

Clague, J.J., 1997. Evidence for large earthquakes at the Cascadia subduction zone. Reviews of Geophysics. 35: 439-460.

Clague, J.J., 1999. The Earthquake Threat in Southwestern Columbia. *The Office of Critical Infrastructure Protection and Emergency Preparedness, Government of Canada*, http://www.epc-pcc.gc.ca/ *Scientific and Technical Reports. Report available at*: http://www.epc-pcc.gc.ca/research/down/clague.pdf

Clague, J.J., and Bobrowsky, P.T. 1994. Evidence for a large earthquake and tsunami 100-400 years ago on western Vancouver Island, British Columbia. Quaternary Research. 41, 176-184.

Clague, J.J., and Bobrowsky, P.T. 1999. The Geologic signature of great earthquakes off Canada s west coast. Geoscience Canada. 26, 1-15

Clague, J.J., Atwater, B.F., Wang, K., Wang, Y., Wong, I., 2000. Penrose Conference - Great Cascadia Earthquake Tricentennial. Episodes, 23(1): 281-282.

Clague, J.J., Naesgaard, E., Ny., A., 1992. Liquefaction features on the Fraser Delta: Evidence

for prehistoric earthquakes> Canadian Journal of Earth Sciences, 29: 1734-1745.

Dallimore, A. 2001. "Late Holocene Geologic, Oceanographic and Climate History of an Anoxic Fjord: Effingham Inlet, West Coast, Vancouver Island." PhD thesis, Carleton University, Ottawa, Ontario, Canada.

De Diego T.A. and Douglas, R.G., 1999. Oxygen-related sediment fabrics in modern "black shales", Gulf of California, Mexico. Journal of Foraminiferal Research. 29(4): 453-464.

Dragert H. and Hyndman, R., 1995. Continuous GPS monitoring of elastic strain in the northern Cascadia subduction zone. Geophysical Research Letters, 22: 755-758.

Einsele, G., 1990. Deep-reaching liquefaction potential of marine slope sediments as a prerequisite for gravity mass flows? (Results from the DSDP). Marine Geology, 91: 267-279.

Environment Canada, 1999. Climate Trends and Variations Bulletin for Canada (1999). http://www.msc-smc.ec.gc.ca/ccrm/bulletin/annual99/page2.htm

Fisher, R.V., 1983. Flow transformations in sediment gravity flows. Geology, 11: 273-274.

Follmi, K.B., and Grimm, K.A., 1990. Doomed pioneers: gravity flow deposition and bioturbation in marine oxygen-deficient environments. Geology, 18: 1069-1072.

Francis, R. C. and Hare, S.R., 1994. Decadal-scale regime shifts in the large marine ecosystems of the Northeast Pacific: a case for historical science. Fish. Oceanogr. 3: 279-291.

Geological Survey of Canada, 2001. Natural Resources Canada, Earthquake Hazards Program: Western Canada, http://www.pgc.nrcan.gc.ca/seismo/table.htm

Gorsline, D.S., 1996. Depositional events in Santa Monica Basin, California Borderland, over the past five centuries. Sedimentary Geology, 104: 73-88.

Gorsline, D.S., de-Diego, T., Nava-Sanchez, E.H., 2000. Seismically triggered turbidites in small margin basins; Alfonso Basin, western Gulf of California and Santa Monica Basin, California Borderland. In: Seismoturbidites, seismites and tsunamiites. T. Shiki, M.B. Cita, D.S. Gorsline (Eds.). Sedimentary Geology, 135(1-4): 21-35.

Gould, S.J., 1989. Wonderful Life: The Burgess Shale and the Nature of History. New York, NY, W.W. Norton and Co., 347 pp.

Grimm K. A. and Orange, D. L., 1997. Synsedimentary fracturing, fluid migration, and subaqueous mass wasting: intrastratal microfractured zones in laminated diatomaceous sediments, Miocene Monterey Formation , California, U.S.A.. Journal of Sedimentary Research, 67(3): 601-613.

Grimm, K.A., Lange, C.B., Gill, A.S., 1996. Biological forcing of hemipelagic sedimentary laminae: evidence from ODP site 893, Santa Barbara Basin, California. Journal of Sedimentary Petrology. 66(3): 613-624.

Hampton, M. A., 1972. The role of subaqueous debris flow in generating turbidity currents. Journal of Sedimentary Petrology, 42: 775-793.

Hawkins, A. B., 1984. Introduction; submarine slope failures. In: Seabed mechanics. Edited by: B. Denness, Graham & Trotman. London, 51-64.

Heezen, B.C., and Ewing, M., 1952. Turbidity currents and submarine slumps, and the 1929 Grand Banks earthquakes. American Journal of Science, 250: 849-873.

Hein, F. J. and Gorsline, D. S., 1981. Geotechnical aspects of fine-grained mass-flow deposits: California Borderland. Geo Marine Letters 1: 1-5.

Herzer R.H. and Bornhold, B.D. 1982. Glaciation and post-glacial history of the continental shelf off southwestern Vancouver Island, British Columbia. Marine Geology, 48(3-4): 285-319.

Hill, P.R. and Marsters, J.C., 1990. Controls on physical properties of Peru continental margin sediments and their relationship to deformational styles. Proceedings of the Ocean Drilling Program, Scientific Results, v. 112. Ocean Drilling Program, College Station, Texas. 112: 623-632

Inouchi, Y., Kinugasa, Y., Kumon, F., Nakano, S., Yasumatsu, S., Tsunemasa, S., 1996. Turbidites as recorders of intense paleoearthquakes in Lake Biwa, Japan. Sedimentary Geology, 104: 117-125.

Karlin, R, E. and Abella, S.E.B., 1992. Paleoearthquakes in the Puget Sound region recorded in sediments from Lake Washington, U.S.A.. Science, 258: 1617-1620.

Karlin, R, E. and Abella, S.E.B., 1996. A history of Pacific Northwest earthquakes recorded in Holocene sediments from Lake Washington. Journal of Geophysical Research, 101(no.B3): 6137-6150.

Keller, G.H., 1983. Coastal upwelling, its influence on the geotechnical properties and stability characteristics of submarine deposits. In: Coastal Upwelling: its sediment record, Part A. J. Thied, E.Suess, (eds), Plenum Press, New York, 181-199.

Kemp, A.E.S. 1996. Laminated sediments as paleo-indicators. In Paleoclimatology and Palaeoceanography from laminated sediments, Ed. A.E.S. Kemp, Geol. Soc. Spec. Pub. #116, vii-xii.

Kemp, A.E.S., 1990. Sedimentary fabrics and variation in laminae style in Peru continental margon upwelling sediments. Proceedings of the Ocean Drilling Project, Scientific Results. 112:43-58.

Linden, R.H. and Clague, J.J., 1993. Paleoseismic implications of sediment cores from Comox Lake, British Columbia. Current Research Part E, Geological Survey of Canada, Paper 93-1E, 41-46.

Lindsley-Griffin, N., Kemp, A., and Swartz, J.F., 1990. Vein structures of the Peru margin, Leg 112. Proceedings of the Ocean Drilling Program, Scientific Results, v. 112. Ocean Drilling Program, College Station, Texas. 112: 3-16.

Lowe, D.R., 1982. Sediment gravity flows: II. Depositional models with special references to the deposits of high-density turbidity currents. Journal of Sedimentary Petrology, 52:279-297.

Mathewes R.W. and Clague J.J., 1994. Detection of large prehistoric earthquakes in the Pacific Northwest by microfossil analysis. Science, 264: 688-691. 1

McCalpin, J.P. and Nelson, A.R., 1996. Introduction to Paleoseismology. *In:* Paleoseismology. *Edited by:* J.P. McCalpin, International Geophysical Series, Volume 62, Academic Press. 583pp.

Middleton, G.V. and Hampton, M. A., 1976. Subaqueous sediment transport and deposition by sediment gravity flows. In: Marine sediment transport and environmental management. Edited by: D.J. Stanley and J.P. Swift, New York, Wiley, 197-218.

Mohrig, D, Elverhoi, A., Parker, G., 1999. Experiments on the relative mobility of muddy subaqueous and subaerial debris flows, and their capacity to remobilize antecedent deposits. Marine Geology, 154: 117-129.

Nakajima, T. and Kanai, Y., 2000. Sedimentary features of seismoturbidites triggered by the 1983 and older historical earthquakes in the eastern margin of the Japan Sea. Sedimentary

Geology, 135: 1-19.

National Research Council, 1985. Liquefaction of Soils During Earthquakes. National Academy Press, Washington, D.C.

Nederbragt, A.J. and Thurow, J.W., 2001. A 6000 yr varve record of Holocene climate in Saanich Inlet, British Columbia, from digital colour analysis of ODP Leg 169S cores. Marine Geology, 175(1-4): 95-110.

Nelson, A.R., Kelsey, H.M., Hemphill-Haley, E., and Witter, R.C., 1996. A 7500-yr lake record of Cascadia tsunamis in southern coastal Oregon. Geological Society of America, abstracts with Programs, 28: 95.

Ozalas, K., Savrda, C.E., Fullerton Jr., R.R., 1994. Bioturbated oxygenation-event beds in siliceous facies: Monterey Formation (Miocene) California. PALAEO. 112: 63-83.

Prior D.B., and Bornhold, B.D., 1988. Submarine morphology and processes of fjord fan deltas and related high-gradient systems: modern examples from British Columbia. In: Fan Deltas: Sedimentology and tectonic setting. ed: W. Nemec, R.J. Steel, Blackie and Son, 125-143.

Prior, D.B., Bornhold, B.D., and Johns, M.W. 1984. Depositional characteristics of a submarine debris flow. Jo. of Geology. 92: 707-727.

Prior, D.B., Bornhold, B.D., Wiseman Jr., W.J., Lowe , D.R., 1987. Turbidity current activity in a British Columbia fjord. Science. 237: 1330-1333.

Prior, D.B.and Bornhold, B.D. 1989. Submarine sedimentation on a developing Holocene fan delta. Sedimentology. 36: 1053-1076.

Riddihough, R.P., 1977. A model for recent plate interactions off Canada's west coast. Canadian Journal of Earth Sciences, 14: 384-396.

Robinson, S.W., Thompson, G., 1981. Radiocarbon corrections for marine shell dates with application to southern Pacific Northwest Coast prehistory. Syesis, 14: 45-57.

Rogers, G.C. 1980, A documentation of soil failure during the British Columbia earthquake of 23 June, 1946. Can. Geotech. J., 17: 122-127.

Rogers, G.C. and Hasewega, H.S., 1978. A second look at the British Columbia earthquake of23 June, 1946. Seismological Society of America Bulletin, 68: 653-676.

Rogers, G.C., 1988. An assessment of the megathrust earthquake potential of the Cascadia subduction zone. Canadian Journal of Earth Sciences. 25: 844-852.

Rogers, G.C., 1998. Earthquakes and earthquake hazard in the Vancouver area, In: Geology and Natural Hazards of the Fraser River Delta, British Columbia. J.J. Clague, J.L. Luternauer, D.C. Mosher (Eds.). Geological Survey of Canada Bulletin, 68: 653-676.

Sancetta, C. and Calvert, S.E., 1988. The annual cycle of sedimentation in Saanich Inlet, British Columbia: implications for the interpretation of diatom fossil assemblages: Deep-Sea Research. 35(1a), 71-9

Sancetta, C., 1989. Spatial and temporal trends in diatom flux in British Columbia fjords. Journal of Plankton Research. 11(3): 503-520.

Savrda, C.E. and Bottjer, D.J., 1991 Trace fossil model for reconstruction of paleo-oxygenation in bottom waters. Geology 14: 3-6.

Savrda, C.E., Bottjer, D.J., Gorsline, D.S., 1984. Development of a comprehensive oxygen-deficient marine biofacies model: Evidence from Santa Monica, San Pedro, and Santa Barbara Basins, California Continental Borderland. AAPG Bulletin, 69(9): 1179-1192.

Savrda C.E. and Ozalas, K.1993. Preservation of mixed-layer ichnofabrics in oxygen-event beds. PALAIOS, 8: 609-613

Seilacher, A., 1969. Fault-graded beds interpreted as seismites. Sedimentology, 13: 155-159.

Seilacher, A., 1984. Sedimentary structures tentatively attributed to seismic events. Marine Geology, 55: 1-12.

Shanmugam, G., 1996. High-density turbidity currents: are they sandy debris flows? Journal of Sedimentary Research, 66(1): 2-10.

Shedlock, K.M., and Weaver, C.S., 1991. Program for Earthquake Hazard Assessment in the Pacific Northwest. U.S. Geological Society Circular 1067, 29 pp.

Shilts, W.W. and Clague, J.J., 1992. Documenting of earthquake-induced disturbance of lake sediments using subbottom acoustic profiling. Can. J. Earth Sci., 29: 1018-1042.

Sims, J.D., 1975, Determining earthquake recurrence intervals from deformational structures in young lacustrine sediments. In: Recent crustal movements. N. Pavoni and R, Green (eds), Tectonophysics, 29(1-4): 141-152.

Soutar, A. and Crill, P.A.,. Sedimentation and climatic patterns in the Santa Barbara Basin during the 19th and 20th centuries. Geological Society of America Bulletin, 88: 1161-1172.

Stuiver, M., and Brazuinas, T.F., 1993. Modeling atmospheric ^{14}C influences and ^{14}C ages of marine samples to 10,000 BC. Radiocarbon, 35: 137-189.

Stuiver, M., and Reimer, P.J., 1993. Extended ^{14}C data base and revised CALIB 3.0 (super 14) C age calibration program. Radiocarbon, 35: 215-230

Syvitski J.P.M., Burrell, D.C. and Skei, J.M., 1987. Fjords - processes and products. Springer Verlag. 379p.

Syvitski, J.P.M. and Schafer, C.T. 1996. Evidence for an earthquake-triggered basin collapse in Saguenay Fjord, Canada. Sed. Geol. 104: 127-153.

Vittori, E., Labini, S.S., Serva, L., 1991. Paleoseismology: review of the state-of-the-art. Tectonophysics, 193: 9-23.

Wells R.E., Weaver, C.S., and Blakely, R.J., 1988. Fore-arc migration in Cascadia and its neotectnic significance. Geology, 26:759-762.

Yorath, C.J., Sutherland, B.A., Massey N.W.D., 1999. LITHOPROBE, southern Vancouver Island, British Columbia; geology. In:. Bulletin, Geological Survey of Canada 145pp.

Appendices

Appendix1 and 2, see back pocket material

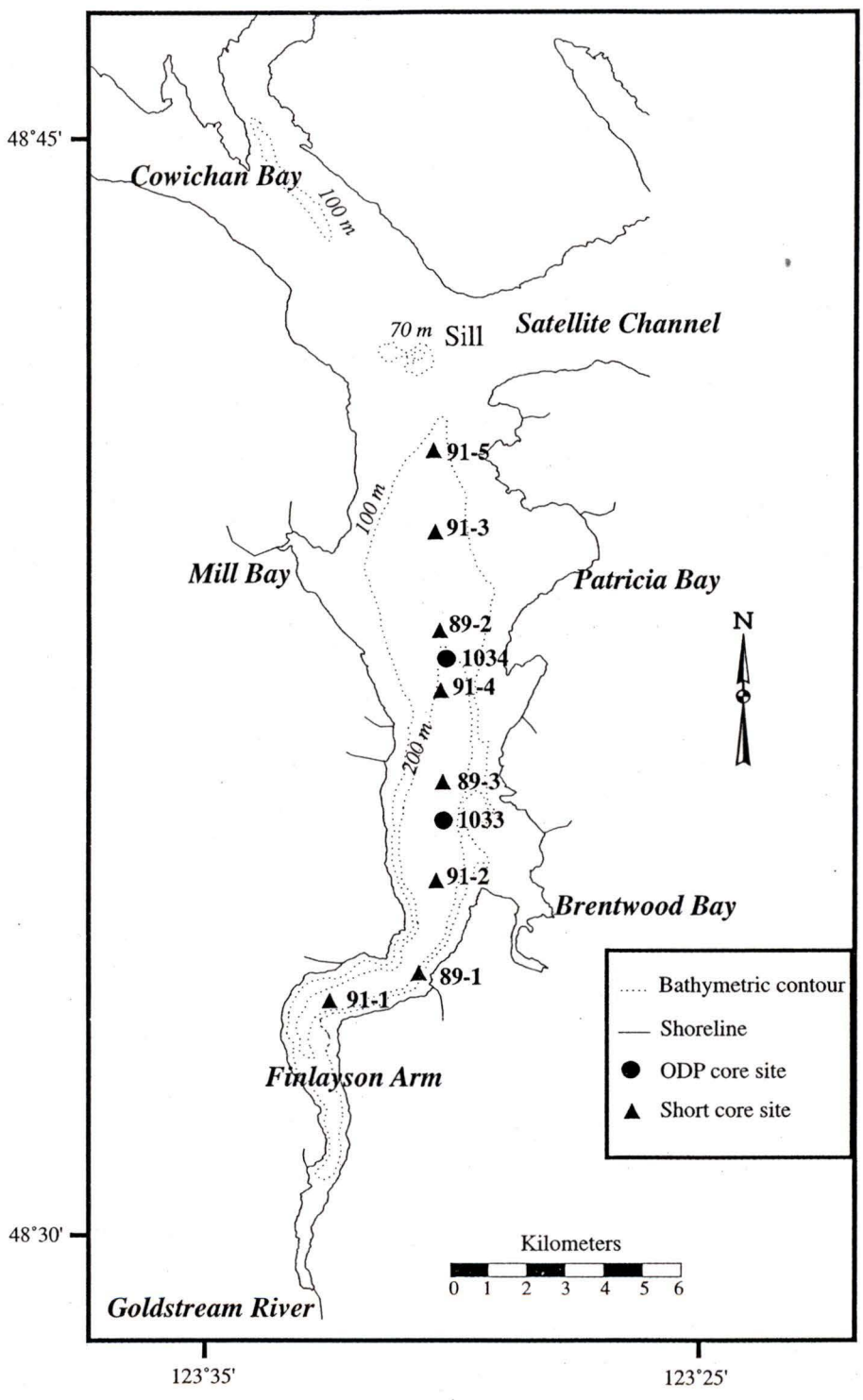

Appendix 3. Map of Saanich Inlet showing ODP Leg 169S core and piston core locations. All cores except 91-3 and 91-5 were incorporated in the Saanich Inlet stratigraphy depicted in appendices 4 and 5.

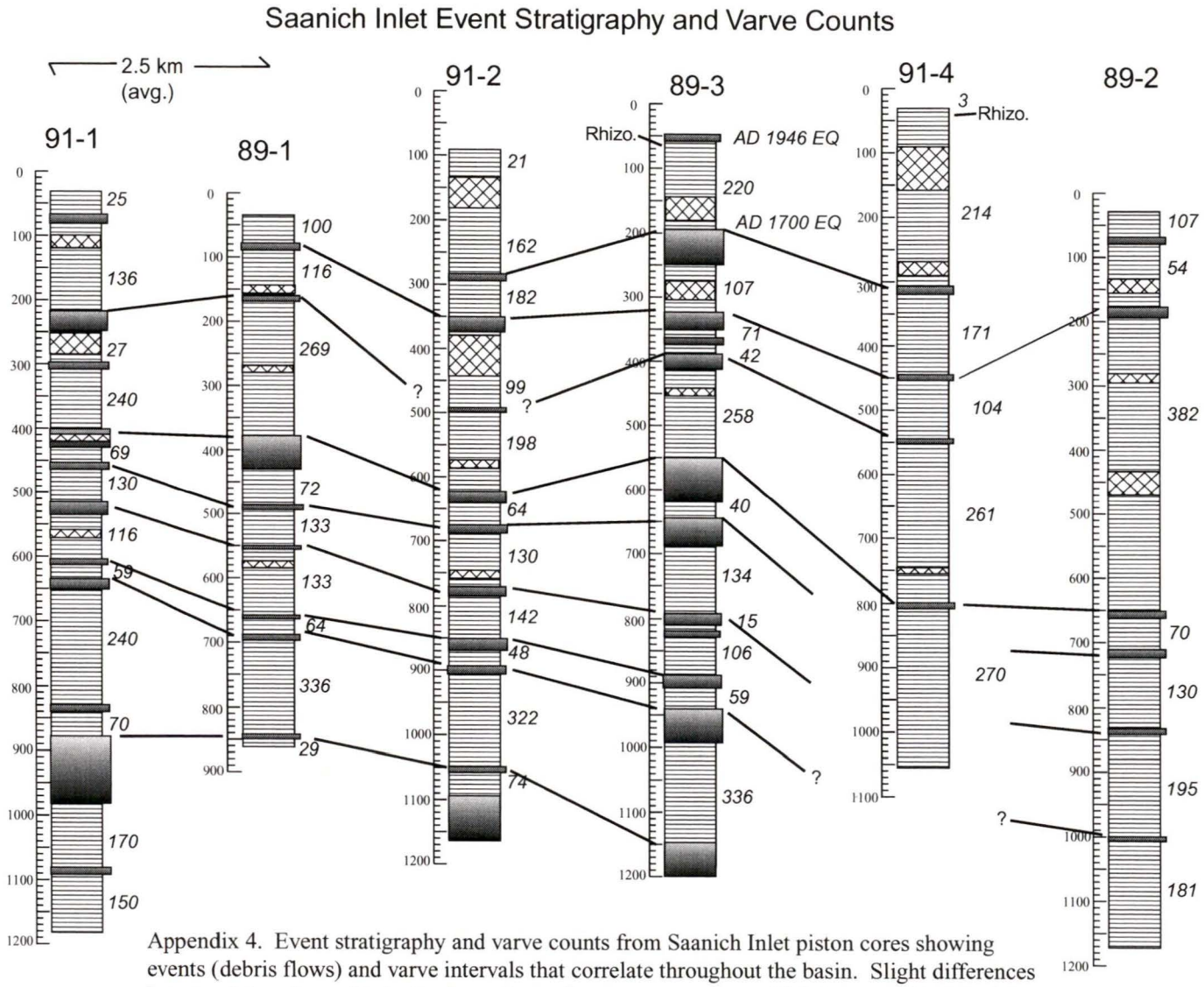

Appendix 4. Event stratigraphy and varve counts from Saanich Inlet piston cores showing events (debris flows) and varve intervals that correlate throughout the basin. Slight differences in varve intervals are likely due loss of core from gas expansion, which is especially prevalent in the upper portions of the piston cores, as well as counting errors. Adapted from Blais (1995) and Blais-Stevens et al., 1997. For legend, see App. 1. "Rhizo." indicates AD 1940 *Rhizosolenia* sp. diatom horizon.

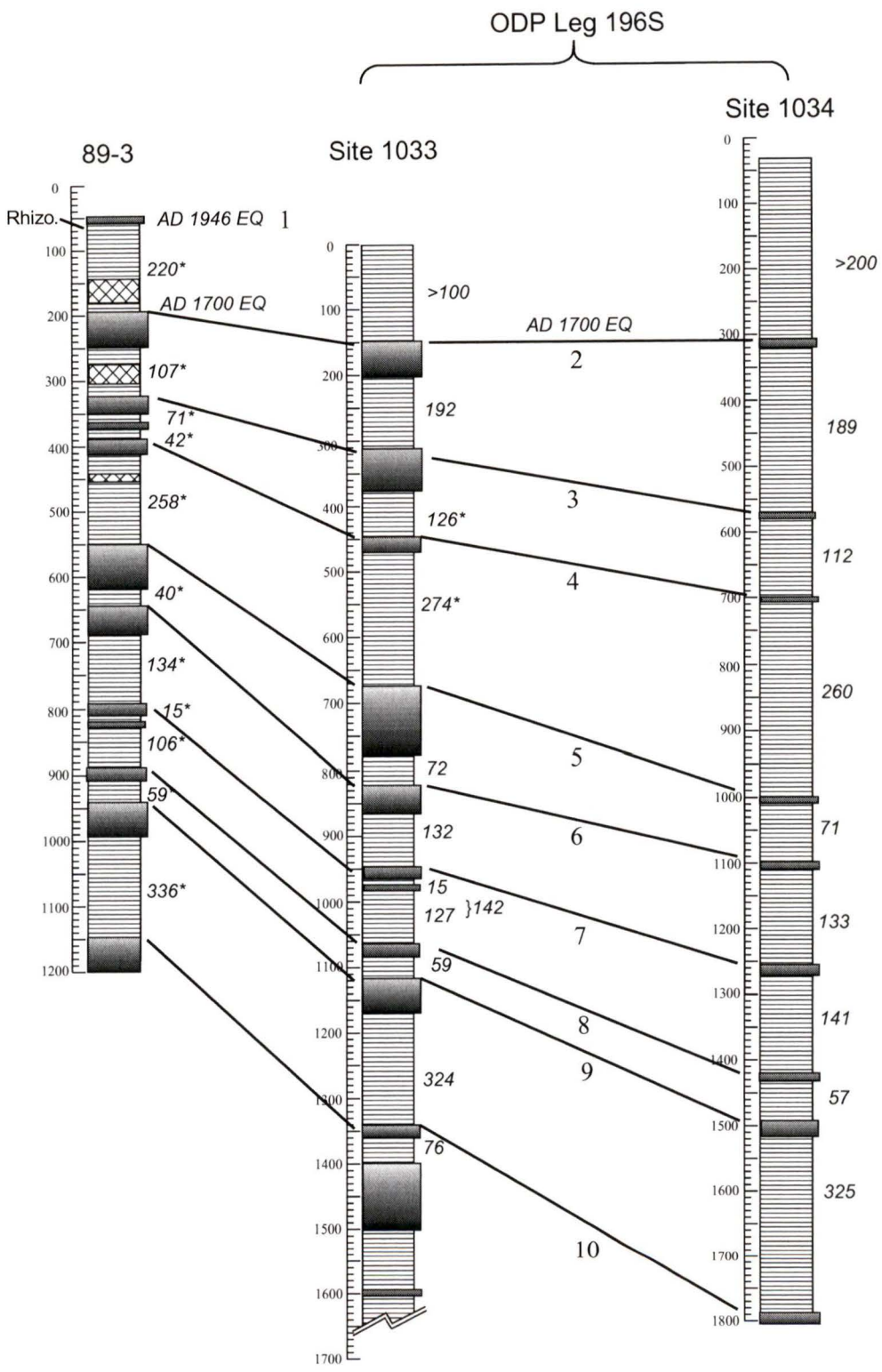

Appendix 5. Event stratigraphy and varve counts from the ODP leg 169S cores and piston core 89-3 from Saanich Inlet showing correlation between sites. Varve counts from Nederbragt and Thurow (2001), except those indicated by an asterisk, which are from Blais-Stevens and Clague, (2001). Varve counts from the ODP cores differ little between sites and are therefore considered to be more accurate than those from the piston cores. Event numbers refer to basin-wide events that are the same as in Table 8. See Appendix 1 for legend.

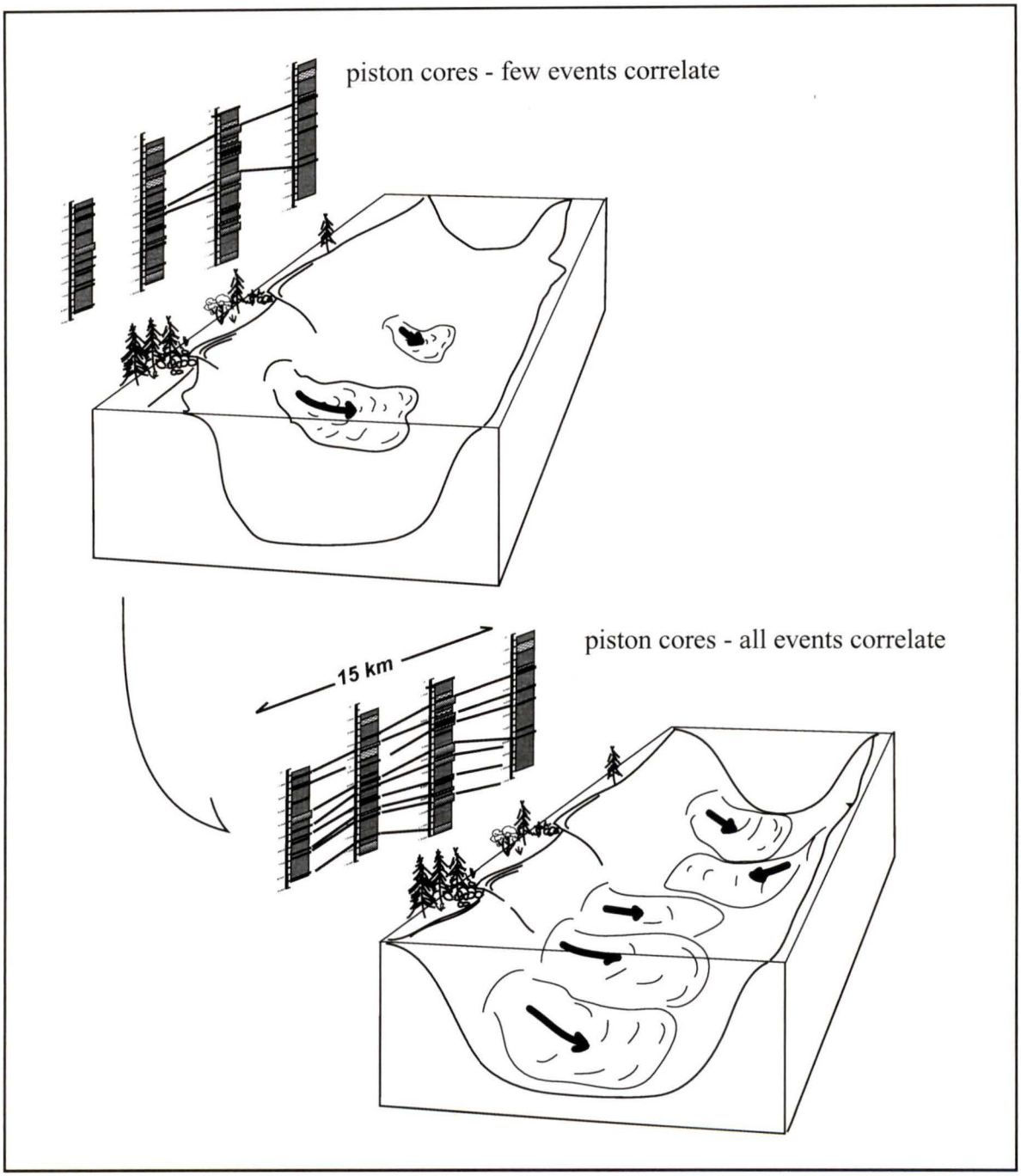

Appendix 6. Cartoon model for mass wasting in Saanich Inlet. The correlation of event deposits along 15 km of the basin axis strengthens the link between mass wasting in the inlet and paleo-earthquakes since no other mechanism could trigger discrete, simultaneous sidewall failures with such a widespread distribution. After Blais, (1995, fig. 3-13).

Comparing Event Chronologies

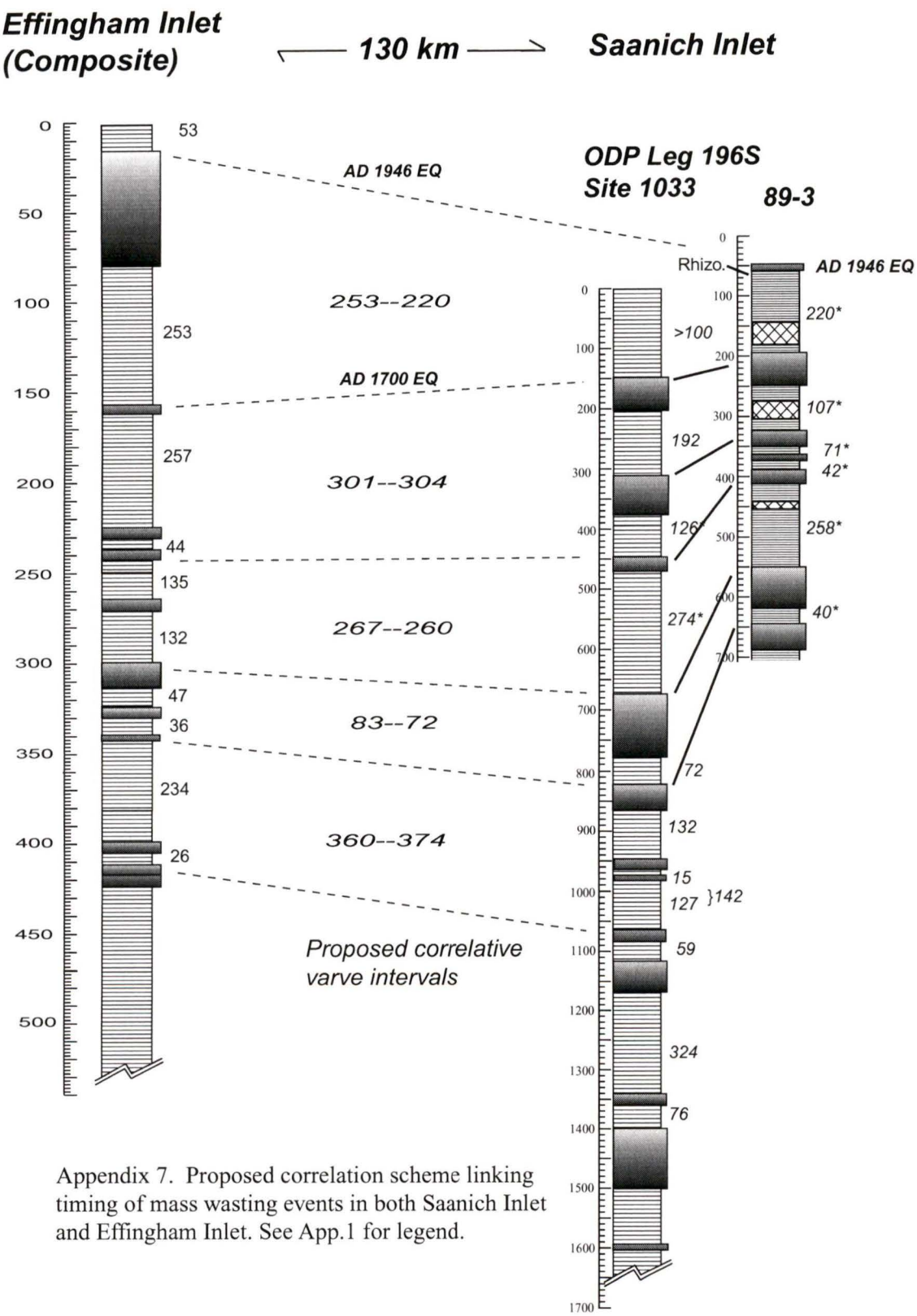

Appendix 7. Proposed correlation scheme linking timing of mass wasting events in both Saanich Inlet and Effingham Inlet. See App.1 for legend.

CURRICULUM VITA

Surname: Skinner Given Names: Matthew Robert

Place of Birth: Ottawa, Ontario, Canada

Educational Institutions Attended:

University of Victoria	1999 - 2002
Queen's University	1993 - 1998

Degrees Awarded:

BSc. (Honours), Geological Sciences	Queen's University

UNIVERSITY OF VICTORIA PARTIAL COPYRIGHT LICENSE

I hereby grant the right to lend my thesis to users of the University of Victoria Library, and to make single copies only for such users or in response to a request from the library of any other university, or similar institution, on its behalf or for one of its users. I further agree that permission for extensive copying of this thesis for scholarly purposes may be granted by me or a member of the University designated by me. It is understood that copying or publication of this thesis for financial gain by the University of Victoria shall not be allowed without my written permission.

Thesis title:

A record of paleoseismicity from the varved marine sediments of Effingham Inlet, Vancouver Island, British Columbia.

Author 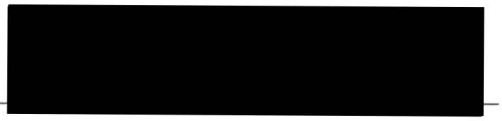

Matthew Robert Skinner

March 1, 2002

Appendix 1 Effingham Inlet - Inner Basin Stratigraphy

Northwest

Southeast

TUL97A02 (100 mbsl)

TUL99B03 (120 mbsl)

TUL99B02 (118 mbsl)

TUL99B05 (120 mbsl)

TUL99B13 (122 mbsl)

TUL99B06 (121 mbsl)

TUL99B09 (122 mbsl)

TUL99B08 (122 mbsl)

(Pilot)

AD 1946 EQ

AD 1700 EQ

200 - 360 BP (wood)

560 - 671 BP (shell)

850-980 BP (wood)

983 - 1104 BP (wood)

1223 - 1344 BP (wood)

1953-2167 BP (wood)

982-1106 BP (wood)

1790 - 1932 BP (wood)

2060 - 2350 BP (wood)

1950-2170 BP (wood)

2904 - 3048 BP (wood)

2305 - 2385 BP (fish bones)

3408 - 3503 BP (wood)

3923 - 4124 BP (wood)

3100 - 3213 BP (shell)

2807-2999 BP (shell)

3833 - 4023 BP (wood)

4475 - 4875 BP (wood)

4623 - 4888 BP (wood)

Sec 1

Sec 2

Sec 3

Sec 4

Sec 5

Sec 6

Sec 7

Sec 8

Legend

- well laminated (varved)
- indistinctly laminated
- bioturbated or disturbed varves
- no core (settling)
- gravity flow deposits (graded/non-graded)
- sandy layer
- folded laminae
- inclined laminae

982 - 1106 BP Calibrated C age before 2000 AD

Italics indicate rejected dates (reworked material)

Scale bars in cm

Appendix 2. Outer Basin Stratigraphy

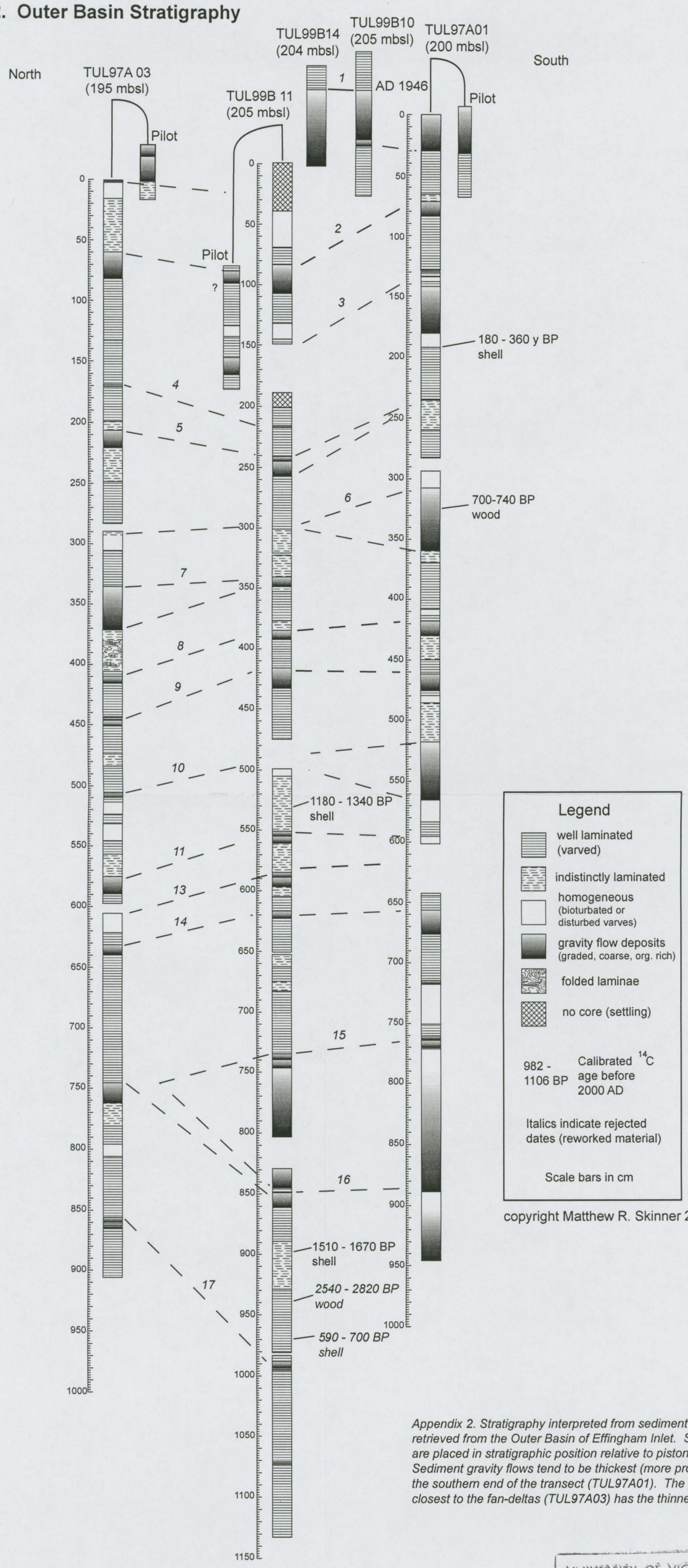

Appendix 2. Stratigraphy interpreted from sediment cores retrieved from the Outer Basin of Effingham Inlet. Short cores are placed in stratigraphic position relative to piston cores. Sediment gravity flows tend to be thickest (more proximal) towards the southern end of the transect (TUL97A01). The piston core closest to the fan-deltas (TUL97A03) has the thinnest units.